**UNIVERSIDAD PONTIFICIA COMILLAS DE MADRID**

**ESCUELA TÉCNICA SUPERIOR DE INGENIERÍA (ICAI)**

Instituto de Investigación Tecnológica

# TECHNICAL AND ECONOMIC ASSESSMENT OF INFORMATION AND COMMUNICATION TECHNOLOGIES FOR SMART GRIDS

Dissertation for the Degree of PhD

**PhD candidate:**

Ing. D. Luis González Sotres

**Directed by**:

Dr. D. Carlos Mateo Domingo

Prof. Dr. D. Pablo Frías Marín


Madrid 2017

# ABSTRACT

The smart grid concept represents a change of paradigm that implies a modernization of current electricity networks to obtain a more efficient and sustainable power system. The first step to achieve the potential advantages of the smart grid is the successful design and implementation of a reliable, secure and cost-effective communication infrastructure.

However, at the present time there is no existing standardized communication infrastructure that has been widely accepted and used to transform the current electric power grid into a smart grid. So, defining the services, requirements and architecture of the communication infrastructure of the power system, besides proper and optimal design techniques for such a network, are live research subjects in this field. With this aim in view, a critical need for tools and methodologies dedicated to analyse the performance of smart grids has been clearly identified. In this thesis, the performance and the impact of Information and Communication Technologies (ICT) in current smart grids applications are analysed from a novel technical and economic perspective.

From all the smart grid communication technologies, Power Line Communications (PLC) is considered the most cost-effective solution because it allows the reutilization of the power infrastructure as communication channel. PLC is especially used for the deployment of Advanced Metering Infrastructures (AMI), but the performance of this technology is highly affected by the local network conditions. Among the different PLC protocols used for AMI, PRIME provides the best performance under favourable conditions. For this reason, a methodology to analyse the performance of PLC PRIME networks has been developed, which is based on a simulation framework that takes into account the characteristics of the physical channel and the network behaviour.

The two Key Performance Indicators (KPIs) used for the previous analysis are the number of registered nodes and the time to read all meters, which have shown a strong influence of the registration process and the high impact of the user density on the communication performance. From the analysed scenarios, it has been concluded that when the registration process is performed correctly, the time to read all the smart meters is usually lower than 15 minutes, which is a typical reference value used for smart metering scenarios. Additionally, other dynamic factors like impulsive noise, load impedances and data traffic have been analysed, where the conclusions encourage the use of impulsive noise cancellation techniques, and the transmission in off-peak hours and with small packet sizes to improve the communication performance.

The developed methodology has been satisfactory applied to a wide range of distribution networks with a tree topology of different sizes. For this purpose, an algorithm to compute the PLC transfer function between any pair of nodes has been proposed, which is based on transmission line theory. Additionally, Reference Network Models (RNMs) have been used to obtain representative networks that can be later analysed with the proposed methodology avoiding the use of confidential data from DSOs. The combination of the simulation framework and the RNM has resulted in a very powerful way to analyse the communication performance of PLC networks at a regional level.

The added value provided by better information and communication systems in smart grids is another open issue for the smart grid development. Then, a new methodology to analyse the impact of these systems in a centralised voltage control application with On-Load Tap Changers (OLTC) and PV based on inverters has been presented. The selection of this application has been motivated by the high dependence of this functionality on ICT, as well as by the expected increase of solar PV in distribution networks and the beneficial effect of voltage control mechanisms to mitigate the voltage problems that might arise in scenarios with large PV penetration. Since this kind of voltage control application aims to send set-points from the central unit to the OLTC and PV inverters to optimize the system operation, the presented methodology is focused on the impact of the accuracy of the forecast used to calculate the set-points and the time interval used to update these set-points in the PV inverters. The voltage deviation cost, the energy curtailment cost, and the energy losses cost have been chosen as economic KPIs.

From the forecasting analysis, the reduction of the forecast error has produced better results of the voltage control application. When PV is underestimated, control actions include less PV curtailment but overvoltages are worse identified, which results in higher voltage deviation costs. Conversely, in the case of PV overestimation, the higher expected PV generation involves the identification of higher overvoltages. Then, on the one hand the corresponding control actions cause lower voltage deviation costs, but on the other hand result in a PV curtailment higher than actually needed. From the communication analysis, the reduction of the set-point interval has involved lower voltage costs thanks to a better adjustment to the actual voltage profiles, especially when the time interval is lower than one hour. The cost reduction obtained with shorter time intervals is usually related to a slight increase of the curtailment cost, which allows maintaining the voltages closer to the admissible limits.

All the conclusions obtained in this PhD provide a significant improvement for the analysis of the performance of smart grids, and encourage the use of the developed methodologies and their extension to other communication technologies and applications.

# CONTENTS

# FIGURES

# TABLES

# NOMENCLATURE

## Acronyms

| | |
|---|---|
| ADA | Advanced Distribution Automation |
| AMI | Advanced Metering Infrastructures |
| AMR | Automatic Meter Reading |
| BER | Bit Error Rate |
| CSMA | Carrier Sense Multiple Access |
| CVPP | Commercial VPP |
| DR | Demand Response |
| DSM | Demand-Side Management |
| DFS | Depth First Search |
| D8PSK | Differential 8 Phase Shift Keying |
| DBPSK | Differential Binary Phase Shift Keying |
| DQPSK | Differential Quaternary Phase Shift Keying |
| DSL | Digital Subscriber Lines |
| DER | Distributed Energy Sources |
| DG | Distributed Generation |
| DMS | Distribution Management Systems |
| DSO | Distribution System Operator |
| EC | European Commission |
| EEGI | European Electricity Grids Initiative |
| FLISR | Fault Location, Isolation and Service Restoration |
| FAN | Field Area Network |
| FT | Forecasting Tools |
| FEC | Forward Error Correction |
| GPS | Global Positioning System |
| HV | High Voltage |
| HAN | Home Area Network |
| ICT | Information and Communication Technologies |
| LLC | Logical Link Control |

| | |
|---|---|
| LV | Low Voltage |
| MAC | Medium Access Control |
| MV | Medium Voltage |
| MST | Minimum Spanning Tree |
| MTL | Multiconductor Transmission Line |
| MIMO | Multiple-Input-Multiple-Output |
| NAN | Neighbour Area Network |
| NSE | Non-Served Energy |
| OLTC | On-Load Tap Changers |
| OPF | Optimal Power Flow |
| OFDM | Orthogonal Frequency Division Multiplexing |
| PER | Packet Error Rate |
| PMU | Phasor Measurement Unit |
| PHY | Physical |
| PEV | Plug-in Electric Vehicles |
| PCC | Point of Common Coupling |
| PLC | Power Line Communications |
| RF | Radio Frequency |
| RNM | Reference Network Model |
| RES | Renewable Energy Sources |
| SCP | Shared Contention Period |
| SNR | Signal to Noise Ratio |
| SISO | Single-Input-Single-Output |
| STATCOM | Static Synchronous Compensators |
| SVC | Static VAR Compensators |
| SCADA | Supervisory Control And Data Acquisition |
| TVPP | Technical VPP |
| VoLL | Value of Loss Load |
| V2G | Vehicle-to-Grid |
| VPP | Virtual Power Plant |
| VC | Voltage Control |
| WACC | Weighted Average Cost of Capital |
| WAN | Wide Area Network |

# Chapter 1: Introduction

## 1.1. Introduction

Traditional power systems are evolving towards more sustainable scenarios based on energy policies that promote the use of low carbon technologies and reduce greenhouse emissions. In Europe, the European Commission (EC) presented in 2007 the so called 20-20-20 objectives for 2020, which are: increasing renewable energy supply to 20% of total demand, reducing energy consumption by 20% with respect to 2020 forecasts and reducing greenhouse gas emissions by 20% with respect to 1990 levels.

With the aim of incentivising the development of technologies that facilitate the achievement of these objectives, the EC created the European Strategic Energy Technology Plan (SET Plan) (European Commission, 2010b), which covers a set of European Industrial Initiatives formed by the main agents of each sector. The European Electricity Grids Initiative (EEGI) was presented as one of the most important areas since power grids will work as enablers for other technologies (ERGEG, 2010). In (EEGI, 2010) EEGI presented a roadmap for the period 2010-2018 of a research, development and demonstration program aimed at accelerating innovation in this area and addressing the most critical aspects of the European power system. The cost of this initiative was estimated at 2 billion €, where more than 60% corresponded to investments exclusively in distribution networks. Nevertheless, global spending on smart grids will reach a total of US$600 billion by 2020 (Chang, Yuan, Lv, Yin, & Yang, 2013).

But, why is so much investment needed in distribution networks? Most of the European network was built more than 30 years ago and was designed to transport energy from big power plants connected to transmission networks, to final customers connected at the distribution side (SmartGrids ERA-NET, 2012). This approach presented the advantage that power flows were very predictable and in just one direction. Moreover, the traditional driver for new investments was only demand growth. However, in order to achieve the 20-20-20's objectives, distribution networks have to cope with scenarios that present high penetration of Distributed Generation (DG), mainly from Renewable Energy Sources (RES). These technologies were not considered in the initial design of power systems, which additionally cause fluctuations and uncertainty in the generation side. As a result of the integration of these technologies, power flows are more difficult to manage and reverse power flows from lower to higher voltage levels may occur, so the planning and operation of distribution networks is becoming more complex.

Distribution System Operators (DSOs) have two ways to adapt the network to these new challenges. The traditional solution is based on the installation of new lines and transformers and the reinforcement of the existing facilities. Instead, the smart grid solution, is supported by Information and Communication Technologies (ICT) to integrate Distributed Energy Sources (DER) in a more efficient and sustainable way, while ensuring good levels of security of supply and quality of service (Pérez-Arriaga & Knittel, 2016). In fact, in the new version of the research and innovation roadmap proposed by EEGI, communications is conceived as a transversal topic of special interest (EEGI, 2013), and EC has acknowledged that ICT-based innovations may provide one of the potentially most cost-effective means to help Member States to achieve the 2020 targets (European Commission, 2009). On the contrary, the required investments to cope with high RES scenarios using traditional reinforcements would be much higher.

Thus, the main objective of the EEGI program was to prepare an effective and efficient deployment of smart grids in Europe. To ensure the achievement of this objective, pilot projects like SUSTAINABLE or DISCERN are being carried out to test different smart grid solutions and evaluate their performance ("DISCERN project," 2016, "SUSTAINABLE project," 2016b). However, there is very little information about rigorous methodological processes to assess these new smart grid technologies and applications (European Commission, 2013a). Indeed, appropriate metrics are not currently available for evaluating the performance of the smart grid from both power and communication sides, and these metrics should be quantifiable and useful to drive operations and planning decisions (NIST, 2013). Furthermore, sound regulatory schemes require the quantification of the effects and benefits of this new distributed intelligence (ERGEG, 2010).

Now, models are required to simulate the interaction between communication systems and smart grids performance. Developing communication and power network performance assessment models will help to adopt cost-effective solutions and leverage communications infrastructure investments. Nevertheless, current planning methodologies and computational tools are not well prepared to assess all the new issues that smart grids are presenting (Kolhe, 2012; Ribeiro, 2012). Indeed, an important aspect of smart grid planning is the decision-making process for selecting the new equipment and technologies that are expected to be deployed in the distribution system and the variables that should be taken into account during this process (IEEE Power and Energy Magazine, 2011). The work developed within this document will aim to propose new methodologies for the assessment of Smart Grid technologies, with special focus on ICT.

## 1.2. Smart Grids overview

The smart grid concept represents a radical change of power systems that implies a modernization of current electricity networks to obtain a more reliable and efficient system. There is a wide range of definitions for smart grid, but all of them share the same essence. Here there is a compilation from some important international institutions:

Eurelectric (EU): A smart grid is an electricity network that can intelligently integrate the behaviour and actions of all its users to ensure a sustainable, economic and secure electricity supply (Eurelectric, 2011).

National Institute of Standards and Technology (US): A smart grid is a modernized grid that enables bidirectional flows of energy and uses two-way communication and control capabilities that will lead to an array of new functionalities and applications (NIST, 2012).

Department of energy & climate change (UK): Building a smart grid is an incremental process of applying ICT to the electricity system, enabling more dynamic 'real-time' flows of information on the network and more interaction between suppliers and consumers (DECC, 2009).

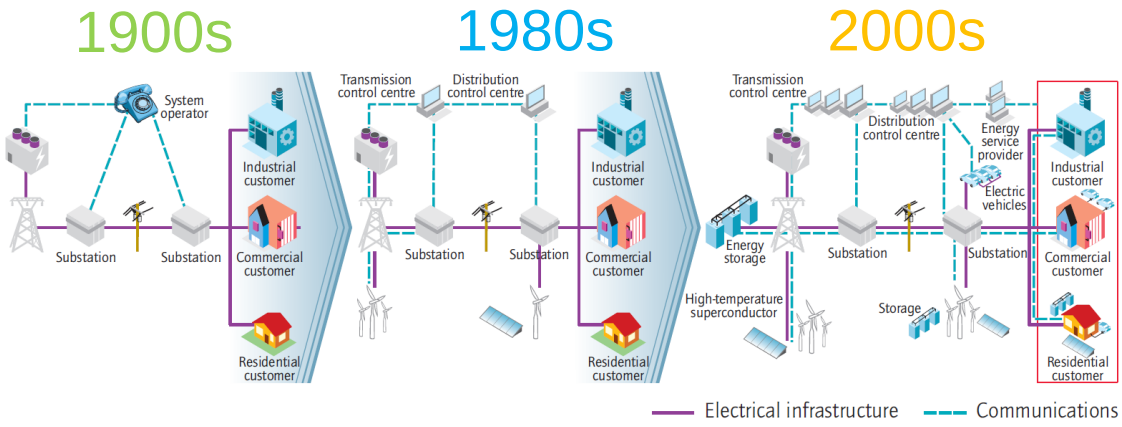


**Figure 1-1 Incremental process of applying ICT to the electricity system** (International Energy Agency, 2011)

The evolution of communications in the power system is represented in Figure 1-1. As it can be seen in the figure, communications have been gradually upgraded from being only used at generation and substation levels to the whole power system. Thus, network infrastructures have to be improved and expanded to enable effective communication between multiple devices and technologies to take full advantage of smart grid capabilities (Sendin et al., 2016).

In (Gungor et al., 2013) the authors divided the whole smart grid into three layers, represented in Figure 1-2 (Ho et al., 2013). The power layer is the physical infrastructure for power supply. The communication layer is the heart of the system and provides interconnection between all of the systems and devices. Finally, the application layer takes advantage of the other two layers to provide advanced services and applications. In the following, a detailed description of each layer will be presented.

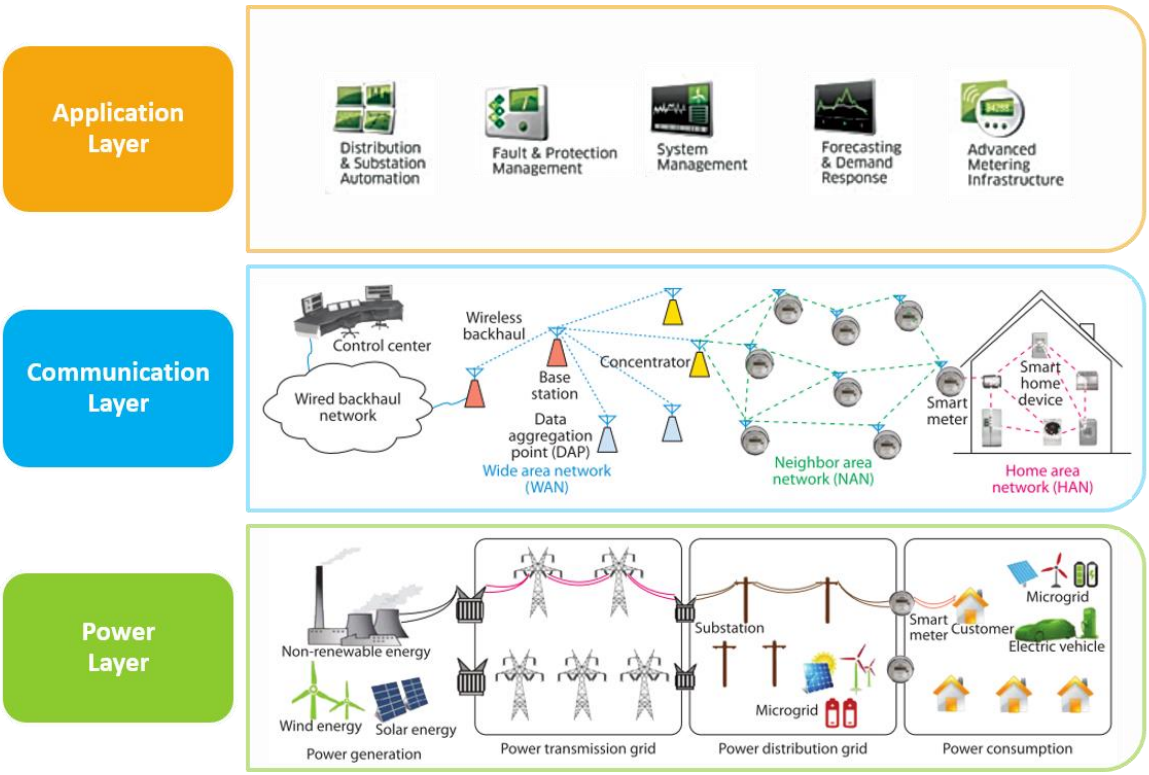


**Figure 1-2 Power layers of the smart grid** (Ho et al., 2013)

### 1.2.1. Power Layer

From a conceptual point of view, power systems can be divided in four main sections: generation, transmission, distribution and consumption. Smart grids are focused on the distribution side, which is the part of the power system that connects the transmission network to the electricity consumers, and requires a large number of facilities to meet all the demand (González-Sotres, Mateo Domingo, Sánchez-Miralles, & Alvar Miró, 2013).

The distribution network is divided in high (HV), medium (MV) and low (LV) voltage levels, which are connected through HV/MV primary substations and MV/LV secondary substations (Gonzalez-Sotres et al., 2011). Most distribution lines are LV and MV. For instance, in Europe LV networks account for 60% and MV networks for 37%, being HV lines just 3% of

total distribution networks, for a total of nearly 10 million km of power lines (Eurelectric, 2013). Usually, LV networks present a radial tree structure, whereas MV networks are normally developed with a mesh configuration but radially operated to allow network reconfiguration, for instance under emergency conditions for fast fault location and service restoration.

Residential consumers are connected to LV networks, whereas high demand consumers like industries or commercial buildings are connected to higher voltage levels. Traditionally, upper levels have presented a higher degree of observability and controllability, because the number of assets is much lower and continuity of supply is more critical. Thus, residential consumers were treated as passive actors and their engagement in the power system was practically null. For this reason, one of the first changes in the evolution of distribution systems is the deployment of smart meters, which help consumers to understand their consumption better and encourage them to adopt a more active role to achieve a more efficient system operation (Morgan et al., 2009). These electronic devices present the advantage of measuring detailed load profiles instead of total energy consumed in the billing period like conventional meters, apart from other advanced functionalities. In Europe, the deployment of smart meters is supported by the European Directive 2009/72/EC, which declares that Member States with a positive cost-benefit analysis for smart meter roll out have to deploy at least 80% by 2020, which involves the installation of nearly 200 million smart meters, with an estimated investment of around 45 billion € (European Commission, 2014).

DG is becoming very important in the power distribution system, which means that more generation units are being connected to the distribution side, mainly from RES. For instance, in the last 10 years the integration of solar PV in power systems all over the world has increased significantly. By 2019 the total installed capacity is expected to be around 450 GW according to market forecasts (SolarPower Europe, 2014), and the vast majority of these PV facilities are installed in LV and MV networks. Additionally, buildings with small scale generators used for self-consumption can help consumers to reduce their energy consumption, like the integration of photovoltaic panels in the rooftops (Glassmire, Komor, & Lilienthal, 2012). As a matter of fact, the European Directive on the energy performance of buildings stated that for 2021 all new buildings must be nearly zero-energy buildings (European Commission, 2010a). These scenarios present new challenges, such as reverse power flows, voltage violations or congestions in distribution grids (von Appen, Braun, Stetz, Diwold, & Geibel, 2013). Additionally, high PV penetration levels may cause power and voltage fluctuations due to cloud shadows, and even an increase on energy losses when reverse power flows are large enough (Ebad & Grady, 2016; Gonzalez-Sotres et al., 2011). In this sense, the smart grid is expected to integrate DG at the

distribution level in a reliable and cost-effective way, reducing the need for network reinforcements and improving distribution system operation thanks to new applications based on ICT.

Energy storage can provide flexibility to the system since it can store energy to contribute to the supply-demand balance or to mitigate current and voltage violations in the distribution networks. In (Falvo, Martirano, Sbordone, & Bocci, 2013) a summary of the characteristics of the main storage technologies is presented. According to (Hidalgo, Abbey, & Joós, 2010) energy storage systems could be of different types. Bulk storage are large units that can be used to supply electricity at peak demand hours for load shaving, as well as to consume the excess of production from renewable integration or provide ancillary services. Distributed storage systems are smaller units that can be used for instance as backup for critical loads. Plug-in Electric Vehicles (PEV) can be considered as Mobile Storage Units from the power system point of view, which can be Hybrid in case they also have a combustion engine, or pure electric in case they only have the battery. These devices may also be used for primary frequency control (Izadkhast, Garcia-Gonzalez, Frias, & Bauer, 2017) as additional storage units under certain conditions with appropriate control mechanisms based on the Vehicle-to-Grid (V2G) concept (Pieltain Fernandez, Gomez San Roman, Cossent, Mateo Domingo, & Frias, 2011).

According to this analysis of the power layer, it can be concluded that the most important changes in power systems due to the development of smart grids are located in the distribution side, especially in LV and MV levels. Moreover, the actual degree of development of smart grids and current legislations pose smart meters and DG as the most widespread technologies. Among the Distributed Energy Sources (DER), solar PV is expected to present a large increase of penetration at these voltage levels in the next years, which shows new challenges for the operation of power systems that can be effectively solved with new applications based on ICT.

### 1.2.2. Communication Layer

Typically, the communications network of a smart grid presents three representative segments depending on the coverage area (Ho et al., 2013). The Home Area Network (HAN) gathers sensor information from different smart devices within the home and delivers control information to them for better energy consumption management. The Smart Meter works as a communication gateway between the HAN and the rest of the system. The Neighbour Area Network (NAN) – also called Field Area Network (FAN) - connects a group of Smart Meters to a central unit called data concentrator. Finally, the Wide Area Network (WAN) aggregates data from multiple NANs and connects them to the control centre. Complementary to the previous

classification, in (Ancillotti, Bruno, & Conti, 2013) authors associate the WAN, NAN and HAN segments to a different tier or domain, which are utility core backbone, distribution backhaul, and access segment, respectively.

There are different types of communication technologies used in smart grids, which can be wired or wireless. Optical fibre is the most flexible and robust wired technology, but the costs of implementation can be too high, especially over large geographical areas. Digital Subscriber Lines (DSL) use the wires of the voice telephone network, so the already existing infrastructure of DSL reduces installation costs. Finally, Power Line Communications (PLC) reuses existing power grids as a communications channel, reducing the investment required to connect the devices, which has placed PLC as a cost-effective technology for utilities.

There are two main types of PLC technologies, narrowband (from 3 kHz to 500 KHz) and broadband (from 1.8 MHz to 250 MHz). Although broadband PLC provides higher data transmission rates, narrowband can be used over longer distances at a lower cost (Amarsingh, Latchman, & Yang, 2014). Within the narrowband solutions, standards and specifications such as PRIME, G3, ITU-T G.hnem or IEEE 1901.2 that take advantage of multicarrier Orthogonal Frequency Division Multiplexing (OFDM) can achieve bit rates of hundreds of kbps, whereas single carrier solutions like Echelon, Meters and More, and G1 can only achieve few kbps (Haidine, Tabone, & Muller, 2013). Broadband solutions have been mainly used for in-home applications like HomePlug, although some access applications can also be found in the industry, for instance with the IEEE 1901 standard or solutions like the ones provided by Main.net or Ascom (Alberto Sendin, Peña, & Angueira, 2014). In Europe narrowband PLC is especially used to deal with large-scale smart meter deployments. The most widespread PLC technologies are PRIME in Spain, Portugal and UK, G3 in France, Meters and More in Italy, and Echelon in Nordic countries. In (Kim, Varadarajan, & Dabak, 2010) authors compared the OFDM solutions, PRIME and G3, concluding that PRIME provides higher data rates under favourable conditions, whereas G3 is more robust under unfavourable conditions. All these technologies are usually combined with the Device Language Message Specification/ Companion Specification for Energy Metering (DLMS/COSEM) application protocol (“DLMS/COSEM,” 2016).

Radio Frequency (RF) networks are easily scaled, reliable and redundant, and can be quickly installed to achieve wide coverage. There are two main types of RF networks being deployed. RF mesh networks enable connectivity and communication between all endpoints and present high resiliency because when a connection point is lost, a device can find alternate routes to communicate with the network by relaying messages to other nodes. Star RF can be more economical than mesh in densely populated areas or areas with difficult topography where its

antenna towers can better reach the maximum number of endpoints than RF mesh. Currently, the typical RF communication technologies for smart grids are GPRS, EDGE, HSPA, LTE and WiMAX which can be owned by the DSO or hired to a telecomm operator. However, the higher cost of these communications technologies poses GPRS as the preferred option for the DSOs. There are other wireless technologies like Zigbee, Bluetooth or IEEE 802.11 (Wi-Fi) with very limited coverage, which can be only used for HAN applications.

The most important aspects of communication networks are bandwidth and latency. The former measures the data transmission rate, whereas the latter represents the time necessary for data to reach an endpoint. Reliability is also important since the communication network has to be robust. Additionally, communication networks convey energy consumption data from millions of customers as well as signals used for grid management and stabilization so they are vulnerable to privacy and security issues. For this reason it is necessary to embrace existing security solutions where they fit. For determining the suitability of communication technologies to a specific application, the typical parameters to take into account are bandwidth and coverage. Typical ranges of these parameters for the described technologies can be found in (Andreadou, Guardiola, & Fulli, 2016; Vehbi C Gungor et al., 2011; Parikh, Member, & Kanabar, 2010; Shrestha & Jasperneite, 2012). However, these references only present approximate values and the final performance depends on the actual implementation conditions.

When designing the architecture of the communication network for the smart grid, the type of control is an important question that has to be solved (Bouhafs, Mackay, & Merabti, 2012). In a centralised control all the sensors are only connected to the control centre, which performs control and optimization functions. However, the network can be designed in a more distributed way, so a set of microgrids managed by intelligent controllers can be deployed. These microgrids under certain situations could be disconnected from the main network and operate in island mode. Figure 1-3 shows the two approaches. Although in this option the communication requirements for the control centre could be lower than in the centralised way, new connections at the same hierarchical level will have to be considered. Nevertheless, the communication network has to be implemented to enable an efficient operation of the smart grid applications, which are analysed in Section 1.2.3.

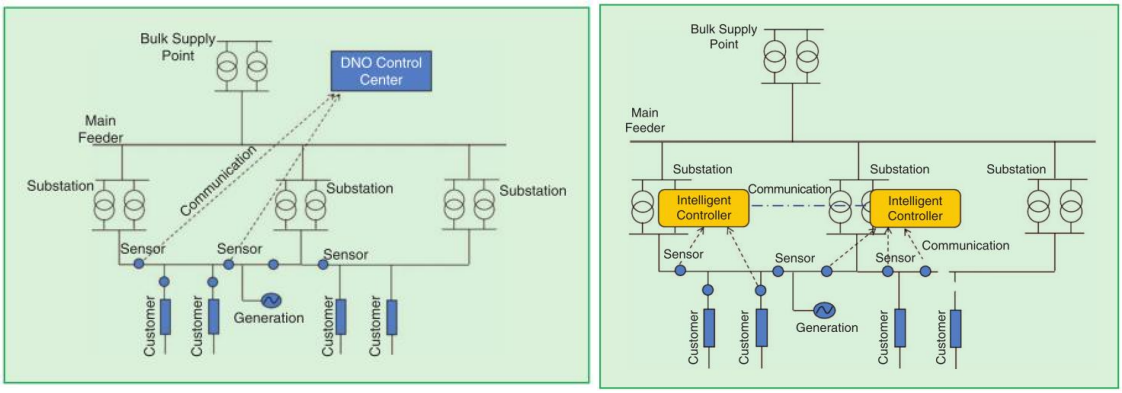


**Figure 1-3 Differences between centralised and distributed control in power networks**

After this review of the communication layer, it can be concluded that despite the wide range of communication technologies for the different network areas, technologies like PLC are especially appropriate for the first stage of the transition towards a smart grid and they are already deployed in different countries. Nevertheless, PLC depends on the topology and characteristics of power systems. Thus, PLC performance is highly affected by the implementation conditions, which makes the analysis of this communication technology of special interest for this PhD. Finally, the communication requirements are defined by the smart grid applications, which will determine the suitability of a specific communication technology based on its performance.

### 1.2.3. **Application Layer**

The development of Advanced Metering Infrastructures (AMI) represents one of the first steps in the smart grid process to take advantage of the massive deployment of smart meters mentioned in Section 1.2.1. Besides the higher level of detail that they provide with respect to traditional metering systems, they also allow utilities to perform Automated Meter Reading (AMR) and remote control, as well as provide differentiated services and tariffs to consumers that will facilitate a more efficient electricity supply (Depuru, Wang, & Devabhaktuni, 2011). For instance, Demand Response (DR) practises can be facilitated through different price-based programs, where consumers may change their consumption based on different electricity prices. Time-of-Use (TOU) tariffs present different prices for different time intervals, whereas real-time prices (RTP) propose more dynamic rates that change periodically in short intervals like 15 minutes or 1 hour. Thanks to the bidirectional communication of AMI, Demand-Side Management (DSM) mechanisms can be also provided. In this case, distribution operators can reduce the consumption of their customers under certain conditions, for example in exchange for an economic incentive (Gellings, 2011).

The high variability of RES production together with the difficulty to perform reliable predictions make Forecasting Tools (FT) a key aspect for system operators to reduce the uncertainty and ensure a secure and stable system operation. An state of the art of solar and PV forecasting can be found in (International Energy Agency, 2013). Forecasts performed for less than 6 hours ahead (intra-day forecasts) normally use stochastic learning techniques that train the algorithms with historical data, but the accuracy of the results can be considerably improved when close to real-time measurements and good weather predictions are available. These forecasts can be also supported by sky or satellite images to track the clouds movement and predict the irradiance. Forecasts more oriented on the day-ahead are usually supported by numerical weather predictions. Forecasting tools aimed at predicting the demand of grid users can also be useful to reduce the uncertainty and adopt better control decisions. For instance, in (Bracale, Caramia, Carpinelli, Di Fazio, & Varilone, 2013) authors presented a probabilistic method for short-term forecasting of DG and demand based on a Bayesian approach.

State estimation applications seek to obtain a fair approximation of the current state of the system to face lack of measurements and provide a certain level of redundancy (Carmona-Delgado, Romero-Ramos, & Riquelme-Santos, 2013). In the same way that prediction tools, these applications require close to real time information to obtain results with a reasonable degree of certainty. Phasor Measurement Units (PMUs) or Synchrophasors can improve state estimation and other applications providing dynamic information of the system referenced to a common time base, which enhances observability and allows coordinated control (Sexauer, Javanbakht, & Mohagheghi, 2013). These devices use the Global Positioning System (GPS) time reference and collect the order of tens measurements per second. The potential applications that can benefit from PMU data are discussed in (Sexauer et al., 2013).

The previous applications are mainly oriented on gathering information from a large number of sensors distributed across the power system that produce a huge amount of information. For instance, Austin Energy in Texas implemented 500,000 smart meters that sent data every 15 minutes and required 200Tb of storage (McHann, 2013). Thus, big data is crucial since this information has to be stored, processed and analysed to be effectively turned into management decisions (Bahramirad, Svachula, & Juna, 2014). Control centres with Supervisory Control and Data Acquisition (SCADA) systems and Distribution Management Systems (DMS) have to manage this information in real time to efficiently operate distribution network assets. Thanks to these systems, distribution automation can be performed to improve protections and Fault Location, Isolation and Service Restoration (FLISR) activities. The existing approaches and future trends in fault location can be found in (Kezunovic, 2011). Since these applications are

critical for the system, their capability to respond almost instantaneously must be guaranteed. For instance, IEEE 1547 requires the detection and elimination of unintentional islanding within two seconds.

Voltage Control (VC) can be performed with devices such as capacitor banks, Static VAR Compensators (SVC) or Static Synchronous Compensators (STATCOM). For instance, in (Aziz, Mhaskar, Saha, & Member, 2013) a methodology to find the best location of STATCOM for fast voltage recovery in the presence of dispersed DG units is described. On-Load Tap Changers (OLTC) are another control mean to keep voltages within admissible ranges by changing the taps of the transformers at the substations.

The inverters associated to DG can also be used for voltage control at the Point of Common Coupling (PCC) by changing the injected or absorbed amount of reactive power. Additionally, active power curtailment can also be considered under certain conditions. These options are very interesting because they do not require additional control devices. Moreover, in the study presented in (Vandenbergh et al., 2013) for the prioritisation of technical solutions for PV integration in power systems, active and reactive power control of PV units were identified as high effectiveness solutions to mitigate voltage problems in LV and MV networks. However, the deployment of these solutions highly depends on the regulatory framework, which should provide adequate incentives to establish a more efficient and coordinated power system where DSOs can procure DG services (Cossent, Gómez, & Frías, 2009; Pérez-Arriaga, Ruester, Schwenen, Battle, & Glachant, 2013).

Another mechanism for DG control is through Virtual Power Plants (VPPs), which integrate the operation of supply- and demand-side assets to meet customer demand (KEMA, 2011). VPPs have two roles: The Commercial VPP (CVPP) is responsible for optimizing the operation of the aggregated units in the energy and ancillary services markets, whereas the Technical VPP (TVPP) manages optimal and secure operation of the system and ensures the technical feasibility of the program submitted by the CVPP (Lloret & Valencia, 2013). An Optimal Power Flow (OPF) formulation can be used by these mechanisms to seek for an economic dispatch, for instance to minimize the price of reactive power purchased by the DSO (A. G. Madureira & Peças Lopes, 2012).

This assessment of the application layer has shown many possibilities that can be achieved by the smart grid, which can be more related to gathering useful information for system operation, or more focused on performing control actions and asset management. From the information side, AMR seems to be the first functionality that can be activated by smart meters,

and presents a huge challenge in terms of communications due to the large amount of devices that are being installed. From the control side, voltage control is really interesting for future scenarios with high PV generation since they can contribute for their efficient integration in the power system. In this case, forecasting was also identified as an important enabler to carry out more effective control actions.

In the next section, a review of the communication requirements of smart grid applications and their performance is presented to identify the major gaps to cover in this PhD taking also into account all the aforementioned conclusions.

## 1.3. Communication requirements and performance of smart grids

As concluded from the previous analysis, communication networks enable the integration of a number of technologies and applications to achieve a better observability and control in the process of turning distribution networks into smart grids. However, these applications present different communication requirements depending on the scope and objective that are aiming for. Typical values of the requirements of smart grid technologies and applications have been discussed in several publications (DOE, 2010; Gungor et al., 2013; Ho et al., 2013; NRECA-DOE, 2013) and a summary of them is presented in Table 1-1.

**Table 1-1 Bandwidth and latency requirements of smart grid technologies and applications**

| Technology / Application | Bandwidth | Latency |
|---|---|---|
| AMI | 10-100 kbps/node,<br>500 kbps for backhaul | 2-15 s |
| Demand Response | 14-100 kbps/device | 500 ms-several minutes |
| Distributed Generation and Storage | 9.6-56 kbps | 20 ms-15 s |
| Electric Vehicles | 9.6-56 kbps | 2 s-5 min |
| Synchrophasor | 600-1500 kbps | 20 ms-200 ms |
| Fault Location, Isolation, and Restoration | 10-30 kbps | few ms |
| Distribution Automation | 2-5 Mbps | 25-100 ms |

In general, applications that have to meet critical requirements and operate close to real-time may need lower latency than others that are less stringent. For this reason, activities related to control and protection functions present latencies on the range of milliseconds, whereas applications related to meter reading or demand response can reach the range of seconds or even

minutes. However, even non-critical applications like smart metering may imply high communication requirements due to the large number of deployed devices, especially in scenarios with short reading intervals like the 15 minutes read that is expected for AMI. For most applications, the required level of reliability should be between 99% and 99.99%, but in the case of synchrophasors it should be of approximately 99.99995%, which means to be out of service 16 seconds a year. Furthermore, in order to achieve these objectives cyber security has to be a must.

Several authors have performed specific studies to analyse the communications requirements of the smart grids. For instance, in (Aggarwal, Member, Kunta, & Pramode, 2010) authors studied the bandwidth requirements of a future medium size smart grid by using queuing theory, and they concluded that the resulting high bandwidth will need optical fiber to meet the latency requirements. In (Luan, Sharp, & Lancashire, 2010) a bottom-up method to estimate the capacity requirements of a WAN for AMI and other smart grid applications was presented. The authors forecasted the number of smart devices to obtain data traffic profiles and they considered two scenarios in the planning process: normal conditions and emergency conditions. Another approach to estimate the capacity limitations of a linear chain wireless communication architecture for AMI is presented in (Karimi & Namboodiri, 2012).

In principle, the most suitable communication technology for a specific smart grid application is the one that fulfils the communication requirements at the minimum cost taking into account the local conditions of the distribution area. To determine whether a technology is technically feasible under certain communication requirements, the communication performance of the technology must be carefully analysed. As concluded in Section 1.2.2, PLC is considered the most cost-effective solution for AMI since it allows the reutilization of the power infrastructure as communication channel. However, power lines were not traditionally designed to this purpose so PLC has to deal with phenomena like the presence of noise or the signal attenuation that worsen and limit the communication (Galli, Scaglione, & Wang, 2011). Thus, the topology and the technical characteristics of the electricity network highly affect the communication performance.

The most precise way to prove PLC performance is to test the technology in field. For instance, in (Olivera et al., 2013) the performance of a real AMI deployment from a Spanish utility is analysed, where typical problems found during the tests are described. In (S. K. Rönnberg, Bollen, & Wahlberg, 2011) the interactions between PLC and end-user equipment are analysed through measurements in a laboratory environment and in the field, where authors concluded that low impedances are the main cause of interference. In (S. Rönnberg, Bollen, & Larsson, 2014) a similar analysis was performed for PV installations on the LV, where the authors concluded that

the interferences caused by these devices can be a concern for PLC. Alternatively, simulation tools can provide a fair approximation of communications performance of ICT for a wide range of specifications and scenarios in a more economical way, so they can be used as a first step for real deployments before installing any equipment and avoiding additional costs (López et al., 2013). In most studies of PLC, the scope of the analysis is usually limited to the physical channel (Kim et al., 2010; Korki, Zhang, & Vu, 2013; Papadopoulos et al., 2013), or only focused on the network behaviour (Alberto Sendin, Guerrero, & Angueira, 2011; A. Zaballos, Vallejo, Majoral, & Selga, 2009), and conclusions applicable to real networks are difficult to obtain. This fact was the motivation of the work presented in (Matanza, 2013) to develop a simulation framework that integrates both approaches. In this framework the attenuation and noise effects are modelled in MATLAB, and the network behaviour is analysed in the discrete event simulation framework OMNeT++ considering PRIME and DLMS/COSEM protocols and specifications.

In (Matanza, Alexandres, & Rodríguez-Morcillo, 2014) the performance of PLC networks for AMR application was analysed with this simulation framework by measuring the latencies of the messages sent between the MV/LV substation and the smart meters. Simultaneous and sequential polling strategies were compared, concluding that sequential polling can obtain a better performance. Additionally, the results obtained from the comparison of the analysed networks shown that a linear increase in the number of smart meters does not necessarily involve a linear increase in the time to read them, because the communication channel acts as a bus where all devices contend with each other for transmitting. Indeed, the threshold of 15 minutes to read all smart meters was exceeded for the most demanding cases. Therefore, a more rigorous analysis of the most critical parameters that affect to the communication performance would be really useful to determine under which boundary conditions PLC may be suitable for AMI applications.

Apart from the assessment of the performance of communication networks, currently there is a high uncertainty related to the level of information and control that should be adopted by these new applications, which can be measured based on different Key Performance Indicators (KPIs) (Dupont, Meeus, & Belmans, 2010). Indeed, despite the number of publications analysing the requirements of the so called smart grid (Khan & Khan, 2013; Patel et al., 2011; Rohjans, Danekas, & Uslar, 2012), most of them provide general recommendations that have to be verified from a technical point of view in order to reveal more practical conclusions (López et al., 2015). In this sense, simulation tools can provide very valuable information to assess the performance of smart grid applications such as advanced metering and voltage control considering both power and communication sides (Mets, Ojea, & Develder, 2014). In addition, technical benefits have to be quantified in monetary terms to adopt the most cost-effective solutions, which may help to

understand the economic implications of these advanced functionalities. But compared to the large amount of previous publications related to technical analyses, a much lower number of authors have tried to provide conclusions combining technical and economic approaches.

The authors in (Shahraeini, 2011) compared the characteristics of centralised and decentralised control strategies. They used the IEEE 118-bus test system to design the backbone network required to communicate a set of state estimators to the control centre. In order to design the network, they obtained the Minimum Spanning Tree (MST) for all installed metering devices in each area. Finally, they concluded that both control strategies present similar costs, but the decentralised one shows better latency and reliability features. With regard to voltage violations, several authors have analysed the impact of different voltage control strategies. For instance, authors in (Han et al., 2014) assessed from a qualitative point of view the technical and market implications of current trends for voltage control, which were classified into four categories: decentralised autonomous control, decentralised peer-to-peer coordination, hierarchical control, and centralised control. In (Delfanti, Merlo, & Monfredini, 2014), autonomous and coordinated local voltage control strategies based on reactive power adjustment were analysed in LV networks, where authors concluded that this mechanism alone is not enough to fully resolve the overvoltage problems caused by DG due to the high R/X ratio at this voltage level. In (Etherden & Bollen, 2014) different active power curtailment techniques were analysed, where the amount of curtailed energy was highly affected by the curtailment method used.

The combination of real and reactive power control of PV inverters was investigated in (Collins & Ward, 2015), which results showed that the inclusion of reactive power compensation helps to reduce curtailment losses that may be derived from the implementation of an active power control strategy alone. This conclusion was also envisaged in (Etherden & Bollen, 2014), although in this case authors also noticed that the reactive power control is less effective where the major overvoltage problems are expected to arise, for instance in rural networks where R/X ratios are higher (Frias, Platero, Soler, & Blázquez, 2010). A coordinated voltage control strategy including also real-time thermal rating was presented in (Degefa, Lehtonen, Millar, Alahäivälä, & Saarijärvi, 2015). In this case, authors proposed an optimal control setting defined by a centralised control that might be used with set-point intervals between few minutes and one day ahead. This type of active distribution network operations planning highly relies not only on the communication infrastructure, but also on the accuracy of the forecasted data required to determine the control actions. In this sense, probabilistic and forecasting tools may help to reduce this uncertainty (Bessa, Trindade, Monteiro, & Miranda, 2014; Klonari et al., 2015). Moreover, voltage control mechanisms may be also performed as ancillary services considering a market

framework as the one presented in (A. G. Madureira & Peças Lopes, 2012), where the market settlement is performed using an OPF formulation. In (Ziadi et al., 2014) a methodology for voltage control with OLTC and PV inverters is presented, where the devices are adjusted considering voltage references with one-day schedule. The forecast error was considered in the performance of the voltage control, so a re-planning of the voltage references was introduced to mitigate this effect.

In (Idlbi et al., 2013) and (Stetz et al., 2014) authors compared from a technical and economic points of view different voltage control strategies in MV and LV networks, respectively. They used MATLAB® and MATPOWER to run power flow simulations for the different voltage control mechanisms and then compared the investment, operation and maintenance costs of each solution. The results for the case of MV networks showed that central control can be much more interesting than grid reinforcement from an economic point of view, and even than local control in scenarios with large amount of DG. In the LV case the authors concluded that the combination of voltage dependent active and reactive power control mechanisms provide the highest benefits. Authors also showed that distribution transformers with autonomously controlled OLTC may be economically effective in the long term despite their higher investment and maintenance costs. Finally, they analysed the economic effectiveness of a centralised control for network loss reduction calculating the optimal reactive power of PV inverters and OLTC set values. They found that the resulting reduction of energy losses was very low so a specific investment in this control strategy for this objective would not be economically efficient, but in case the required infrastructures were already deployed an additional benefit could be obtained.

From the literature review of voltage control strategies it can be concluded that centralised voltage control through OLTC and PV inverters is a promising control mechanism to economically mitigate voltage violations due to high PV penetration levels. However, none of the previous references analyse the value of the information in such application in terms of forecast accuracy or set-point timing, so this is another gap found in this review.

## 1.4. International experiences on Smart Grids performance

The Steering Committee for Innovation in Smart Grid Measurement Science and Standards stated that appropriate metrics are not currently available for evaluating the performance of the smart grid (NIST, 2013). They highlighted that these metrics should be quantifiable and useful to drive operations and planning decisions. Moreover, the European

Commission in one of their latest reports concluded that there is a need for a methodological approach to estimate the costs and benefits of Smart Grids, based as much as possible on data from smart grid pilot projects (European Commission, 2013b). With these aims in view, a number of smart grid pilot projects have been developed. A non-exclusive list of projects that cover the key topics identified in the previous analysis is presented below.

InovGrid: EDP's umbrella project for smart grids. It presents an answer to several challenges, including: the need for increased energy efficiency; the pressure to reduce costs and increase operational efficiency; the integration of a large share of dispersed generation; the integration of electric vehicles and the desire to empower customers and support the development of new energy services (Gouveia et al., 2015). The Joint Research Center (JRC) of the European Commission has recognized the unique positioning of project InovGrid by choosing it as the single case study on which to base the development of its "Guidelines for Conducting a Cost-Benefit Analysis of Smart Grid Projects" (JRC, 2012a), which was then applied to the specific case of smart meter metering deployment in (JRC, 2012b). Additionally, InovGrid was the first national project receiving the Core Label by the European Electricity Grid Initiative (EEGI).

INCREASE: It focuses on how to manage renewable energy sources in LV and MV networks, to provide ancillary services (towards DSO, but also TSOs), in particular voltage control and the provision of reserve. It also investigates the regulatory framework, grid code structure and market mechanisms for DER, and proposes adjustments to facilitate successful provisioning of ancillary services that are necessary for the operation of the electricity grid, including flexible market products.

SINGULAR: The Smart and Sustainable Insular Electricity Grids Under Large-Scale Renewable Integration project investigates the effects of large-scale integration of renewables and demand-side management on the planning and operation of insular electricity grids, proposing efficient measures, solutions and tools towards the development of a sustainable and smart grid.

RESERVICES: The Economic grid support from variable renewables project was the first study to investigate wind and solar based grid support services at EU level. It has provided technical and economic guidelines and recommendations for the design of a European market for ancillary services, as well as for future network codes within the Third Liberalisation Package.

ADDRESS: The Active Distribution network with full integration of Demand and distributed energy RESourceS project is targeted to enable the Active Demand in the context of the smart grids, or in other words, the active participation of small and commercial consumers in power system markets and provision of services to the different power system participants.

KIC-ASS: The goal of the Knowledge and Innovation Community – Active Sub Stations project is to bring research institutes and industry together to develop key cost efficient components for future smart secondary substations, thus contributing to improved distribution network operation through better distribution network monitoring technologies.

I3RES: The ICT-based intelligent management of integrated RES for the smart grid optimal operation project develops the I3RES Management Tool, which is an ICT system designed to balance energy production and consumption in an optimized, controlled and secure way in power networks with massive distributed and renewable sources. It is made up of the following elements: A monitoring infrastructure that integrates information from multiple sensors and legacy systems in the grid. Algorithms for forecasting, state estimation and optimisation that assist DSOs in the management of the network. Data mining and artificial intelligence tools for aggregators to analyse demand, generate tariffs dynamically and send demand response signals to its customers.

UPGRID: Real proven solutions to enable active demand and distributed generation flexible integration, through a fully controllable low voltage and medium voltage distribution grid. UPGRID project focuses on addressing the constraints and needs arisen from poor observability of LV grid, local accumulation of distributed generation, risks and difficulties in managing the distribution network, aging infrastructure and social and environmental restrictions that inhibit the grid development. To be successful, UPGRID proposes an open, standardised and integral improvement of the LV grid. UPGRID has objectives in three interrelated areas: technical, economic and social. In the technical area it is aimed at developing tools to operate the LV grid, improving LV power system observability and integrating active demand in the LV Network Management System. From an economic point of view the project explores the increase of LV infrastructure capabilities and resulting boost of value provided by DSO to the Electrical System and the development of new LV products & services (manufacturers & ICT providers). Finally, its social objective is focused on the creation of conscious behaviour of efficient electrical energy use by consumer and the improvement of the service provided to consumers (better restoration time, more accurate info, etc…)

MEREGIO: It targeted an ICT integration in all parts of the energy value chain in order to meet the demand for efficient, yet decentralised energy systems. In order to establish the system, the physical level had to be connected to the market level. MeRegio sought to trial the integration of energy consumers and the integration of DER in the market to induce an increase in energy efficiency. The primarily rural regions around Göppingen and Freiamt/Eppingen appeared to be suitable for the project’s goal and were chosen as test sites, since a large array of

decentralised generation unit had already been connected to the local distribution grids and in fact, served to trial future scenario that might be relevant for other regions in Germany and Europe.

E-DEMA: aimed at designing ICT-based solutions enabling the intelligent utilisation of all resources at the model region's disposal. Additionally, the project targeted the optimisation as well as the integration of the energy system starting from generation to storage, up to the distribution of electricity leading to an efficient final consumption through new services based on metering data and energy management services.

SUSTAINABLE: The smart distribution system operation for maximizing the integration of renewable generation project develops the SUSTAINABLE concept. It is based on the cloud principle, where the distribution system operator collects data from smart metering infrastructure and other distributed sensors, and communications from external partners, market operators, and maintenance staff; transforms data into information using tools such as distribution state-estimation, prediction tools, data mining, risk management and decision-making applications; communicates settings to power quality mitigation devices, protection relays and actuators, distribution components and distributed flexible resources; and assesses its market strategy as a provider of ancillary services and balancing services (Matos & Messias, 2013).

DISCERN: The Distributed Intelligence for Cost-Effective and Reliable Distribution Network Operation project utilizes the experience of major European DSOs with innovative and efficient distribution network monitoring technologies to provide best-practise system solutions. Based on the recommendation from DISCERN, DSOs can implement solutions that have been tested and validated in various countries and circumstances. The complementary nature of the demonstration sites with regard to the specific challenges as well as technological and operational solutions serve as the main resource of DISCERN.

GRID4EU: a large-scale demonstration project of advanced smart grids solutions with wide replication and scalability potential for Europe. Grid4EU consists of six demonstrators tested over a period of four years. The emphasis is on fostering complementarity between these projects, and on promoting transversal research and sharing results between the different DSOs involved. The project is led by six European DSOs (one per demo) covering more than 50% of the electricity supply in Europe: CEZ Distribuce (Czech Republic), Enel Distribuzione (Italy), ERDF (France), Iberdrola Distribucion (Spain), RWE (Germany) and Vattenfall Eldistribution (Sweden).

IGREENGRID: The core of IGREENGRID is to share knowledge and promote the best practices identifying potential solutions for the effective integration of DRES in the six existing Demo Projects in LV and MV grids participating to the project and validating them via simulation in other environments to assess the scalability and replicability at EU level.

INTEGRIS: proposes the development of a novel and flexible ICT infrastructure based on a hybrid Power Line Communication-wireless integrated communications system able to completely and efficiently fulfil the communications requirements foreseen for the Smart Electricity Networks of the future. This includes encompassing applications such as monitoring, operation, customer integration, voltage control, quality of service control, control of DER and asset management and can enable a variety of improved power system operations, some of which are to be implemented in field trials that must proof the validity of the developed ICT infrastructure (Selga, Zaballos, & Navarro, 2013; Agustin Zaballos, Vallejo, & Selga, 2011).

The main characteristics of analysed projects are summarized in Table 1-2. From this analysis it can be concluded that almost all the projects take into account MV and LV networks, and AMR and VC applications. Despite all projects presented a technical analysis, approximately half of them developed an economic assessment and just one third were also focused on the analysis of the communication performance.

**Table 1-2 Main characteristics of analysed Smart Grid projects**

| | Voltage level | | Application | | | | Assessment | | |
|---|---|---|---|---|---|---|---|---|---|
| | MV | LV | AMR | FT | DSM | VC | TEC | ECO | COM |
| INOVGRID | X | X | X | X | X | X | X | X | |
| INCREASE | X | X | | | | X | X | X | |
| SINGULAR | X | X | X | X | X | X | X | | |
| METER-ON | | X | X | | | | X | | |
| RESERVICES | X | X | | | | X | X | X | |
| ADDRESS | | X | X | X | X | | X | | X |
| KIC-ASS | X | X | X | | | X | X | X | |
| I3RES | X | X | X | X | X | X | X | | |
| UPGRID | X | X | X | X | X | X | X | X | X |
| MEREGIO | X | X | X | X | X | X | X | | |
| E-DEMA | | X | X | | X | | X | | X |
| SUSTAINABLE | X | X | X | X | | X | X | X | X |
| DISCERN | X | X | X | | X | X | X | X | X |
| GRID4EU | X | X | X | X | X | X | X | X | |
| IGREENGRID | X | X | X | | X | X | X | X | |
| INTEGRIS | X | X | X | | X | X | X | | X |

*TEC: Technical; ECO: Economic; COM: Communications*

## 1.5. Scope and objectives of the thesis

From the previous analysis it can be concluded that the first step to achieve the potential advantages of the Smart Grid is the successful design and implementation of a reliable, secure and cost-effective communication infrastructure (Ho et al., 2013). Nevertheless, to date there are no sufficiently comprehensive engineering models that can cope with the higher level of complexity of future electric grids (Ribeiro, 2012). This is because the existing planning methodologies and computational tools were not designed to handle the new challenges introduced by these new technologies (IEEE Power and Energy Magazine, 2011). For this reason there is a critical need for research, development, and demonstration of Smart Grid systems, which will modernize the design, planning, and operation of future power system networks (Kolhe, 2012). At the present time there is no existing standardized communication infrastructure which has been widely accepted and used to transform the current electrical power grid into a smart grid. So, defining the services, requirements and architecture of the communication infrastructure of the power system, besides proper and optimal design techniques for such a network, are live research subjects in this field.

From the applications point of view, AMI and DG management have been analysed in many publications given their important role in the power system and their current degree of deployment. However, the number of different alternatives to handle the efficient integration of AMI and DG through advanced monitoring and control mechanisms suggests that further research on these issues is required, especially related to the design of their required communication infrastructures. Among all the communication technologies, the most interesting one for the DSO seems to be PLC since it uses power lines as communication channel. And among all PLC protocols, according to their specifications and previous studies, PRIME seems to provide the best performance under favourable conditions. However, since the topology and characteristics of the network considerably affects the actual performance, the first step of any deployment should be its assessment under real implementation conditions to ensure an effective two-way communication. Gathering information from smart meters is crucial to improve the observability of current power systems, and sending information to the control devices is critical to maintain reliability and quality of supply. Furthermore, the amount and accuracy of information are two important aspects for an efficient system operation, which affect the benefits that may be provided by the smart grid applications. These issues are especially interesting for AMR, voltage control and forecasting functionalities, which are closely related to AMI and DG technologies.

Thus, the main objective of this PhD is to assess the performance of PLC for smart metering and control applications to provide practical conclusions that can help their effective deployment, as well as to understand the impact of information and communication in a voltage control application.

The specific objectives that will be covered in the PhD are the following:

1. Define a methodology to assess the communication performance of PLC-PRIME to identify the most critical parameters.
2. Analyse the communication performance of PLC-PRIME in real LV and MV distribution network topologies to obtain more practical conclusions.
3. Assess the value of information and communication on a voltage control application from a technical and economic point of view.

## 1.6. Outline of the document

The thesis is divided in four chapters to address the specific objectives defined before. As a result of this research work, four articles have been produced. At the time of writing this document, three of them have been already published in JRC impact factor journals, and one is under review.

Chapter 2 presents the developed methodology to assess the communication performance of PLC for a smart metering application, explaining the details of the communication channel and network behaviour. In this chapter, the main parameters from the topological design of distribution networks that may affect to the communications are analysed to identify the most critical ones.

Chapter 3 adapts and extends the previous methodology for the application to real distribution network topologies. To do so, a method to model the PLC channel taking into account the characteristics of these networks is used to analyse different LV and MV networks, obtained from real data as well as from a large-scale distribution network planning tool.

Chapter 4 describes the assessment of the value of information for a centralised voltage control functionality. In this chapter the impact of forecast accuracy and set-point timing are analysed in two real distribution networks used in a smart grid pilot project. A future scenario with large amount of DG is considered to better show these effects.

Chapter 5 summarizes the main conclusions provided in each chapter as well as general conclusions derived from the PhD, and provides a set of open issues for further research. Finally, this chapter includes a list of all published papers and attended conferences related to this thesis.

Appendix A details the methodology used to obtain representative networks with the large-scale distribution network planning tool used in Chapter 3. Appendix B presents the statistics of the results obtained in the simulations performed in Chapter 2. Appendix C includes the network data of the LV and MV networks used in Chapter 3. Appendix D shows the attenuation matrix for the LV network case. Appendix E summarizes the KPIs obtained in Chapter 4.

# Chapter 2: Methodology for Performance Analysis of Power Line Communications

## 2.1. **Introduction**

The development of smart grids involves the integration of Information and Communications Technologies (ICT) in the electric power system, where Advanced Metering Infrastructures (AMI) represents one of the first and most important outcomes of this change of paradigm (Depuru et al., 2011). Thanks to AMI, every single costumer may get detailed information of their energy consumption and enjoy new services to improve energy efficiency. Furthermore, Distribution System Operators (DSOs) may count on a higher level of network observability, so the system operation may be improved through the adoption of new monitoring and control strategies (Canale et al., 2013; Hashmi, Hänninen, & Mäki, 2011).

In Chapter 1, Power Line Communications (PLC) was identified as one of the most widespread technologies for AMI, especially in Europe, where massive smart meters roll-outs are being deployed based on PLC. However, the communication performance of this technology is highly affected by the network topology, which may jeopardize its effectiveness when low latencies like the ones presented in Table 1-1 are required. Among the typical PLC standards used for AMI, the specifications defined by PRIME provide the highest data rates, so an upper bound for PLC performance can be obtained with this technology. PRIME is a consolidated and worldwide narrowband PLC standard for smart metering, monitoring and control applications ("PRIME Alliance," 2016), but in order to avoid future problems and minimize deployment and operation costs, the performance of this technology should be analysed in advance considering the local implementation conditions. As concluded in the literature review carried out in the previous chapter, the simulation framework developed in (Matanza, 2013) represents a cutting-edge tool that allows assessing the communication performance of PLC PRIME networks taking into account both physical and network behaviour aspects. Nevertheless, a room for improvement was found in previous studies with this framework, where a thorough analysis of the critical parameters that affect to the communication performance of this technology was missing.

Then, the aim of this chapter is to present a methodology to analyse the critical parameters that affect the performance of PLC communication networks used for smart grids, specifically for Automatic Meter Reading (AMR) applications using PRIME standard. The methodology is based

on the assessment of two Key Performance Indicators (KPIs) related to the stability of the nodes and the latency of the smart meters readings. Simulation scenarios are defined considering critical design parameters of distribution networks, which take into account the number and length of distribution feeders, as well as the number of buildings and smart meters at each feeder. Although these networks have been created synthetically, the values of these parameters are chosen to model representative networks topologies to provide more practical results. After the definition of the initial scenarios, a sensitivity analysis is presented to show the impact of each individual parameter in the communication performance. This chapter is divided as follows. First an introduction of the simulation framework is included and the performance assessment methodology is described, with special focus on the selected KPIs. Then, a set of base case studies are presented. Finally, the results of the performance of the case studies and their sensitivities are analysed and the main conclusions are summarized.

## 2.2. Simulation framework

The simulation framework used to develop the performance assessment methodology presented in this chapter was developed in (Matanza, 2013). The objective of this tool is to simulate the network behaviour of all the communication nodes connected to a PLC network taking into account the effects of the physical channel. Figure 2-1 presents the architecture of this framework, where it can be seen that the effects of the physical communication channel are implemented in Matlab, whereas the characteristics of the network behaviour are implemented in the OMNeT++ event simulator.

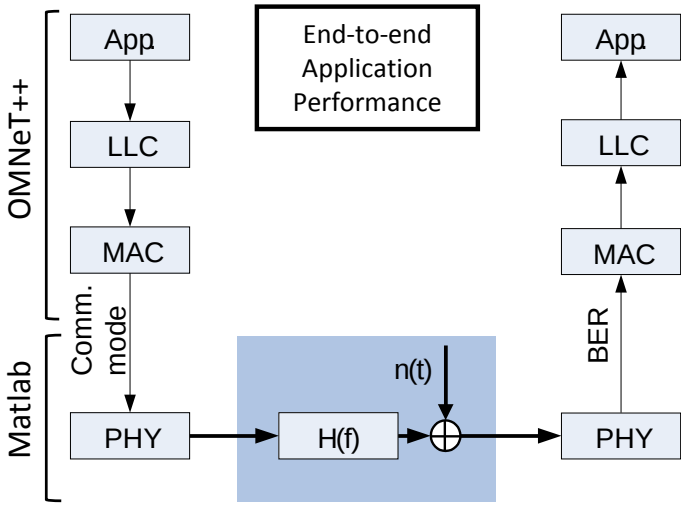


**Figure 2-1 Architecture of the simulation framework used for the analysis**

The communication nodes are modeled considering the implementation of the application layer protocol DLMS/COSEM to encapsulate data related to energy consumption of each device, and the PRIME standard to transmit this information through the electric distribution network.

PRIME defines a protocol for the Logical Link Control (LLC), Media Access Control (MAC) and the Physical (PHY) layers. The LLC layer controls the logical connections between the communication nodes, since PRIME is a connection-oriented protocol. The MAC layer is responsible for managing the access to the communication channel, since the PLC channel is shared by all the nodes connected to the network. Finally, the PHY layer is in charge of modulating the digital data so that the transmission errors are minimized.

Table 2-1 shows the communication modes used by PRIME, each one of them with different level of robustness to disturbances in the channel. In order to increase the robustness, a lower-order constellation can be used when modulating the digital information. The terms DBPSK, DQPSK and D8PSK stand for Differential Binary/Quaternary/8 Phase Shift Keying and represent differential phase modulations with 2, 4 and 8 symbols respectively. The higher the number of symbols, the more sensitive the transmission is to noise but the higher data rates are achieved; and vice-versa. This robustness can be increased by the use of Forward Error Correction (FEC) techniques, where the basic principle is that the transmitter inserts redundant information in the message. The receiver uses this extra payload to try to correct the errors that might have occurred during the transmission. A clear drawback of this technique is the decrement of effective data rate, as shown in Table 2-1.

**Table 2-1 Communication modes used by PRIME**

| **Mode** | **FEC-ON** | **FEC-OFF** |
|---|---|---|
| DBPSK | 21.4 kbps | 42.9 kbps |
| DQPSK | 42.9 kbps | 85.7 kbps |
| D8PSK | 64.3 kbps | 128.6 kbps |

PRIME also defines two types of nodes in the communication network: the base node and the service node.

- Base node: the node responsible for managing the communication with the rest of the nodes. It is located in the data concentrator installed in a secondary substation.
- Service node: the node that establishes the communication with the base node. They are located in the smart meters installed in the consumer dwelling.

PRIME networks follow a master-slave communication protocol, where the base node plays the role of master and communicates with all the service nodes, which behave as slaves. Additionally, service nodes may operate in three different functional states: disconnected, terminal and switch.

- Disconnected: the service node has not been registered by the base node and is not able to transmit information.
- Terminal: the service node is registered and communications with the base node can be performed.
- Switch: the service node is able to retransmit information, enabling the communication between nodes that otherwise would not be able to communicate because of high attenuation or noise problems.

The communication channel is usually modelled considering two main characteristics: the transfer function and the noise sources.

The transfer function provides the attenuation between the transmitted signal and the received signal in the channel, which can be obtained through empirical (top-down) or analytical (bottom-up) methods (Domingo, Alexandres, & Rodriguez-Morcillo, 2011). A bottom-up approach commonly used in previous references to assess the transfer function is based on a Single-Input-Single-Output (SISO) multi-conductor transmission line (MTL) model (T. Banwell & Galli, 2005; Lazaropoulos & Cottis, 2009). However, recent studies have proposed the use of a Multiple-Input-Multiple-Output (MIMO) channel (Versolatto & Tonello, 2011), or even hybrid approaches to include the goodness of both models (Cañete, Cortés, Díez, & Entrambasaguas, 2011). Since all approaches seem to provide a good agreement between simulated and measured values in previous publications, the simulation framework uses an MTL-SISO model for simplification reasons. Further details on the computation of PLC transfer functions will be presented in the next chapter to apply this methodology in more complex network configurations.

The effect of the noise sources on communications is the increase of the transmission errors. PLC networks usually present two types of noises: background noise and impulsive noise. In this simulation framework, both types of noise are considered, following the models proposed in (O.G. Hooijen, 1998) for the background noise and in (Middleton, 1972) for the impulsive noise.

The Middleton model is defined by two main parameters: the impulsive index A, which models the number of impulses during the interference time, and the Gaussian-to-impulsive ratio

Γ, which models the amplitude of these impulses. In (Kural & Şafak, 2002) authors reported measurements for impulsive noise sources in narrowband PLC networks that have a mean duration of 34.95μs and mean inter-arrival time of 237ms. As explained in (Ferreira, Lampe, Newbury, & Swart, 2010), the impulsive index A for Middleton noise is computed as the product of the average number of impulses per unit time and the mean duration of the emitted impulses entering the receiver. The value $A=1.47\cdot10^{-4}$ can be obtained by applying this definition to the previous data sample, as it is shown in Eq. (2.1).

With respect to the background-to-impulsive ratio, as presented in Eq. (2.2) a value of Γ= 0.1 is selected to produce an impulsive noise of roughly 50 dB more powerful than the background noise, according to maximum levels reported in previous references (Ferreira et al., 2010; Nassar, Gulati, Mortazavi, & Evans, 2011).

$$A = \frac{1}{t_{IAT}} \cdot t_w = \frac{1}{237ms} \cdot 35\mu s = 1.47 \cdot 10^{-4} \tag{2.1}$$

$$\sigma_1^2 = \sigma_g^2 \cdot \frac{1}{\Gamma \cdot A} + \sigma_g^2 \equiv 10 \cdot log_{10}\left(\frac{1}{0.1 \cdot 1.47 \cdot 10^{-4}} + 1\right) = 48.3\ dBx \tag{2.2}$$

The disturbance caused by the attenuation and the presence of noise is typically modelled by the Bit Error Rate (BER) parameter, which is defined by the number of bits that are mistakenly received divided by the total number of bits that are transmitted. This parameter is computed in Matlab considering the communication channel conditions, which include the attenuation H(f) and noise n(t) parameters shown in Figure 2-1. Additionally, the BER is used by OMNeT++ to represent the hypothetical errors in the communication. Thanks to this approach, both logical and physical effects are considered simultaneously in this simulation framework, which provides more realistic results for the performance analysis defined in the next section.

## 2.3. **Performance analysis**

The developed methodology for PLC performance analysis is based on two KPIs:

- Number of smart meters registered by the base node at each instant of time, which provides information about the stability of the network and the availability of the nodes.
- Time required to read all the smart meters at each round carried out by the base node, which provides information about the latency of the communication process.

Thanks to these KPIs, the operating limits of PLC for Smart Metering applications can be assessed. The fundamentals to assess both KPIs are explained in the next subsections.

### 2.3.1. Registration process

The registration process begins when a service node correctly receives one beacon from the base node. The success of this delivery depends on the Packet Error Rate (PER), which can be obtained from the BER according to Eq. (2.3) considering the number of bits of the packet (*Nbits*).

$$PER = 1 - (1 - BER)^{Nbits} \tag{2.3}$$

For the analytical implementation, a random number between 0 and 1 can be generated, and in case that it is below the value of PER, this packet is considered lost. To maximize the probability of success and according to PRIME, the registration process is performed with the most robust communication mode (DBPSK FEC-ON). The BER can be assessed from the Signal to Noise Ratio (SNR) through empirical curves like the ones shown in Figure 2-2 that relate the BER and the SNR for each communication mode considering impulsive noise (Matanza et al., 2014).

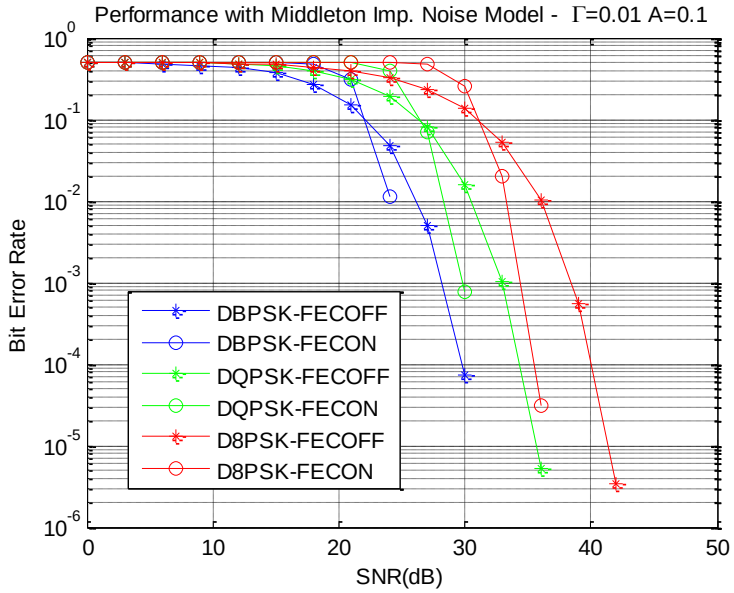


**Figure 2-2 Performance of PRIME communication modes with impulsive noise** (Matanza, 2013)

An estimation of the SNR can be obtained with Eq. (2.4), where $P_{Tx}$ is the transmitting power, $L$ is the attenuation between the transmitter and the receiver, and $P_{Noise}$ is the channel noise power introduced by the noise sources, all in decibels.

$$SNR = P_{Tx} - L - P_{Noise} \tag{2.4}$$

Then, the process to assess whether a packet is correctly delivered results as follows:

1. Calculate the SNR for the noise and attenuation of the channel.
2. Estimate the BER for the corresponding SNR and communication mode.
3. Evaluate the PER for that BER taking into account the size of the received message.

Thanks to this procedure, both BER and PER are calculated every time a message is received and their computation is specific for a given pair of transmitting and receiving nodes, which leads to a more realistic modelling. For example, considering a transmitting power ($P_{Tx}$) of -3 dBm, which is the maximum power defined in PRIME standard, and assuming a channel attenuation ($L$) of 7 dB and a noise power ($P_{Noise}$) of -50 dBm, the SNR would be 40 dB according to Eq. (2.4). Then, it can be seen in Figure 2-2 that a BER of $10^{-4}$ can be achieved with D8PSK FEC-OFF, which is the fastest communication mode as indicated in Table 2-1. Finally, assuming that a 200 Bytes message is sent between these two nodes under these conditions, the PER for the received message taking into account Eq. (2.3) would be 14.79%, which means that approximately 15 messages out of 100 would not be correctly received.

In Figure 2-3 the process to register one node is illustrated. After receiving the beacon, the service node sends a registration request (REG.req). This packet, as the rest of the conversation, can be sent directly to the base node or re-sent through intermediate switches. After this, the base node sends a registration response (REG.res) to allow the service node to connect to the network. Finally, the service node confirms the reception sending a registration acknowledgement (REG.ack).

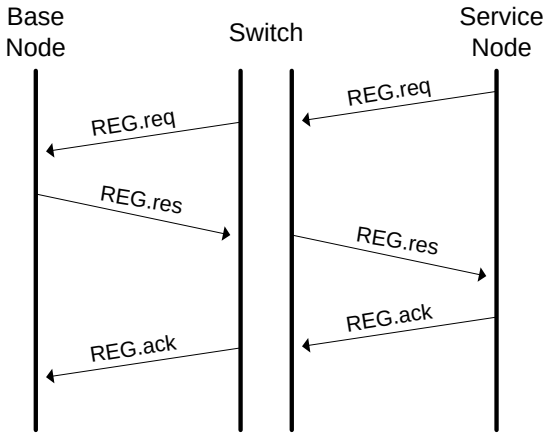


**Figure 2-3 Registration process dialog**

Additionally, in case that a service node does not receive any beacon in a certain time, the promotion process is initiated to try to register it by setting the state of a service node between the disconnected node and the base node to the switch state, so that it can successfully retransmit the required information. In this process, the disconnected node sends a promotion needed signal and all the service nodes that receive this message send a promotion request to the base node, including the information related to the quality of the received promotion needed message. Finally, the base node may accept the promotion of the service node that receives the promotion needed with the highest quality. However, PRIME does not specify the criteria to promote a service node to a switch node, so other assumptions can be also considered.

### 2.3.2. **Reading process**

When the registration process is finished properly, the data from all nodes can be gathered through the reading process. Figure 2-4 shows the process to read one meter, where the actions related to the DLMS/COSEM and PRIME protocols have been differentiated. The reading process starts when the base node sends a request to get the data from one meter (GET.req). Then, the connection establishment (EST) is performed according to PRIME protocol to ensure that the information can be transmitted properly. After this, the instruction to get the data (DAT) is sent to the service node, and then the reading is sent back to the base node.

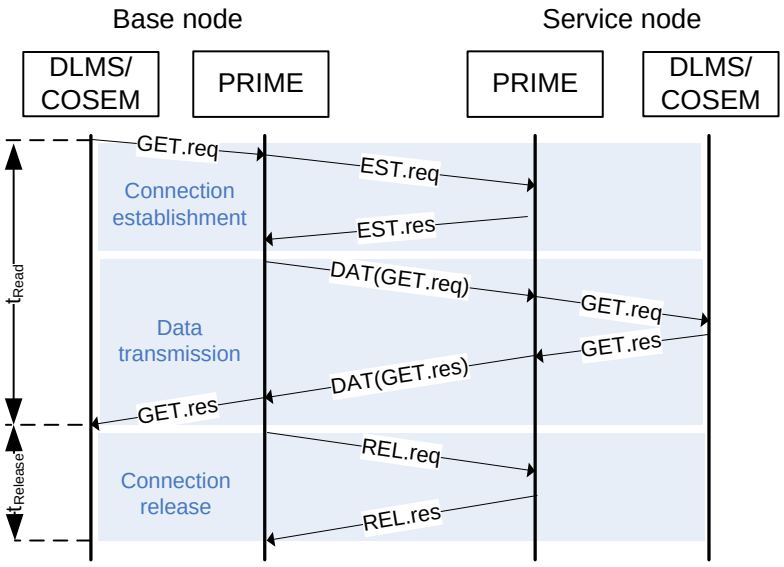


**Figure 2-4 Reading process dialog**

According to the previous description, the time required to read a meter ($t_{Read}$) can be obtained with Eq. (2.5). After a data transmission is finished, the connection needs to be released (REL), and the corresponding time ($t_{Release}$) can be computed using Eq. (2.6). In these

expressions, *BL* stands for the length of the messages in *bits*, and *BR* for the bitrate in *bps*. As in the registration process, the establishment and release control messages use DBPSK with FEC, whereas data is transmitted using the most convenient communication mode to optimize robustness and transmission speed. In addition to this, PRIME uses Carrier Sense Multiple Access with Collision Avoidance (CSMA/CA) as a medium access technique. In order to minimize collisions in the channel, PRIME nodes wait for a random amount of time before transmitting data in the channel. The statistics of this time period are defined in the standard and depend on the channel congestion and on the priority of the packets. Then, the term $t_{CSMA}$ is added in expressions (2.5) and (2.6) as many times as the corresponding number of channel accesses in each stage of the process (EST, DAT and REL). Finally, the overall time required to read *N* meters ($t_{ReadAll}$) in a communication network could be obtained with Eq. (2.7).

$$t_{Read} = \frac{BL_{EST.req} + BL_{EST.res}}{BR_{EST}} + \frac{BL_{DAT.req} + BL_{DAT.res}}{BR_{DAT_i}} + 2 \cdot t_{CSMA\_EST} + 2 \cdot t_{CSMA\_DAT} \quad (2.5)$$

$$t_{Release} = \frac{BL_{REL.req} + BL_{REL.res}}{BR_{REL}} + 2 \cdot t_{CSMA\_REL} \quad (2.6)$$

$$t_{ReadAll} = \sum_{i \in N} t_{Read_i} + (N-1) \cdot t_{Release} \quad (2.7)$$

As example, the time to read all meters in a simple network with just one meter (*N*=1) is now presented. The size of the application messages are defined to 132 Bytes for the application request ($BL_{DAT.req}$) and 200 Bytes for the application response ($BL_{DAT.res}$), considering standard practices in the industry, whereas the size of the establishment request and response messages ($BL_{EST.req}$, $BL_{EST.res}$), are defined by PRIME to 176 and 128 bits, respectively. Regarding the CSMA algorithm, a level 2 priority is defined for the control packets $\left(t_{CSMA_{EST}}, t_{CSMA_{REL}}\right)$ and a level 5 priority for the data packets ($t_{CSMA_{DAT}}$), which leads to 17.6ms and 88.4ms for their average values, respectively. Evaluating Eq. (2.7) with the transmission rates of DBPSK FEC-ON for the connection establishment and D8PSK FEC-OFF for the data transmission, the theoretical roundtrip latency is 246.9ms, as shown in Eq. (2.8):

$$t_{ReadAll} = \frac{176 + 128}{21.4} + \frac{132 \cdot 8 + 200 \cdot 8}{128.6} + 2 \cdot 17.6 + 2 \cdot 88.4 = 246.9\, ms \quad (2.8)$$

The same network was analysed in the simulation framework to contrast this result, from which 160,000 roundtrip latencies were obtained. The results are shown in Figure 2-5 in the form

of a box plot, where the central mark represents the median, the edges of the box correspond to the 25 and 75 percentiles, the whiskers extend to the most extreme data points not considered outliers, and the individual crosses represent the outliers. In this case, results have an average value of 251.1ms, which is 1.7% higher than the result obtained in Eq. (2.8).

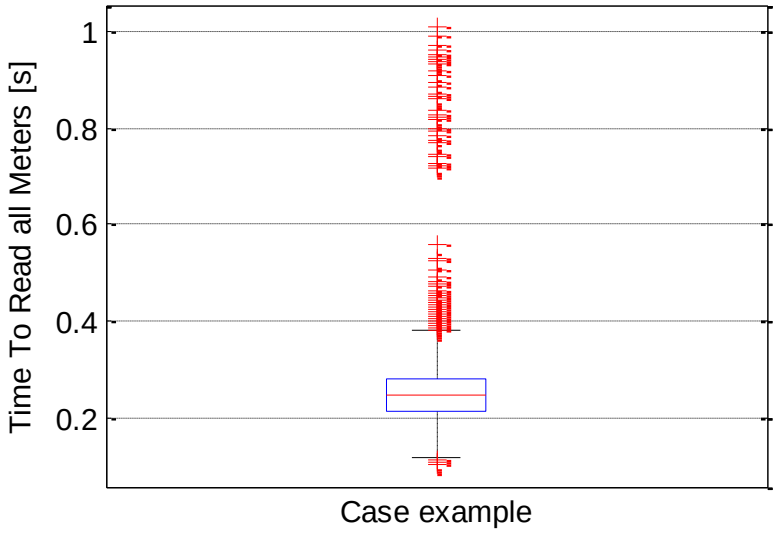


**Figure 2-5 Time to read all meters in a case example with one meter**

From the previous comparison, two ideas may be pointed out. First, it can be concluded that the simulation framework is reliable, since the results obtained analytically are very similar to the average values obtained through the simulations. And second, one might think that the simulation framework is not necessary, precisely for the same reason. However, it must be noted that in the analytical approach there are a number of effects that have been neglected. According to PRIME, nodes are not allowed to transmit on any time instant but only on certain periods. These periods are called Shared Contention Period (SCP). The rest of the time is used to transmit network management messages. Besides, the CSMA procedure used in all nodes to access the channel also adds randomness to the computation. Furthermore, there are other asynchronous events such as the transmission of beacon messages, which make the mathematical approach more complex.

Then, since the simulation framework takes into account all these concepts, the results are more realistic and the dispersion and statistics of the expected communication performance can be obtained as shown in Figure 2-5, which represents an additional contribution of this approach. Additionally, as indicated in (Matanza et al., 2014), a linear increase in the number of smart meters does not necessarily involve a linear increase in the time to read them because the communication channel is shared by all the service nodes, and the network behaviour is more

complex in networks larger than the simple test case used in the previous example with just two nodes. Thus, the differences between the analytical and the simulated approaches would be higher in these cases.

Nevertheless, the communication performance may not be only affected by the number of nodes. For this reason, in the next sections the communication performance of PLC is analysed with the simulation framework considering the impact of different parameters that are characteristic from distribution networks to determine the most critical ones.

## 2.4. Case Studies

A set of case studies are presented to analyse their communication performance based on the KPIs introduced in the previous section related to the registration and reading processes. In Figure 2-6 the typical configuration of a LV network is shown, where the main parameters that characterize the case studies are included. Every case study is made up of a MV/LV transformer substation (base node) and a set of customers with smart meters (service nodes), connected through a certain number of LV feeders (branches). Additionally, every group of customers represents a building. With the combination and variation of these parameters, four case studies aimed to be representative of distribution network configurations were created, keeping the number of service nodes per group uniform within the same case study. The characteristics of each case study are summarized in Table 2-2.

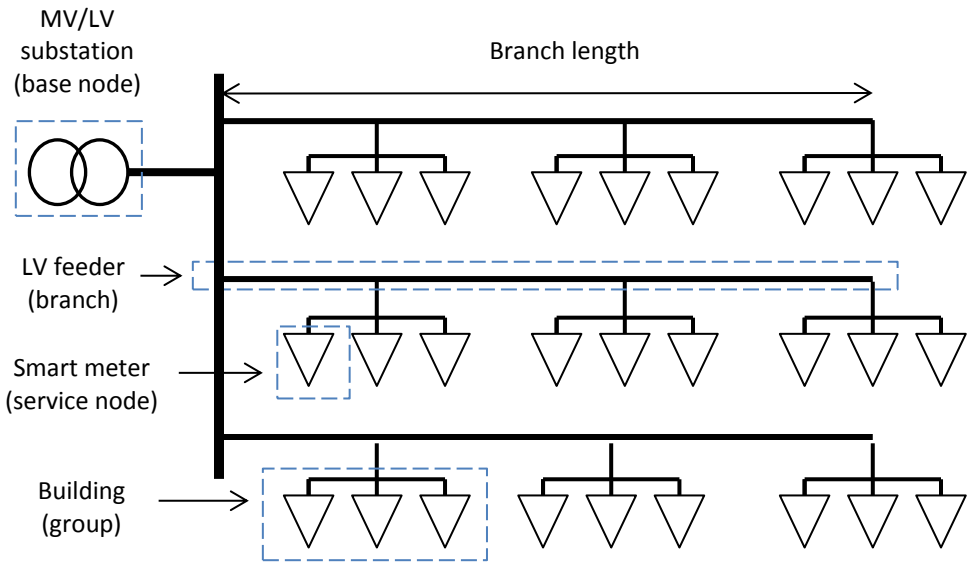


**Figure 2-6 Configuration of an urban LV network to represent the case studies**

**Table 2-2 Case studies characteristics**

| | Case U-L | Case U-M | Case U-S | Case U-XS |
|---|---|---|---|---|
| User density | High | Medium | Low | Very low |
| Branch length (m) | 100 | 200 | 300 | 400 |
| Number of total users | 252 | 198 | 144 | 108 |
| Number of branches | 3 | 6 | 6 | 9 |
| Number of users per branch | 84 | 33 | 24 | 12 |
| Number of groups per branch | 3 | 3 | 6 | 6 |
| Number of users per group | 28 | 11 | 4 | 2 |

The parameters of the case studies are chosen to represent high, medium, low and very low values of user density. These are based on typical data for electricity grids in the European Union, so the conclusions may be applicable to different types of regions (Alberto Sendin et al., 2014). Case U-L corresponds to an urban area with large buildings and Case U-M to one with medium size buildings, whereas Case U-S and Case U-XS represent residential areas with small houses of four and two homes per building, respectively. It can be noted that cases with higher user density present higher number of users ($N$), shorter branches, as well as lower number of branches and groups per branch, which were the topology parameters used to configure their distribution. The data required to model the parameters of the cables were obtained from the NAVY150SE and NAVY50SE models described in (Lampe & Vinck, 2011) and used in (Matanza et al., 2014).

For each case study, a simulation process representing 5,000 seconds is carried out, where the first 3,000 seconds (50 minutes) are used exclusively for the registration of the service nodes, and the remaining 2,000 seconds (33 minutes) are devoted to collect the smart meter readings using the same data sizes of the analytical example described in Section 2.3.2. In case the registration process is finished properly, the reading process is started and continues in an iterative way until the end of the simulation. Otherwise, the registration process is extended, so the reading process is only performed if all the service nodes are correctly registered. Additionally, to take into account the randomness related to communications channel factors such as the noise and the CSMA procedure, each scenario has been simulated 20 times with different seeds for the generation of the random numbers. Finally, the communication performance of each case study is presented according to the results obtained for the two selected KPIs: the number of smart meters registered by the base node at each instant of time, and the time required to read all the smart meters at each round carried out by the base node.

Figure 2-7 shows the number of registered nodes in the four case studies for the first 4,000 seconds of simulation, where an instance from the 20 simulations has been selected for each scenario. It can be seen that in the four cases all nodes are registered in less than 3,000 seconds, so this threshold represents a conservative amount of time to finish the registration process for these cases. Cases U-S and U-XS present some instability problems that cause the disconnection of few nodes for a certain time. Thus, the stability is not only affected by the number of nodes, but also by the topology and characteristics of the network.

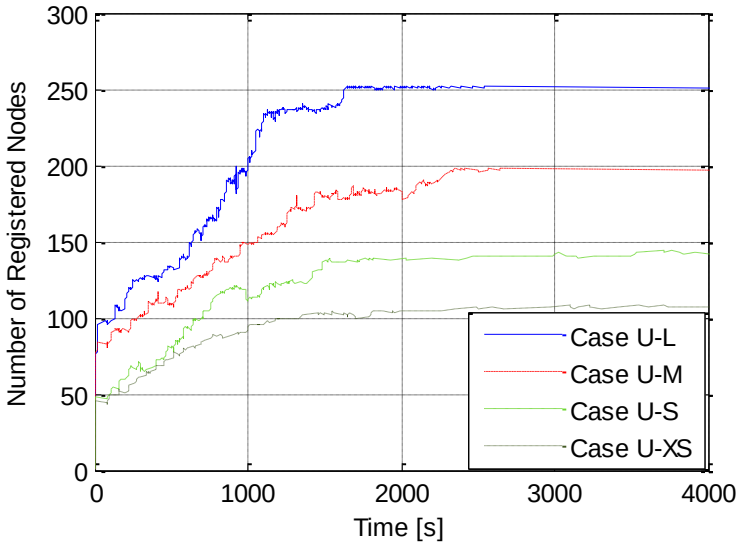


**Figure 2-7 Evolution of registered nodes in the analysed case studies**

In Figure 2-7 three different stages can be identified. The first stage presents a very steep slope where a high number of service nodes are registered very fast. Then, in the second stage the evolution of the registered nodes presents several steps until the total number of service nodes is reached. Generally, every step with a new increase of registered nodes indicates the promotion of one service node from the terminal state to the switch state to extend the transmission range, enabling new nodes to be correctly registered. Finally, the third stage shows a horizontal line that represents a stable behaviour of the network where all the service nodes remain registered unless instability problems appear. For instance, Case U-L registers almost 100 smart meters in the first 15 seconds of simulation, which represents the first stage. Then, the number of registrations increases more gradually until simulation reaches 1,645 seconds, when all the smart meters are registered for the first time. Finally, the number of registered nodes is kept close to 252 until the end of the simulation, eventually oscillating between 250 and 252 because of instability problems with two service nodes. This is mainly due to collisions in the medium or channel congestion, as it also happens in reality.

With regard to the reading process, Figure 2-8 shows the box plot of the time to read all nodes in the four cases, where it can be seen that the minimum reading time for case U-L is approximately 600 seconds (10 minutes), whereas in the other cases the time required is normally below this value. Additionally, the case studies with higher user density show higher reading times and more dispersion in the results, although the outliers of case studies with lower user density can surpass the average values obtained by the previous ones. The main reason for these outliers is that the network conditions cause continuous registration and deregistration of certain nodes as explained before. These situations introduce delays in the process of gathering all the measurements that can be extended for long periods if the nodes are not able to register properly.

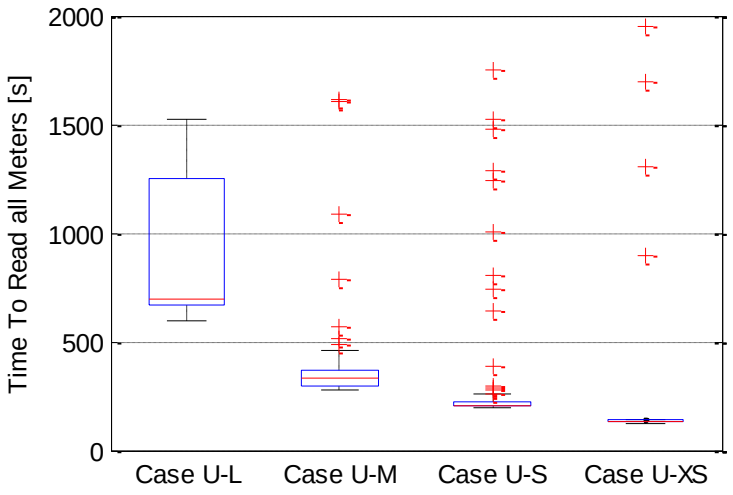


**Figure 2-8 Time to read all meters in the analysed case studies**

Comparing both figures, it can be concluded that a shorter registration process does not necessary involve shorter reading times, as it happens between Case U-L and U-M. This means that certain network topologies like Case U-M may be more challenging in terms of registration but then present a better communication performance. However, instability problems related to frequent deregistration of nodes can seriously affect this performance, as it can be seen with the outliers of Case U-S and Case U-XS. Therefore, user density can be used as a first indicator of the communication performance that can be expected in the network, where higher density networks generally present more demanding traffic management conditions, and networks with higher dispersion of users are more likely to show registration problems focused on specific nodes.

## 2.5. Sensitivity Analysis

Since the previous results are affected by the differences between the design parameters of each case study, a sensitivity analysis is carried out to assess the impact of the variation of specific parameters of the network. For each original network, a different sensitivity analysis with one of the following topology parameters is performed: branch length, number of total users, number of groups per branch and number of branches. Table 2-3 shows the sensitivity parameter for each case study and the values used for the sensitivity scenarios. In this section the results of these sensitivities for the defined KPIs are presented, and a summary can be found in Appendix B.

**Table 2-3 Sensitivity analysis scenarios**

| | **Case U-L** | **Case U-M** | **Case U-S** | **Case U-XS** |
|---|---|---|---|---|
| **Sensitivity parameter** | **Branch length (m)** | **Number of total users** | **Number of groups** | **Number of branches** |
| Scenario 1 | (*) 100 | 108 | 3 | 1 |
| Scenario 2 | 200 | 144 | (*) 6 | 3 |
| Scenario 3 | 300 | (*) 198 | 9 | 6 |
| Scenario 4 | 400 | 252 | 12 | (*) 9 |

*(*) represents the scenario for the original case study of Table 2-2*

### 2.5.1. Branch length

Case U-L is chosen to assess the effect of the branch length in the performance of the communication network. Thus, the four scenarios maintain identical structure but present more distance between groups. In Figure 2-9 it can be seen that the registration process takes more time when the branch length is higher. Furthermore, in the scenario with 400m the time for the registration process exceeds the 3,000s threshold due to the disconnection of a significant number of nodes, so this reference cannot be set as an upper limit for all cases, although it works for most.

Figure 2-10 shows the results of the metering process. A linear trend can be observed for the median values related to this parameter, which can be approximated by the following expression as a function of the branch length ($l$): $t_{ReadAll} = 353.6 + 3.3 \cdot l$. In general, branches with longer distances exhibit higher attenuations (Papadopoulos et al., 2013). Notice that in the 200m scenario the median already surpasses the threshold of 900 seconds (15 minutes), which is a time interval commonly used for smart metering (Bari, Jiang, Saad, & Jaekel, 2014; Claessen & La Poutré, 2014). Nevertheless, the base case chosen for this sensitivity (Case U-L) presents the highest number of users, so the effect of the branch length in this network has a bigger impact.

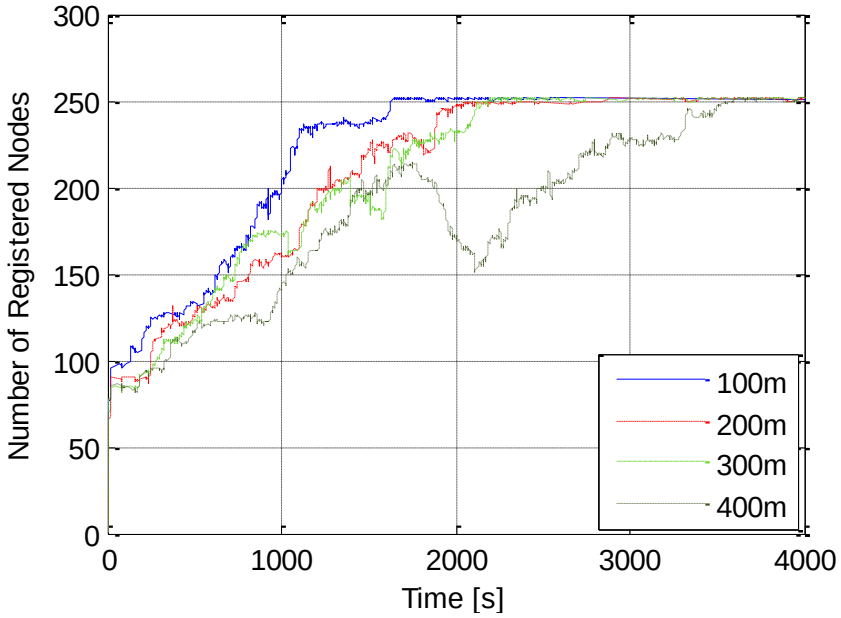


**Figure 2-9 Evolution of registered nodes in Case U-L varying the branch length**

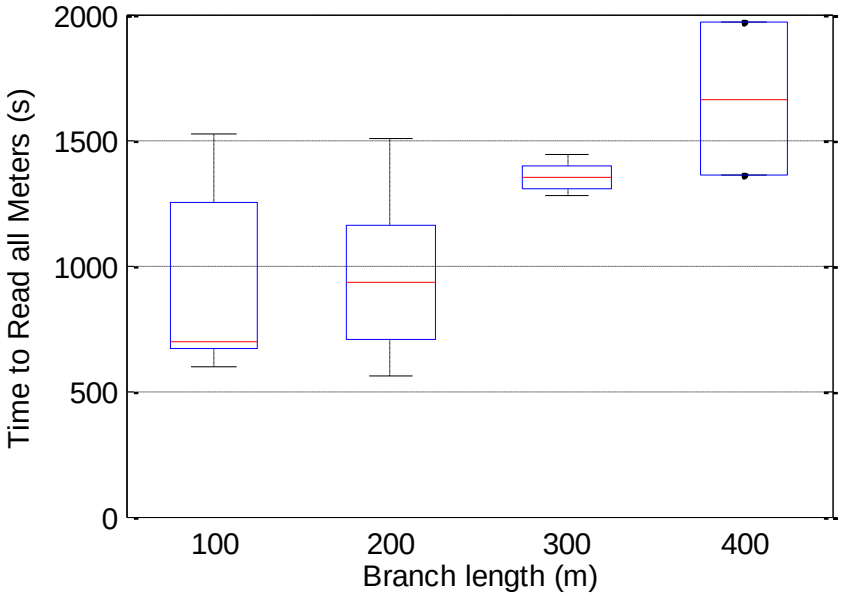


**Figure 2-10 Time to read all meters in Case U-L varying the branch length**

### 2.5.2. **Number of total users**

The sensitivity to the number of total users is analysed in Case U-M. Figure 2-11 shows that in the four scenarios all service nodes are registered in less than 3,000 seconds, but in the scenario with 252 users there is a slight instability that makes the registration process longer and involves adding new switches to the network. The sudden disconnection of a group of nodes is related to the disconnection of a switch, which causes the disconnection of all the service nodes that were connected to it. These results highlight the importance of the criterion to choose the promotion of the service nodes. The algorithm to choose the most favourable switch used in this simulation framework is described in (Alonso et al., 2014).

Figure 2-12 shows the results for the reading time, where it can be seen that this parameter has a high impact in the communication performance. Moreover, the scenario with the highest number of users shows a time to read all meters much higher than the other cases, which is aligned with the conclusions derived from Figure 2-11. On the contrary, in the scenarios with 108 or 144 users, the time to read all nodes is always lower than 5 minutes (300 seconds). Indeed, the results of the median values for the four cases can be approximated by the following polynomial: $t_{ReadAll} = 0.0013 \cdot N^3 - 0.5638 \cdot N^2 + 80.7190 \cdot N - 3.7293 \cdot 10^3$. These results are also coherent with conclusions from previous studies of the physical layer, where the addition of new loads is shown as an important factor of attenuation increase (Papadopoulos et al., 2013).

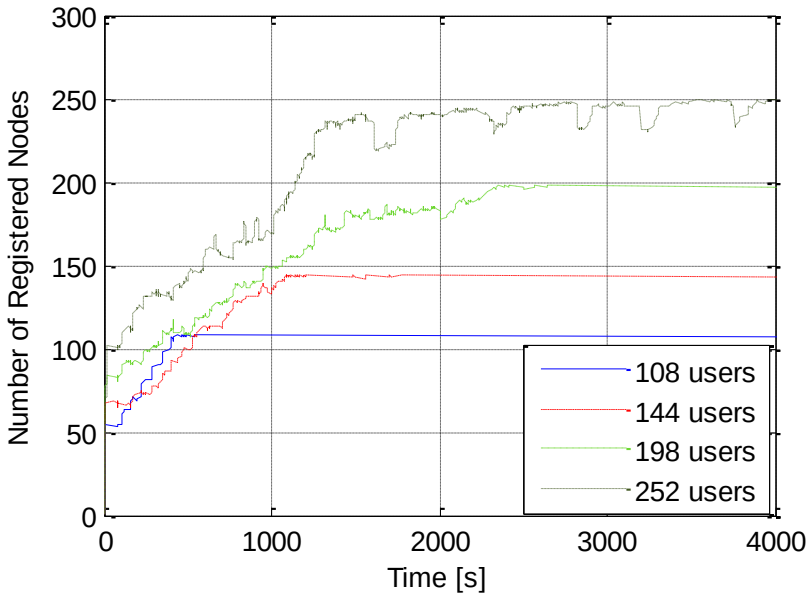


**Figure 2-11 Evolution of registered nodes in Case U-M varying the number of total users**

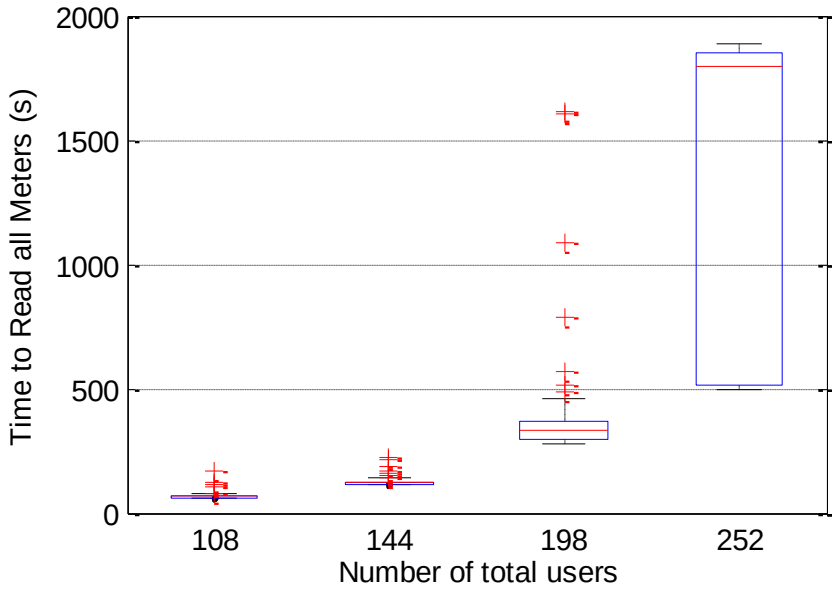


**Figure 2-12 Time to read all meters in Case U-M varying the number of users**

### 2.5.3. Number of groups

The variation in the number of groups is studied in Case U-S. This time the four scenarios have the same total number of users (144) and branch length (300m), and only the spatial distribution of groups along the 6 branches is affected. Thus, as indicated in Table 2-4, Scenario 1 has 3 groups of 8 users, Scenario 2 has 6 groups of 4 users, Scenario 3 has 6 groups of 3 users and 3 groups of 2 users, and Scenario 4 has 12 groups of 2 users.

**Table 2-4 Number of groups and users per group in the sensitivities of Case U-S**

| | Scenario 1 | Scenario 2 | Scenario 3 | Scenario 4 |
|---|---|---|---|---|
| Number of groups | 3 | 6 | Type A: 6<br>Type B: 3 | 12 |
| Number of users per group | 8 | 4 | Type A: 3<br>Type B: 2 | 2 |

Figure 2-13 shows a similar behaviour for all scenarios except for the one with 6 groups, where the registration process is quite instable and presents several disconnections before all nodes are registered. Figure 2-14 shows the effect of this instability in the highest time for the reading process and in the amount of outliers.

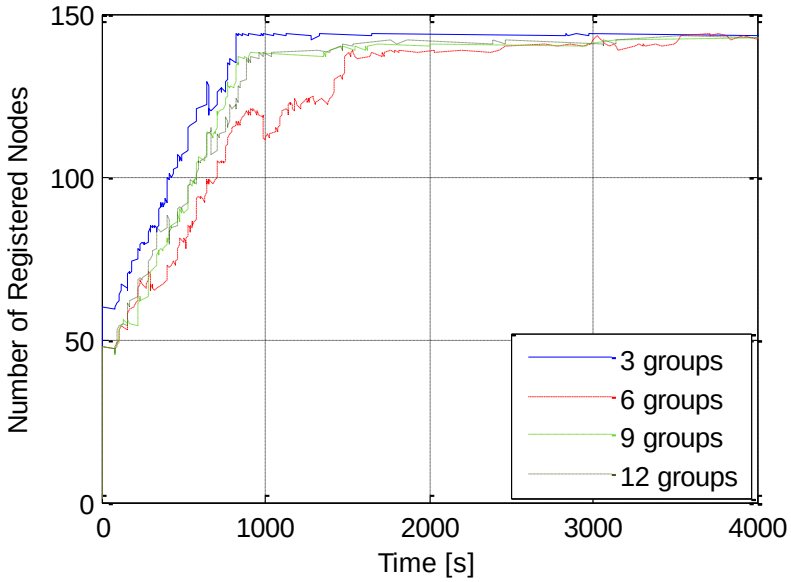


**Figure 2-13 Evolution of registered nodes in Case U-S varying the number of groups**

Nevertheless, in this case the variation of the number of groups does not have a significant impact in the reading process since the four scenarios present in average terms very similar results, although a maximum might be found between the scenarios with 3 and 9 groups. This means that for the same number of users, scenarios with lower user dispersion along the feeder favour the communication performance. This can be due to high user concentration in the groups (scenario 1), or high group concentration in the feeders (scenario 4).

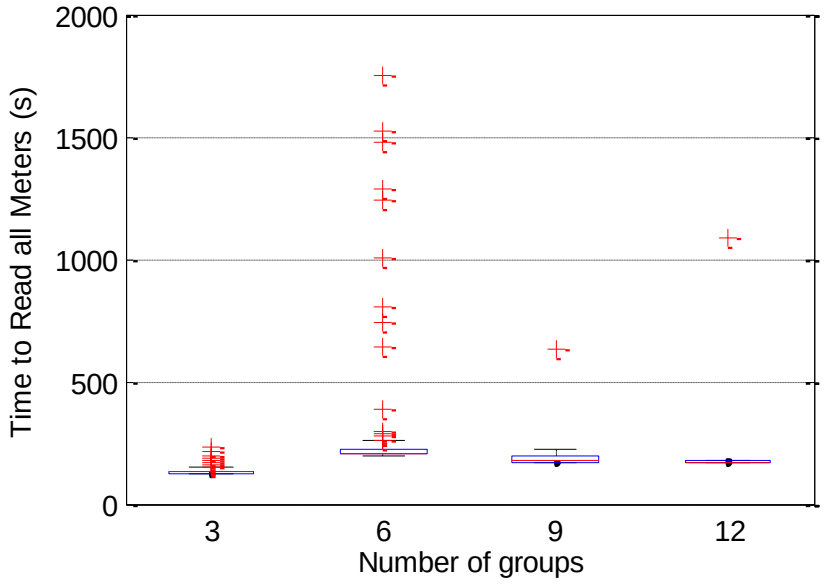


**Figure 2-14 Time to read all meters in Case U-S varying the number of groups**

### 2.5.4. Number of branches

Finally, the sensitivity to the number of branches is assessed in Case U-XS. The total number of users is left invariant to 108, so the scenarios with less branches have more users per branch, but the number of groups is also set to 6. Therefore, scenarios with 1, 3, 6 and 9 branches have 108, 36, 18, and 12 users per branch, and 18, 6, 3 and 2 users per group, respectively, as it is indicated in Table 2-5.

**Table 2-5 Number of branches and users per branch and group in the sensitivities of Case U-XS**

| | Scenario 1 | Scenario 2 | Scenario 3 | Scenario 4 |
|---|---|---|---|---|
| Number of branches | 1 | 3 | 6 | 9 |
| Number of users per branch | 108 | 36 | 18 | 12 |
| Number of users per group | 18 | 6 | 3 | 2 |

In this case, the registration process depicted in Figure 2-15 shows an interesting feature, where the scenarios with lower number of branches present less registered nodes in the first stage of the process, but then the process is finished in less time.

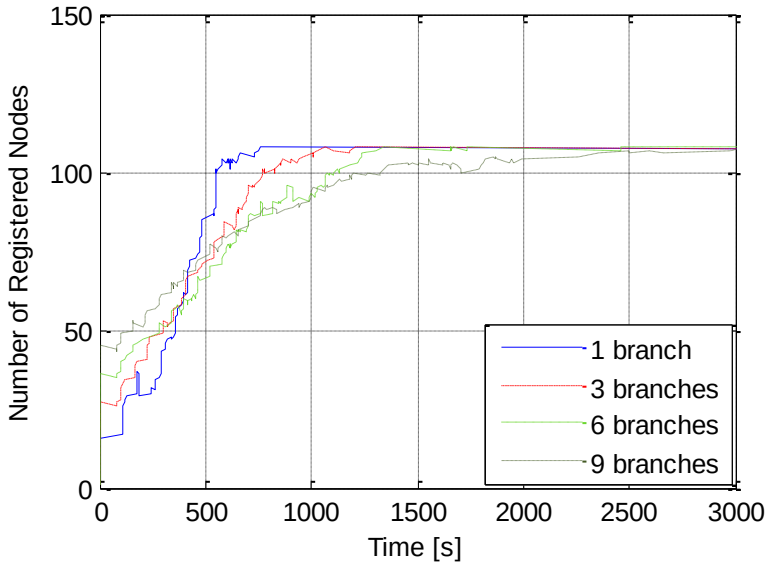


**Figure 2-15 Evolution of registered nodes in Case U-XS varying the number of branches**

However, in Figure 2-16 the scenario with 1 branch is the one with the highest reading time, which indicates that faster registration processes does not necessary involve faster reading times, as it was already commented at the end of Section 2.4 when the original case studies were compared. In this case, when all nodes are located in the same branch the logical connection is

simpler since the amount of service nodes that can be connected through a switch is higher, but then the network can be more congested because of worse traffic conditions. Finally, as in the sensitivity for the number of groups, the variation of this parameter does not show a big impact in the communication performance, although for the analysed configurations a minimum value for the reading time was found between scenarios with 3 and 9 branches.

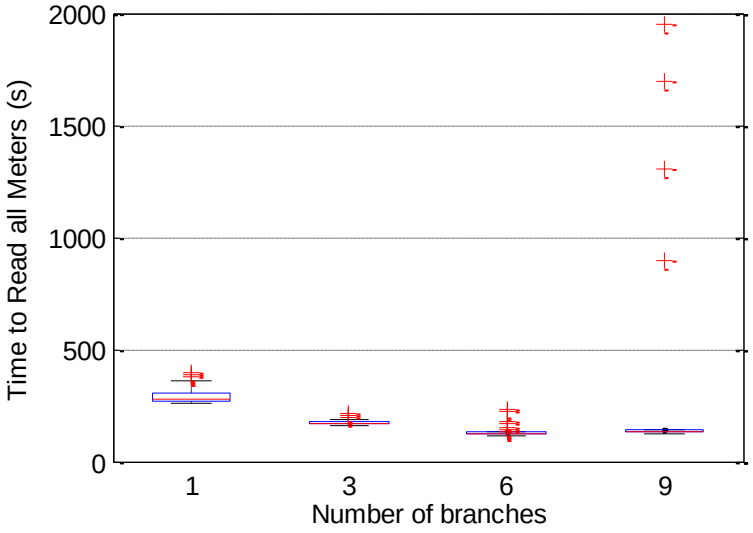


**Figure 2-16 Time to read all meters in Case U-XS varying the number of branches**

## 2.6. Conclusions

This chapter has presented a novel methodology to assess the performance of Power Line Communications (PLC) networks based on PRIME standard. The simulation framework used for the application of this methodology has proved to be a very useful tool to determine the impact of different parameters that vary from one network to another. Additionally, the Key Performance Indicators (KPIs) used in the analysis have provided practical insights to understand the network behaviour of these networks. From the results of the simulations, it can be concluded that the registration process takes an important role in the communication performance, where the time to complete this process is not as important as the stability of the network. This is because the registration of the nodes is an essential requirement to proceed with the reading tasks properly, and in certain scenarios the base node is not able to maintain all the service nodes correctly registered. In most cases where the registration process was performed correctly, the reading time was usually lower than 15 minutes, which is a typical reference value used for smart metering scenarios. However, in the scenarios with the highest number of users (252) this threshold was

normally exceeded. Conversely, in networks where user density was not very high, results indicated that PLC-PRIME was able to read all meters in less than 5 minutes.

With regard to the sensitivities of the topology parameters, it has been concluded that the parameters that affect the most are the total number of service nodes (smart meters) and the branch (feeder) length. For both of them, it has been shown that when these parameters increase, the time to read all meters also increases, but more steeply in the case of the number of users. However, the influence of the number of groups and the number of branches is not so obvious. In the former, a maximum value for the reading time was found between scenarios with 3 and 9 groups, which means that network topologies with lower dispersion present scenarios more favourable for the communication. In the latter, a minimum value was found between the scenarios with 3 and 9 branches, where a trade-off between logical connection and traffic congestion was identified.

All the aforementioned conclusions may be of great interest for the deployment of smart metering applications that are built on the communications infrastructure as well as for their replication to different types of networks. In this sense, the results provided by this study can be used as a first estimation of whether PLC-PRIME can be used or not in a certain network with similar characteristics like the analysed case studies. However, this study was limited to topologies with simple radial configurations, but the presented methodology can be extended to more realistic networks with more complex topologies and larger size. The adaptation and application of this methodology to real network topologies is presented in the next chapter.

# Chapter 3: Power Line Communications Performance in Real Distribution Networks

## 3.1. Introduction

Despite Power Line Communications (PLC) is considered the most cost-effective solution for certain smart grids applications, the reutilization of the electric infrastructure as communication channel makes local network conditions to highly affect the communication performance of this technology. This idea was proved in Chapter 2, where the impact of different topology parameters was analysed in simple network configurations. The main limitation found in the simulation framework used for that study is that the computation of the channel transfer function is only focused on specific network topologies where all service nodes have to be connected to a main feeder, which is a fair simplification but it is not generally applicable to real networks. Then, the aim of this chapter is to adapt the methodology presented in the previous chapter to real distribution networks to present practical results that can be useful for the deployment of PLC technologies.

Traditionally, transmission-line theory has been widely used to carry out analytical studies of PLC networks to compute the channel transfer function, which provides the attenuation between the transmitted and the received signal (Banwell & Galli, 2001; Durbak & Stewart, 1990; Olaf G. Hooijen, 1998). These concepts have still been applied in more recent studies (Duche & Gogate, 2014; Korki, Vu, Foh, Lu, & Hosseinzadeh, 2011; Zaw, Kyaw, & Ye, 2013), which demonstrates the validity of these techniques and the interest for this research topic in the transition to the smart grid. Nevertheless, none of the analysed previous work has applied these analytical methods to real network topologies, but rather they have analysed simple use cases and small configurations. For instance, in (Di Bert, D'Alessandro, & Tonello, 2014) a simulation platform for PLC access networks was proposed considering the G3 protocol, where two simulators were presented: one for the physical layer implemented in Matlab, and the other for the data link and adaptation layer implemented in OMNeT++. However, the considered scenario represents a LV network with a simple tree topology like the ones presented in the previous chapter. Indeed, the channel frequency responses between pairs of nodes were obtained with a bottom-up channel generator generally applied to in-home networks (A. M. Tonello & Versolatto, 2011). In (Aalamifar, Schl, Harris, & Lampe, 2013), the authors presented a PLC channel simulator, which also used a bottom-up approach implemented in the ns-3 network simulator (an

open simulation environment similar to OMNeT++), although the presented analysis was only focused on the physical layer.

In this chapter a step-by-step methodology to systematically compute the channel transfer function between any pair of nodes in real electric power network configurations of any scale is presented. The algorithm for the transfer function computation is based on transmission-line theory and graph theory concepts. This algorithm is used to generate the signal attenuation matrix, which includes the attenuation between all the communication paths in the network. First, the PLC channel modelling is introduced and the algorithm to compute the transfer function is described. Then, the proposed methodology is applied to a LV and a MV distribution network. So, the signal attenuation matrix is obtained for these networks, and then their network behaviour is analysed in the PLC simulation framework. To extend the application of this methodology to large-scale networks, a process to identify and analyse the most critical networks in larger regions is presented, based on a large-scale distribution network planning tool. Additionally, other local conditions different from the topology parameters covered in the previous chapter are analysed in each case study. Finally, the main conclusions are presented.

## 3.2. PLC transfer function in distribution networks

Following the transmission-line theory principles, the transfer function of a two-port network describes the relationship between their voltage (*V*) and current (*I*) at its input (*1*) and output (*2*). In Figure 3-1, the PLC network is represented by a two-port network circuit that connects a source $V_s$ with impedance $Z_s$ to a receiver with an impedance $Z_n$. Although this two-port transmission line approach cannot exactly reflect all transmission modes of multi-conductor power line cables, it is very useful to provide an approximation of the transfer characteristics of PLC networks as indicated in (Lampe & Vinck, 2011).

The voltage and current transfer characteristics of the two-port network can be defined by the transmission matrix *T* with the *ABCD* parameters according to (3.1). Then, the frequency response of the channel ($H_1$) can be obtained with (3.2), whereas the access impedance ($Z_a$) is computed with (3.3). For the case of a transmission line, the *ABCD* parameters of the transmission matrix adopt the expression (3.4), where *l* represents the length of the line, $Z_0$ the characteristic impedance, and $\gamma$ the propagation constant of the line. These last two parameters can be obtained with the resistance *R'*, capacitance *C*,' inductance *L'*, and admittance *G'* per unit length of the line according to (3.5) and (3.6). Notice that there is an implicit frequency (*f*) dependency in equations (3.1) to (3.6), which in case of PRIME is between 41.992 kHz and 88.867 kHz.

The previous method to obtain the PLC transfer function can be applied to distribution networks considering their general tree structure. A simple distribution network topology can be represented by a set of nodes (*N*), lines (*L*), and impedances (*Z*) as shown in Figure 3-2.

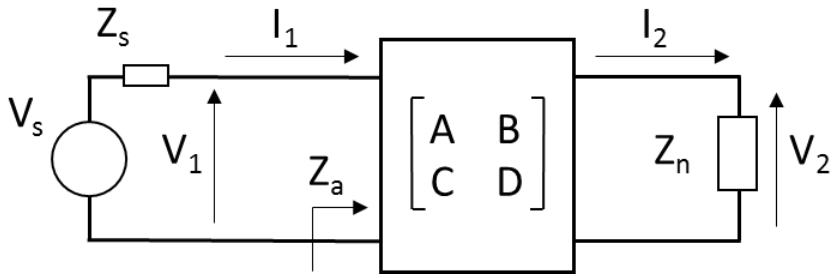


**Figure 3-1 Two-port network and equivalent model**

$$\begin{bmatrix} V_1 \\ I_1 \end{bmatrix} = T \begin{bmatrix} V_2 \\ I_2 \end{bmatrix} = \begin{bmatrix} A & B \\ C & D \end{bmatrix} \begin{bmatrix} V_2 \\ I_2 \end{bmatrix} \tag{3.1}$$

$$H_1 = \frac{V_2}{V_1} = \frac{Z_n}{A \cdot Z_n + B} \tag{3.2}$$

$$Z_a = \frac{A \cdot Z_n + B}{C \cdot Z_n + D} \tag{3.3}$$

$$T(L) = \begin{bmatrix} \cosh(\gamma \cdot L) & Z_0 \cdot \sin(\gamma \cdot L) \\ \frac{1}{Z_0} \cdot \sin(\gamma \cdot L) & \cosh(\gamma \cdot L) \end{bmatrix} \tag{3.4}$$

$$Z_0 = \sqrt{(R' + j \cdot 2 \cdot \pi \cdot f \cdot L')/(G' + j \cdot 2 \cdot \pi \cdot f \cdot C')} \tag{3.5}$$

$$\gamma = \sqrt{(R' + j \cdot 2 \cdot \pi \cdot f \cdot C') \cdot (G' + j \cdot 2 \cdot \pi \cdot f \cdot C')} \tag{3.6}$$

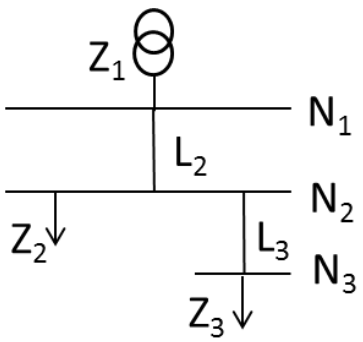


**Figure 3-2 Equivalent circuit of a distribution network topology with two lines**

In this example, the substation is connected at the beginning of the feeder, which is the source node ($N_1$) of the tree and has its own impedance ($Z_1$). This source node is connected to the node $N_2$ through the distribution line $L_2$. At this new node there is an impedance $Z_2$, and a line $L_3$, which in turn connects the previous node to node $N_3$, where the last impedance of the network is located ($Z_3$). Notice that these impedances can represent either a consumer or a supply point associated to a smart meter or any other sensor or actuator, but in this case we assume they are all loads. Distribution networks can be modelled as a series of cascade segments, so the transmission matrix of the complete channel can be obtained by multiplying the individual matrices of the different segments (Duche & Gogate, 2014). Given that, the transmission matrix $T$ from the substation to one of the loads, for instance $Z_3$, is computed following (3.7). In this equation, $T(L_2)$ and $T(L_3)$, which represent the transmission matrices of lines 2 and 3, are computed with (3.4). By contrast, $T(Z_2)$ is obtained with (3.8) as the transmission matrix of an impedance $Z$ connected in parallel to a line. Note that this $Z$ can be a single element or the access impedance of a set of elements.

$$T_{1\to3} = T(L_2) \cdot T(Z_2) \cdot T(L_3) \tag{3.7}$$

$$T(Z) = \begin{bmatrix} 1 & 0 \\ \frac{1}{Z} & 1 \end{bmatrix} \tag{3.8}$$

Based on this approach of cascade elements, a systematic process is applied to compute the PLC transfer function in distribution networks considering basic concepts of graph theory. The main idea is to define a path between the transmitter ($Tx$) and the receiver ($Rx$) to obtain the transfer function of the communication channel in between ($T_{Tx\to Rx}$). Any node of the network can act as transmitter or receiver depending on the type of communication and message that has to be sent. In a tree topology without cross edges, the communication path can be upwards or downwards. The flowchart of the downwards path is presented in Figure 3-3.

The general process starts assessing the transfer function of the transmitter connected to the main line ($T_{Tx}$). Then, the transfer function of the access impedance of the rest of the network in the opposite direction to the receiver is computed based on equations (3.3) and (3.8). Thus, the transfer function of an access impedance can be computed following a downstream ($T_{down}$) or upstream ($T_{up}$) direction. As shown in Figure 3-3, the access impedance in the former case is indicated as $Z_aD$, whereas in the latter is $Z_aU$. The equivalent impedance $Z_{eq} = (Z_1 \cdot Z_2) / (Z_1 + Z_2)$ has to be obtained when two impedances $Z_1$ and $Z_2$ are parallel connected.

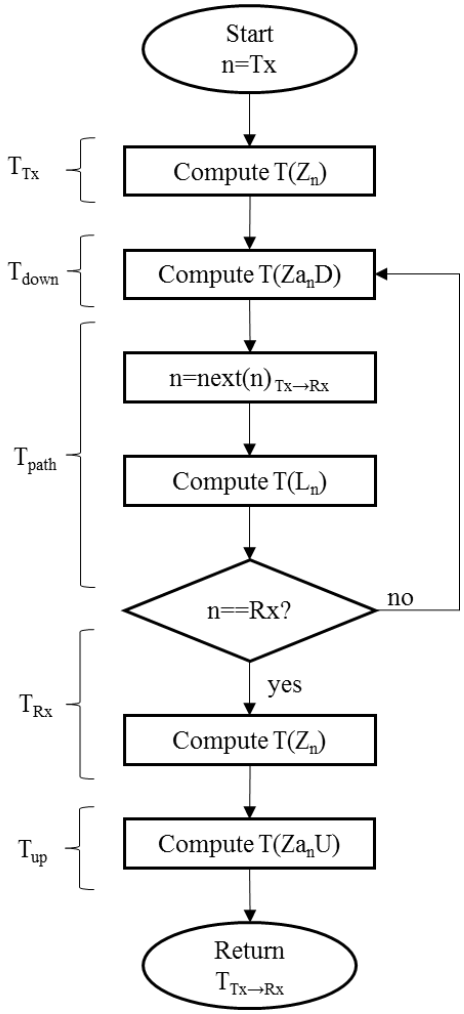


**Figure 3-3 Flowchart to obtain the transmission matrix between two nodes with an upwards path**

After this, the transfer function of the next line of the network from the transmitter to the receiver is obtained with equation (3.4), and then the access impedance of the shunt segment connected at the end of this new line with (3.3) and (3.8) again, repeating this process until the receiver is reached to complete the transfer function of the communication path ($T_{path}$). Then, the transfer function of the receiver connected to the main line is obtained ($T_{Rx}$), and then the access impedance of the rest of the network is computed, when it is applicable. Note that when the access impedance is calculated, a sub-tree may exist, so its calculation has to consider all the downstream elements, which can at the same time have new sub-trees. To identify a sub-tree, the Depth First Search (DFS) order of a set of nodes is obtained, which starts at the root and explores as far as possible along each line before backtracking (Saputro, Akkaya, & Uludag, 2012). Thus, starting a path from the last node to the source node following the reverse order of the DFS, a new sub-tree is found when the parent of the analysed node does not coincide with the immediately below number of the DFS.

Finally, the signal attenuation matrix is obtained with the transmission matrix of all the communication channels between every pair of nodes expressed in dB. For a better comprehension, an illustrative example with a basic distribution network topology is shown in Figure 3-4, for which the previous process has been applied to three different paths. The computation of their transfer functions is included in equations from (3.9) to (3.11), where the elements of $T_{Tx \to Rx}$ are identified. The index after $Z_a$ indicates the node where it is computed, and the numbers at the end show the nodes that are included in the calculation of $Z_a$.

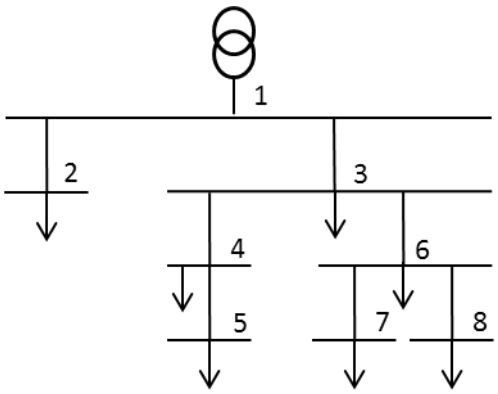


**Figure 3-4 Illustrative example for PLC transfer function computation in a distribution network**

$$T_{6\to1} = \overbrace{T(Z_6)}^{T_{Tx}} \cdot \overbrace{T(Za_6D_{7-8})}^{T_{down}} \cdot \overbrace{T(L_6)\cdot T(Za_3D_{3-4-5})\cdot T(L_3)}^{T_{path}} \cdot \overbrace{T(Z_1)}^{T_{Rx}} \cdot \overbrace{T(Za_1U_2)}^{T_{up}} \tag{3.9}$$

$$T_{1\to4} = \overbrace{T(Z_1)}^{T_{Tx}} \cdot \overbrace{T(Za_1U_2)}^{T_{up}} \cdot \overbrace{T(L_3)\cdot T(Za_3D_{3-6-7-8})\cdot T(L_4)}^{T_{path}} \cdot \overbrace{T(Z_4)}^{T_{Rx}} \cdot \overbrace{T(Za_4D_5)}^{T_{down}} \tag{3.10}$$

$$T_{4\to6} = \overbrace{T(Z_4)}^{T_{Tx}} \cdot \overbrace{T(Za_4D_5)}^{T_{down_1}} \cdot \overbrace{T(L_4)\cdot T(Za_3U_{3-2-1})\cdot T(L_6)}^{T_{path}} \cdot \overbrace{T(Z_6)}^{T_{Rx}} \cdot \overbrace{T(Za_6D_{7-8})}^{T_{down_2}} \tag{3.11}$$

The presented methodology can be used to systematically calculate the signal attenuation in any type of distribution network. Based on this formulation, it can be seen that the attenuation highly depends on the topology and the electrical characteristics of all the elements connected to these networks, which have a significant impact in the communication performance. These parameters can be easily taken into account for communication performance analysis according to geographical and technological local conditions of each network, as discussed in the next section. Additionally, to take into account the frequency dependency of equations from (3.4) to (3.6), the methodology can be repeated for different frequencies in the analysed frequency band.

## 3.3. **Case studies**

The aim of this section is to apply the previous methodology to obtain the attenuation matrix in real distribution networks, and then assess their communication performance with the simulation framework presented in Chapter 2. Two case studies are analysed, a LV network and a MV network. These networks have been used in European R&D projects like ("SUSTAINABLE project," 2016b) to test different smart grid functionalities. The parameters that characterize each network are detailed in (André Guimarães Madureira, 2010) and included in Appendix C. Additionally, the effects of other non-stationary parameters are considered in each case study. Thus, in the LV network the effect of the presence of impulsive noise is analysed, whereas in the MV network the effect of the variation of the node impedances is studied.

### 3.3.1.**LV network**

The LV distribution network is represented in Figure 3-5, which has 2.5 km and consists of a secondary substation with three LV feeders that connect 32 nodes. As it can be seen in the picture, a consumer (arrow), a DG unit (circle) or both can be located at each node. The LV feeders have different segments that present different conductors with different properties, which affect to the attenuation as shown in the previous section. The electrical parameters of each segment are taking into account in equations (3.5) and (3.6) to obtain the characteristic impedance and the propagation constant of the lines, where the admittance *G* has been neglected.

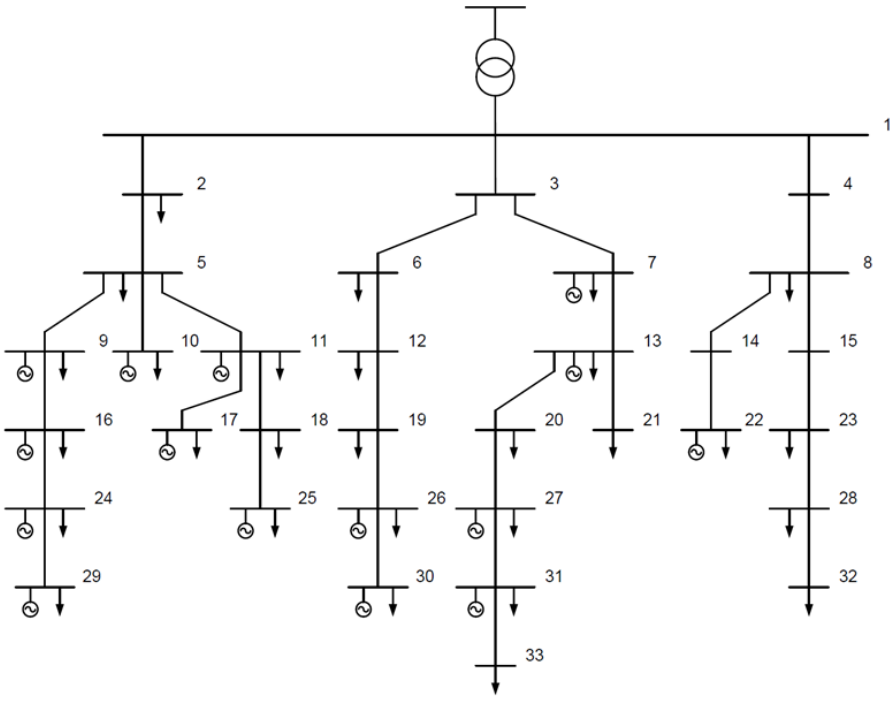


**Figure 3-5 LV distribution network**

The PLC communication network aims to communicate the sensors and actuators related to each load and generator of the network with the secondary substation, where the data concentrator is located. In order to simplify the case study, only one control device per node is considered. The impedance of the nodes is modelled considering a nominal power of 8.8 kVA to represent a LV customer, which corresponds to an equivalent impedance of 6 Ω connected in 230 V. In a real scenario the value of this impedance depends on the electrical devices connected at each time, but to avoid distorting the effects of the physical channel in the network performance, all the loads have been considered static and equal.

The signal attenuation between each pair of nodes of the LV network is shown in the attenuation matrix presented in Figure 3-6, which is computed with the process described in Section 2 considering each node as a transmitter and a receiver, where the index of each node in the matrix refers to the order of the DFS. This process was applied to 25 frequencies linearly equally spaced from 42 kHz to 89 kHz (PRIME frequency range), and results show the median value of the attenuation in dB obtained for each frequency. According to the results of this matrix and for a better illustration of the attenuation between different nodes, the attenuations for the communication paths between the base node and two service nodes located at the end of the feeders (nodes 32 and 33 from Figure 3-5) are shown in Figure 3-7.

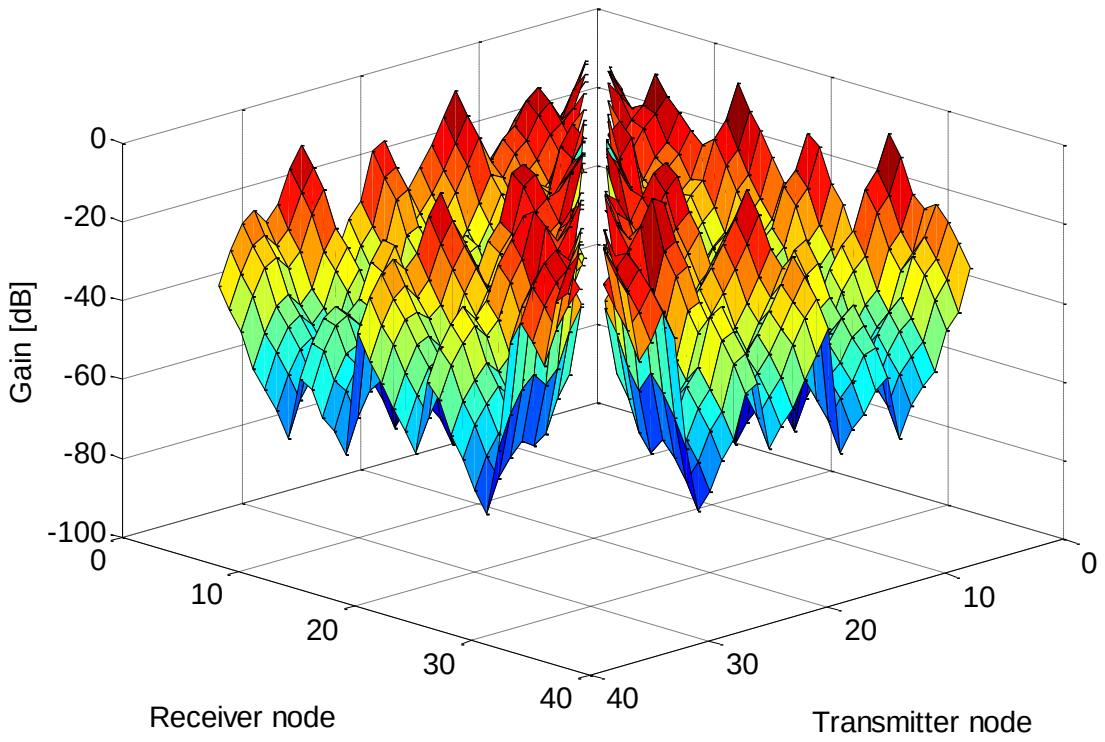


**Figure 3-6 Attenuation matrix of the LV distribution network**

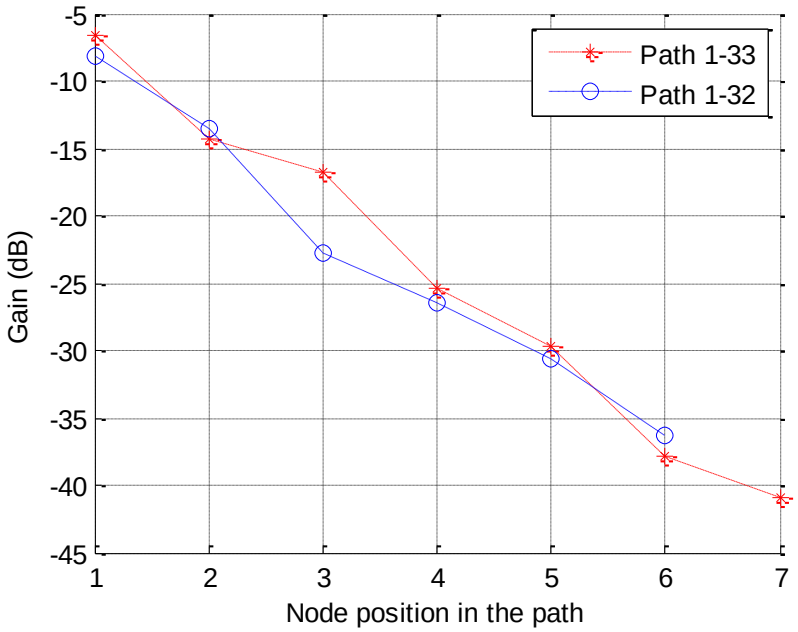


**Figure 3-7 Attenuation of two communication paths of the LV distribution network**

It can be seen that the maximum attenuation is reached for the pair of nodes representing the base node and the last service node in the path, which corresponds to 36 dB from node 1 to 32 and 41 dB from node 1 to 33. Additionally, it can be observed that neighbour nodes show attenuations between 3 and 9 dB approximately, depending on network topology. These results are in the same order of magnitude as the attenuations showed in (Aalamifar et al., 2013), where the signal attenuation between neighbour nodes in a network with similar size (1 km) and frequency band (50-100 kHz) was between 2 and 10 dB approximately. The complete values of the attenuation matrix can be found in Appendix D.

The performance of the network is assessed in the PLC simulation framework. The analysed scenario is run for 5,000 seconds of simulation, where the first 3,000 seconds are exclusively dedicated to register all the service nodes by the base node located in the secondary substation, and the next 2,000 to send messages of 200 Bytes to all the nodes in a sequential manner, repeating this process until the simulation finishes. Under these conditions, two different simulations are carried out to analyse the effect of the impulsive noise in the communication performance, which represents a big challenge for PLC in distribution networks. For this reason, several authors have proposed techniques for the cancellation of these disturbances in the communication channel (Hu, Chen, & Yin, 2014; Lin, Nassar, & Evans, 2013). In the case of the simulation framework used for this analysis, a compressed sensing technique is implemented to substantially remove the impulsive noise (Matanza, 2013).

Figure 3-8 shows the box plot of the obtained one-way latency for all nodes of the LV network, which indicates the statistics of the time that a message sent from the base node takes to reach a service node. In this case, the propagation delay is very low for all the nodes, so the differences in the topology are not very well appreciated. However, it can be noticed in the figure that the longest delays are obtained for the nodes 31 and 33. Precisely, these nodes are the ones that exhibit a higher attenuation in Figure 3-7, which lead to the need of more robust (therefore slower) communication modes. In addition to this, the outliers are produced because the network needs to synchronize during some periods, which involves occasional higher latency due to data queued on the transmitting devices.

The results of the one-way latencies from the simulation with the same impulsive noise conditions described in Section 2.2 are presented in Figure 3-9. In this figure it can be seen that the one-way latency for all nodes is higher than in the previous case due to the presence of noise, especially for those nodes that are located at the end of the feeders where the throughput has been reduced to increase error robustness. These results show the vulnerability of PRIME-PLC networks to impulsive noise sources and encourages the implementation of effective noise cancellation techniques.

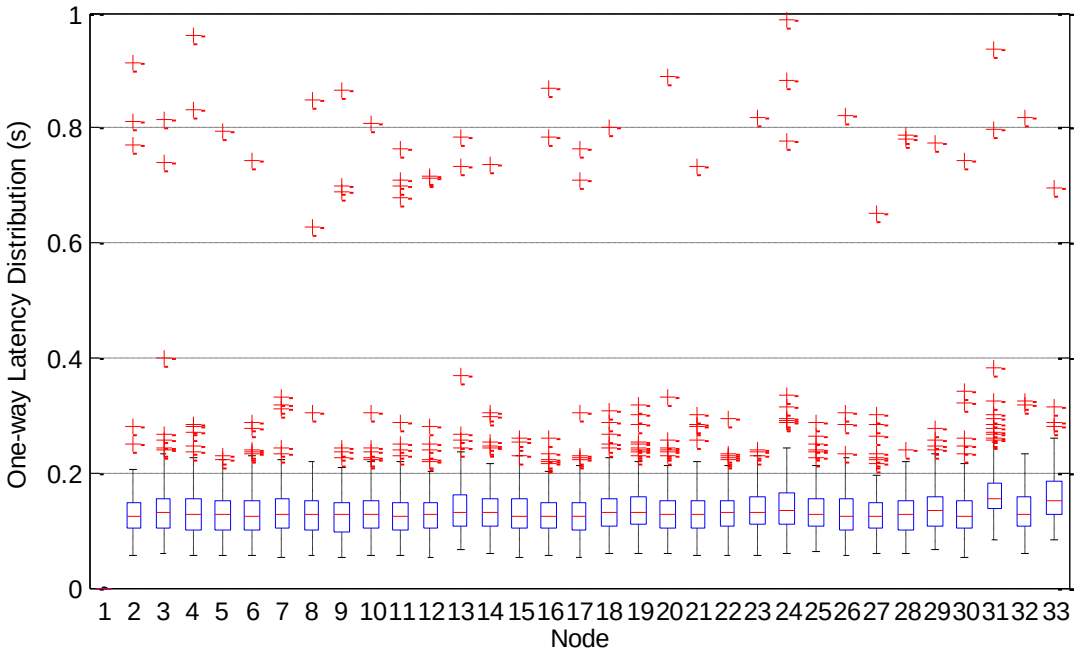


**Figure 3-8 One-way latency of the LV distribution network only with background noise**

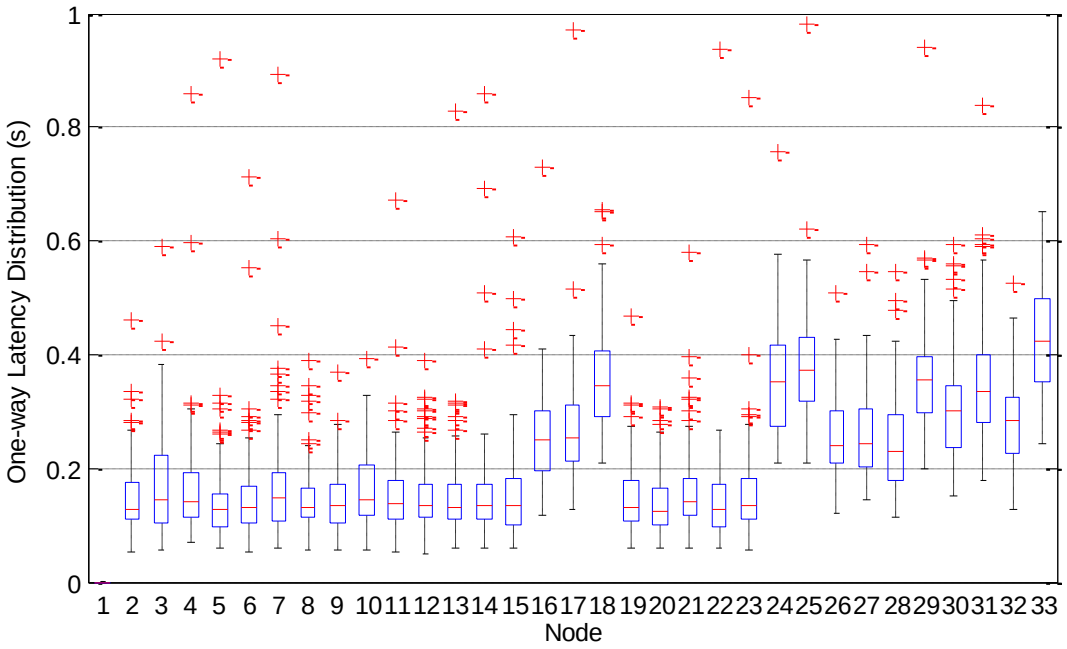


**Figure 3-9 One-way latency of the LV distribution network with background and impulsive noise**

### 3.3.2. **MV network**

Although PLC is more commonly used in LV networks, their application at MV might be also interesting for monitoring and network management (Papadopoulos et al., 2013). Then, the second case study is shown in Figure 3-10 and represents a rural MV distribution network of 103 km length, which consists of a primary substation with three MV feeders that connect 136 nodes. At each node, a secondary substation can be located, which can also have DG units based on Doubly-Fed Induction Generation (DFIG), Combined Heat and Power (CHP), or microgrids.

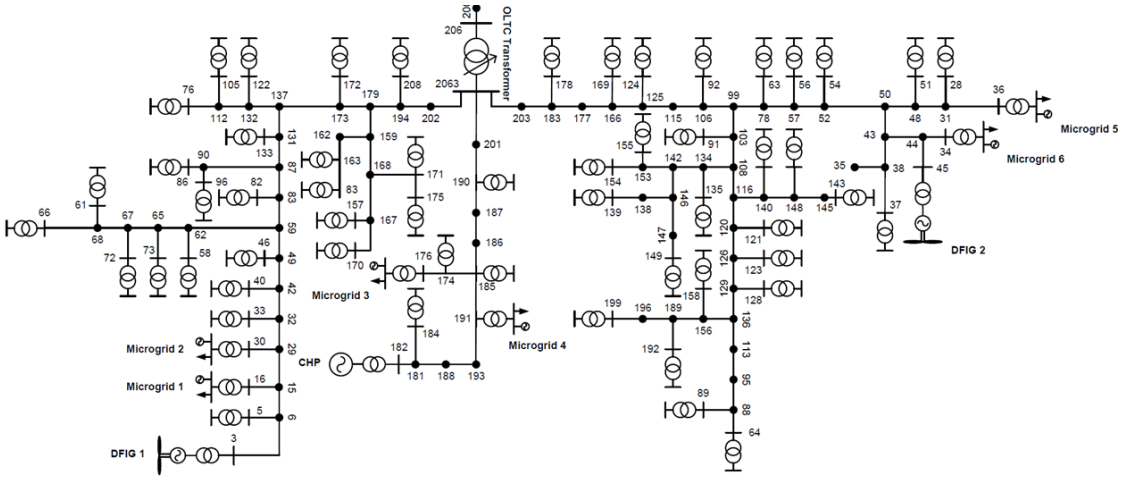


**Figure 3-10 MV distribution network**

As in the previous case, for this analysis all nodes are considered with the same impedance. A value of 4 kΩ was initially considered to represent a secondary substation with a nominal power of 56 kVA connected in 15 kV. The resulting attenuation matrix of the MV network is presented in Figure 3-11, where the index of the nodes again refer to their position in the DFS. In this figure it can be easily identified that nodes that are close to each other (for instance those close to the diagonal) present lower attenuations than nodes that are farther connected. Compared to the attenuation matrix of the LV network, it can be seen that the attenuations are much higher in this case. This can be due to the higher length of the lines and the higher number of connected nodes, which are the parameters that affect the most to network performance according to the conclusions from Chapter 2. This higher attenuation in the MV network contrasts with (A. Tonello, Song, Weiss, & Yang, 2012), where authors stated that in general MV channels exhibit lower attenuation than LV distribution channels because LV topologies are usually characterized by higher number of lines. However, in this case the MV network has more lines than the LV network, so these results are aligned with their justification.

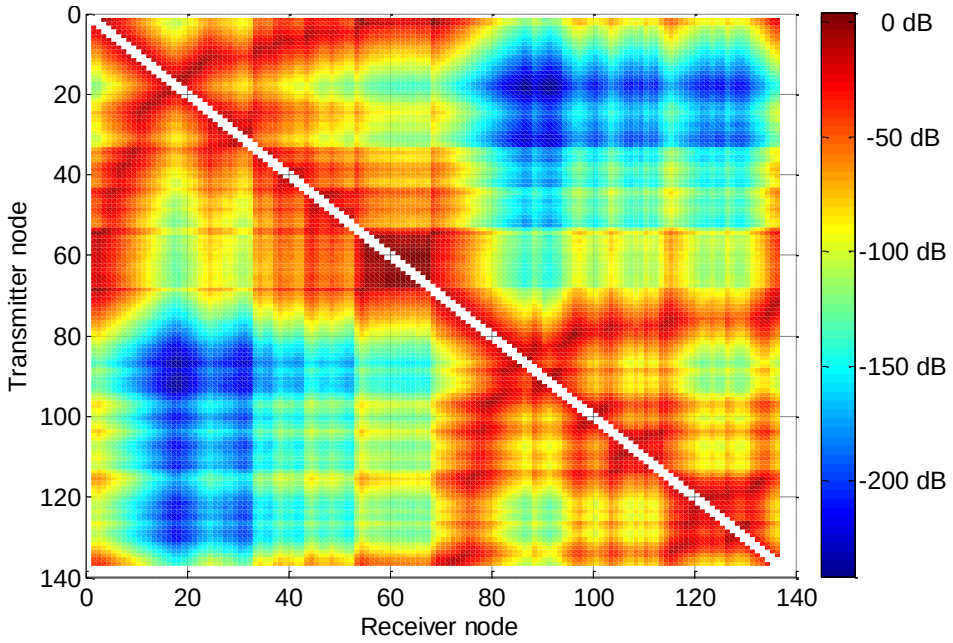


**Figure 3-11 Attenuation matrix of the MV distribution network**

In this case study, the effect of the variation of load impedances is analysed. With this aim in view, the attenuation matrix was computed with different values of this parameter. These values were chosen based on the actual characteristics of the analysed network. The secondary substations of the analysed MV network present a nominal power between 25 kVA and 1.36 MVA. The average peak demand of these substations is 65 kVA and the peak demand in the largest secondary substation is 585 kVA, which represents a 0.44 capacity factor.

Since the considered load impedance corresponds to a rated power in the lower bound of the capacity of the secondary substations, lower impedance values were chosen for the new scenarios. The attenuation matrix was obtained for load impedances with 2 kΩ, 1 kΩ and 500 Ω, which in 15 kV correspond to nominal powers of 113 kVA, 225 kVA and 450 kVA, respectively.

Figure 3-12 shows the attenuation of the communication path between the primary substation (node 206) and the secondary substation with DFIG 2 (node 45) considering the aforementioned load impedances. In this figure it can be clearly seen that lower values of load impedances (i.e. higher consumptions) cause higher signal attenuations. For instance, attenuation between neighbour nodes with Z=4 kΩ range between 3 dB and 10 dB, similarly to the results obtained in the LV network, whereas with Z=500 Ω these attenuations vary between 9 dB and 23 dB. Considering base node communications with the service nodes, it can be concluded that reducing the impedance by half (i.e. doubling the consumption) entails doubling the attenuation between them.

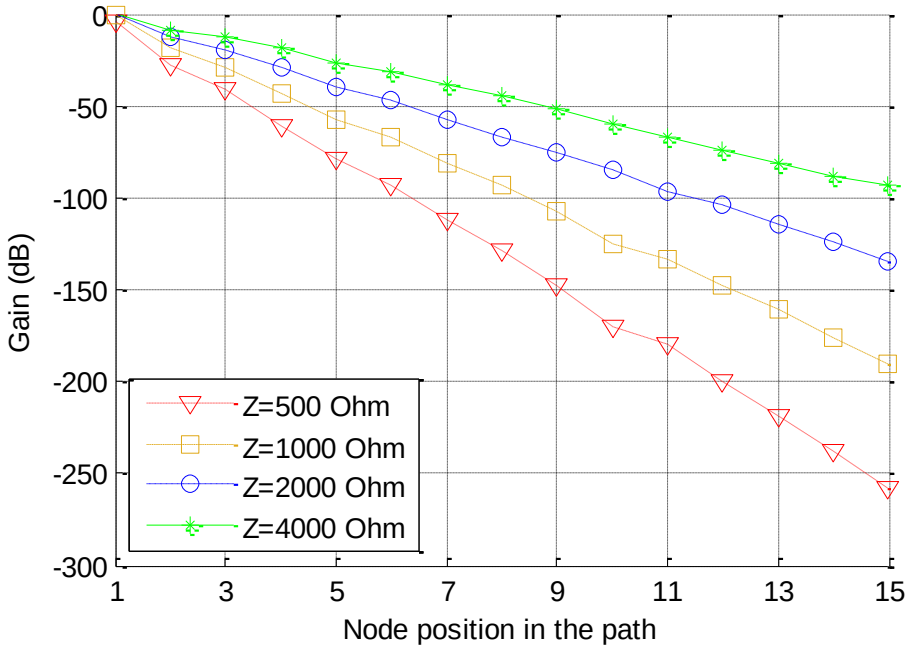


**Figure 3-12 Attenuation of the communication path 206-45 of the MV distribution network with different values of load impedances**

After this analysis of the physical channel, the communication performance is evaluated in the PLC simulation framework for these four scenarios with 3,000 seconds for the registration process and 2,000 for the reading process, as in Chapter 2. Taking into account the higher attenuations observed in the physical channel, the impulsive noise is again cancelled with the compressed sensing technique used in (Matanza, 2013).

Figure 3-13 shows the number of registered nodes during the registration process of the MV network in the four scenarios of load impedance for which the attenuation matrix was previously obtained. In this figure, the impact of the higher attenuations caused by lower load impedances can be observed. Thus, in the scenario with 500 Ω the base node is not able to register all the service nodes because the messages arrive with too much error to be correctly interpreted. As a consequence, the sequential process to communicate with all the service nodes cannot be carried out and the network cannot be fully communicated with PLC with the considered conditions. However, as the base node is able to register a significant number of nodes, it can be expected that PLC can be used for the communication of a specific region of the network. So, in case these were the normal operation conditions, the option of using a hybrid architecture combining PLC and a different communication technology could be analysed. Then, finding the sub-network that maximizes the PLC coverage would be an interesting topic for research.

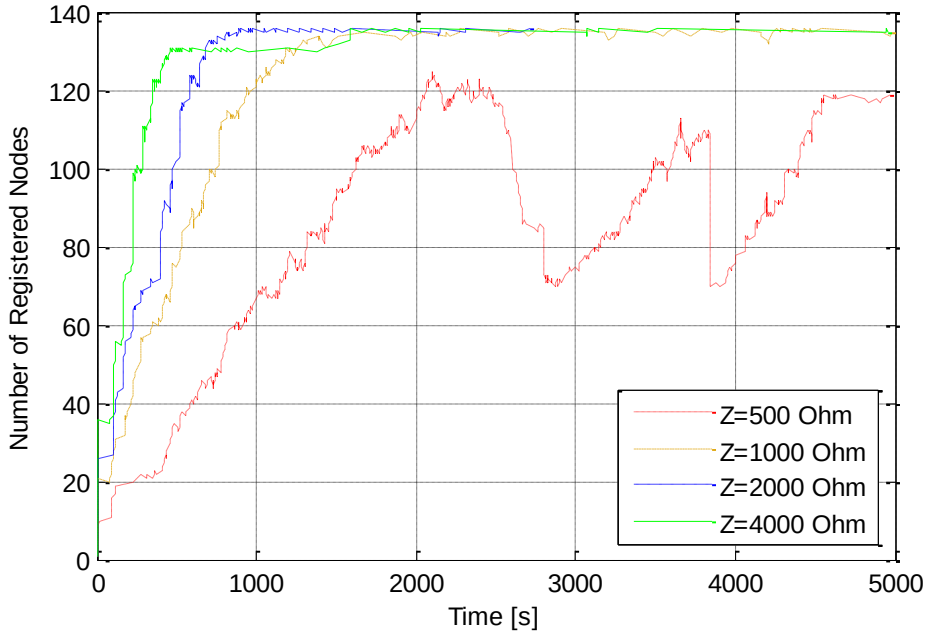


**Figure 3-13 Registration process in the MV distribution network with different values of load impedances**

In Figure 3-13 it can be also observed that for higher values of load impedance, the registration process turns more stable and nodes are also faster registered. Indeed, the results of the time to read all meters show better performance in these cases, as it can be seen in Figure 3-14 where the results for the same simulations presented in Figure 3-13 are shown. The simulation for the lower value of load impedance does not obtain any measurement because the registration process was not properly finished, as explained before. For the rest scenarios, it can be appreciated that when the load impedance is increased from 1 kΩ to 2 kΩ the reading time is reduced by 60%, but when the increase is from 2 kΩ to 4 kΩ the achieved reduction is lower than 40%.

Then, although there was a reverse-proportional relationship between the value of the load impedances and the resulting attenuation of the network, the communication performance does not maintain the same rule and the pattern is similar to the one presented in Figure 2-12 with the variation of the number of users, which was likened to an exponential behaviour. Based on these results, it can be concluded that PLC the performance is much better in off-peak hours. Then, communications for non-critical processes should be carried out taking into account this consideration. This is especially important in large networks with high number of users, which are the topology parameters identified in Chapter 2 that have the highest impact in the performance.

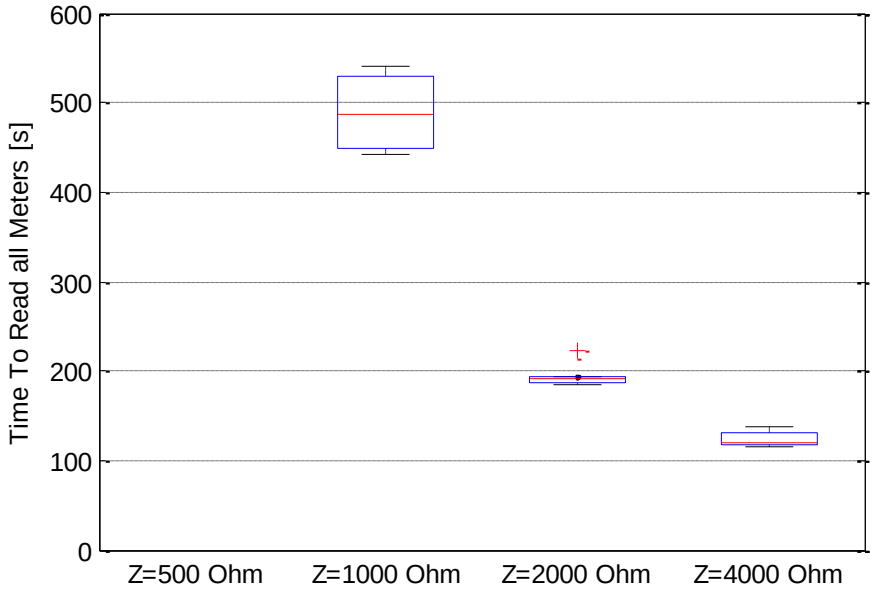


**Figure 3-14 Time to read all meters of the MV network with different values of load impedances**

## 3.4. Application to large-scale networks

From the analysis of the previous case studies it can be concluded that the performance of PLC is highly affected by the characteristics of distribution networks, which can be static like the network topology and line impedances, or dynamic like the channel noise and load impedances. Thus, in case of unfavourable local implementation conditions, the communications with this technology can be seriously jeopardize. Furthermore, the characteristics of distribution networks are very different from one region to another. For instance, in Europe there are nearly 10 million km of power lines connecting around 260 million customers, and distribution networks in different countries present contrasting characteristics in terms of line length, customer density

or voltage levels (Eurelectric, 2013). Then, to facilitate the identification of the most critical networks for PLC performance, a methodology based on the conclusions from previous analysis can be defined.

This methodology builds on the use of Reference Network Models (RNMs), which are large-scale planning tools that design efficient distribution networks aimed at minimizing total investment and associated operational costs while taking into account technical constraints (thermal and voltage limits) and reliability of supply targets in the different supply areas (Gonzalez-Sotres et al., 2011). Then, these models are used to have representative networks avoiding confidentiality problems of DSOs related to sharing real data from their networks.

Figure 3-15 shows a simplified scheme of the RNM used to obtain the large-scale networks analysed in this section.

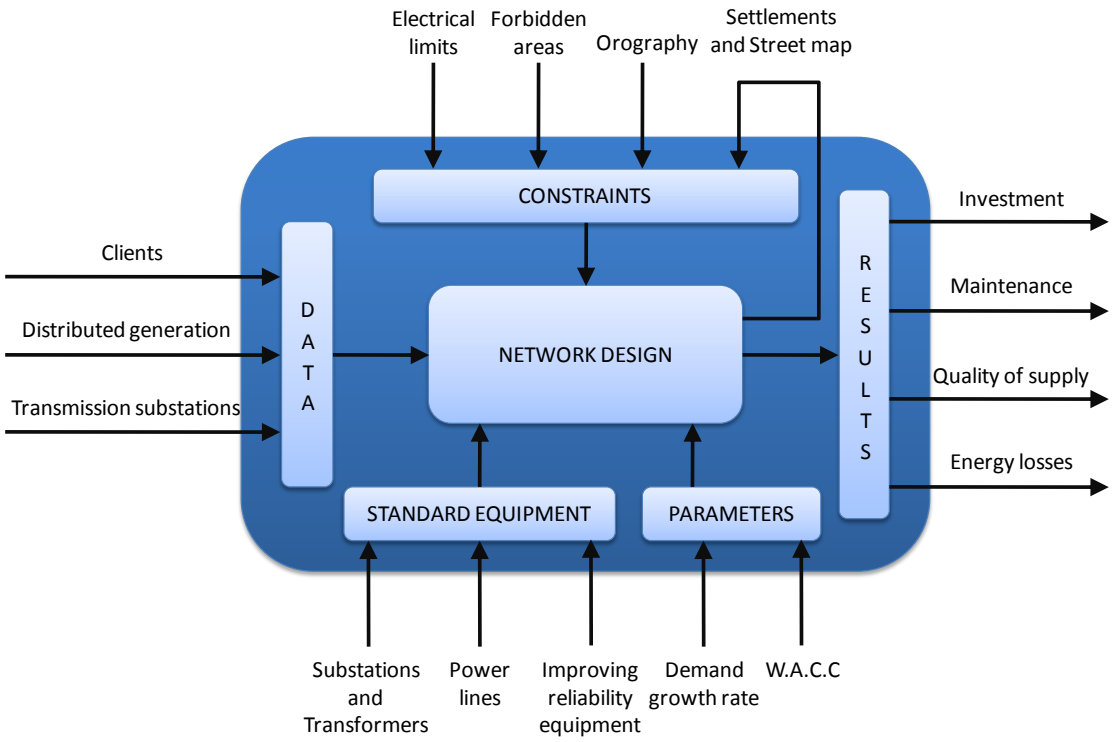


**Figure 3-15 Reference Network Model simplified scheme**

The model takes as inputs the GPS location and the characteristics of the consumers and the DG connected to the high (HV), medium (MV), and low (LV) voltage grid, and also the data of the transmission substations that connect the distribution network to the upper voltage level network. Then, it calculates the efficient location and capacity of the MV/LV transformers, the HV/MV substations and all the lines and conductors that are required to supply the demand, selecting the distribution assets from a library of standardized equipment. Additionally, the

location and characteristics of distribution transformers and substations can also be included as inputs to the model in order to obtain a network more similar to the actual ones. The model takes into account the technical constraints, the forbidden areas, the orography of the area, and the street map of the settlements, which is automatically generated from the location of the load points. There is a set of parameters that can be adjusted when planning the network, such as the demand growth rate or the WACC (Weighted Average Cost of Capital).

Since the location of the secondary substations is critical for PLC networks, the details of the planning algorithm used for this purpose can be found in Appendix A. Then, the efficient networks obtained with the RNM can be considered as reference networks, which results can be used to help the regulator in the task of setting reference efficiency levels. For instance, RNMs have been used by the Spanish regulator to assess the allowed revenues of the distribution companies, and also to set the efficiency targets for energy losses in current distribution areas, comprising millions of customers. With regards to the presented methodology, the described RNM was used by the Joint Research Centre (JRC) of the European Commission to create representative networks from European regions, taking into account data gathered from 79 DSOs that distribute more than 2,000 TWh of electricity to over 200 million customers per year, covering a total area of more than 3 million square km (JRC, 2016).

The large-scale reference networks analysed are the rural and semi-urban networks described in (JRC, 2016). The rural network is depicted in Figure 3-16, where several small settlements and farms can be identified, whereas the semi-urban network is illustrated in Figure 3-17, where the outskirts of a city can be found. In these figures, the blue triangle represents the HV/MV primary substation, the blue lines the MV feeders, the red circles the MV/LV secondary substations, and the black thin lines the LV feeders. The main characteristics of both networks are summarized in Table 3-1.

These reference networks can be divided in a set of LV networks made up of a MV/LV secondary substation and all the LV customers connected by the LV feeders that come from this substation. Thus, the rural network presents 152 LV networks, and the semi-urban network 161 LV networks. In all these networks, the PLC transfer function can be obtained following the process explained in Section 3.2, and then carry out the performance assessment like in the case studies of Section 3.3. However, as it was concluded in Chapter 2, the two main topology parameters that affect the performance of PLC networks are the number of nodes and the branch length. Then, a first analysis can be performed with the most critical networks based on these two parameters, which are expected to present the worst performance.

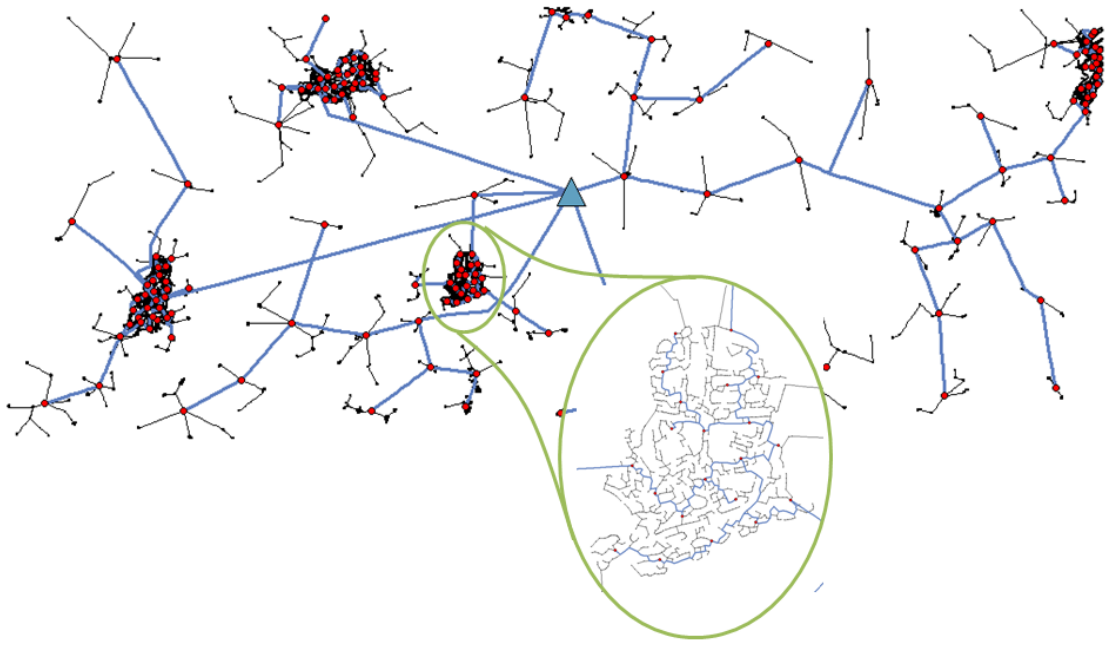

**Figure 3-16 Large-scale rural reference network (JRC, 2016)**

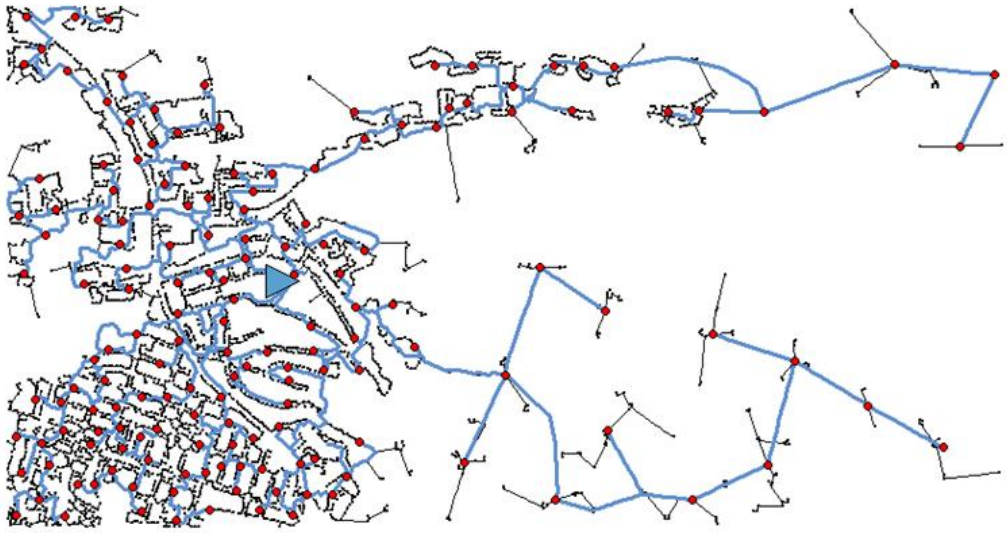

**Figure 3-17 Large-scale semi-urban reference network (JRC, 2016)**

**Table 3-1 Characteristics of the rural and semi-urban reference networks**

| | Rural | Semi-Urban |
|---|---|---|
| Number of MV/LV secondary substations | 152 | 161 |
| Number of LV customers | 7,727 | 13,998 |
| Length of LV feeders (km) | 211 | 115 |

Figure 3-18 and Figure 3-19 show the analytics in terms of number of customers and network length of all the LV networks included in the rural and semi-urban reference networks, respectively. In these figures, the LV networks with the maximum number of customers and maximum network length are highlighted, and the main characteristics of these networks are summarized in Table 3-2.

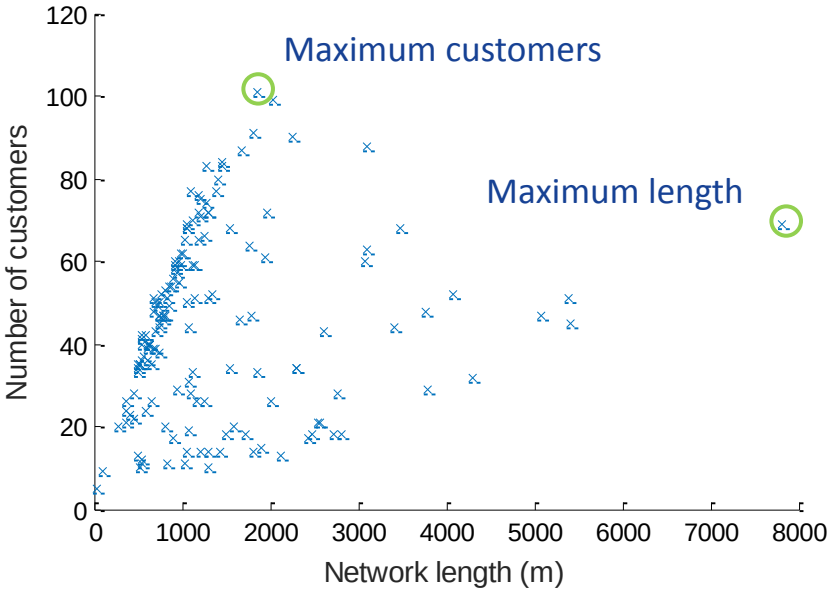


**Figure 3-18 Number of users and network length of all LV networks in the large-scale rural reference network**

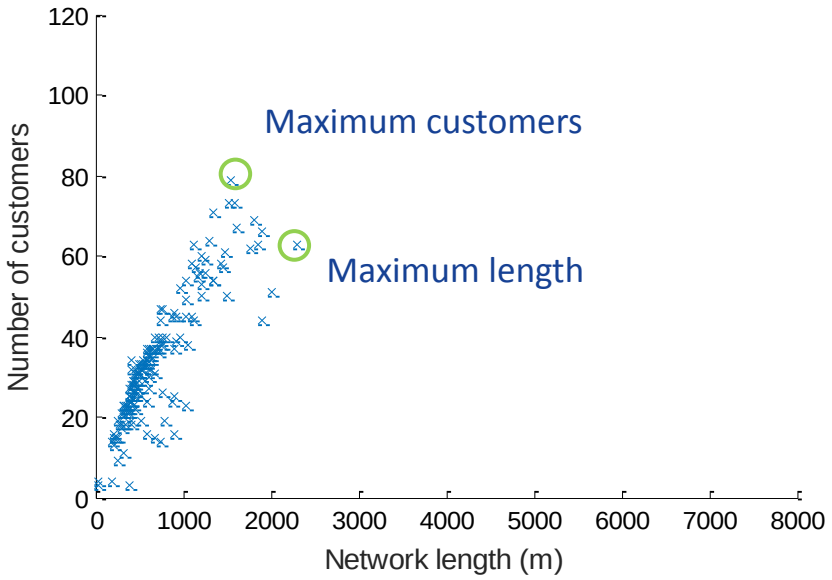


**Figure 3-19 Number of users and network length of all LV networks in the large-scale semi-urban reference network**

**Table 3-2 Characteristics of the LV networks with maximum number of customers and maximum network length in the rural and semi-urban reference networks**

| | Rural | | Semi-Urban | |
|---|---|---|---|---|
| | **Max customers** | **Max length** | **Max customers** | **Max length** |
| Number of customers | 100 | 68 | 78 | 62 |
| Network length (m) | 1,850 | 7,811 | 1,544 | 2,296 |
| Longest feeder length (m) | 358 | 2,078 | 294 | 545 |

Note that the number of customers and the longest feeder length of the LV rural network with the maximum number of clients are similar to the Case U-XS from Table 2-2. However, since the RNM merges the customers that are located close to each other, here the number of customers is equivalent to the number of groups (buildings). Hence, the semi-urban cases have less customers than the rural ones but with a higher electricity demand, since they represent nodes with higher load density. This effect that can be simplified from an energy perspective is not negligible from the communication point of view, because despite the consumption is the same, the number of smart meters to communicate is very different and this has a big impact in the performance. However, for illustrative purposes the number of users is taken directly from the number of customers, but the impedances are still set to 6Ω for all the loads, as in the LV case study.

Then, the PLC performance assessment of these four networks is analysed with the PLC simulation framework considering same conditions than in Chapter 2: 5,000 seconds of simulation, first 3,000 for registration and the next 2,000 to gather messages of 200 Bytes from all the nodes in a sequential manner, and carrying out 20 simulations for each scenario. Figure 3-20 shows the results of the time to read all meters considering the effect of the impulsive noise, where it can be seen that in the four networks all the readings are performed in less than 5 minutes. For a deeper comparison between the four cases, another simulation is performed increasing the packet size to 2,000 Bytes. This effect can be produced by the aggregation of information in the smart meter, for instance when the readings are carried out in longer time intervals and more historic data locally recorded has to be transmitted. In fact, in (Aalamifar, Hassanein, & Takahara, 2012) authors suggest that packet sizes are usually between 200 and 2,400 Bytes for smart metering applications. In this case, to analyse the availability of the nodes, when the base node cannot communicate with a service node over a certain period, instead of repeating the messages until the connection is successfully achieved like in all previous simulations, now the connection is considered lost and the reading process is continued with the next service node.

The results of the reading process for the 2,000 Bytes scenario are presented in Figure 3-21, where it can be seen that the differences between the four networks are higher than in the scenario with 200 Bytes. Comparing with the 200 Bytes results, it can be seen that in average terms an increase of ten times the packet size results in an increase of three times the time to read all meters.

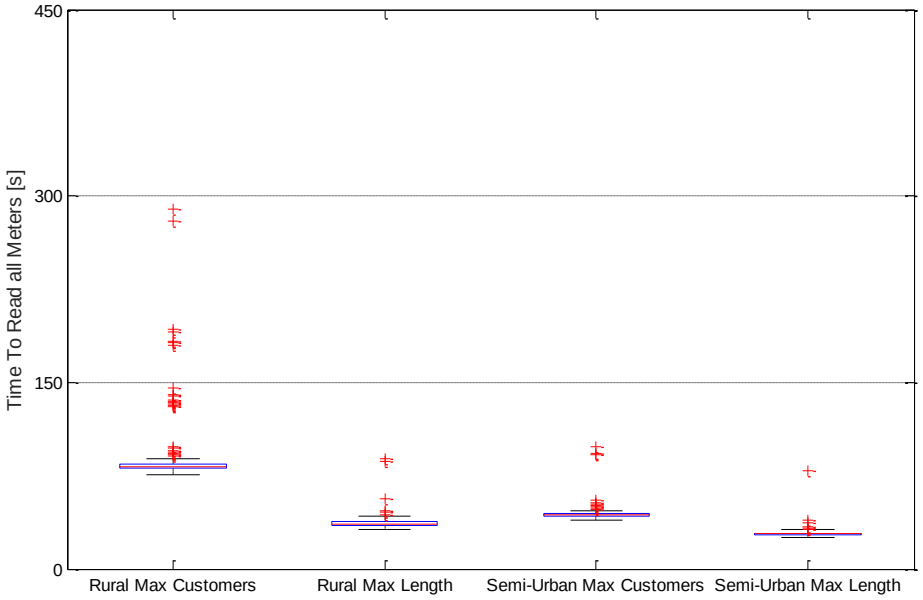


**Figure 3-20 Time to read all meters in the selected cases from the reference networks**

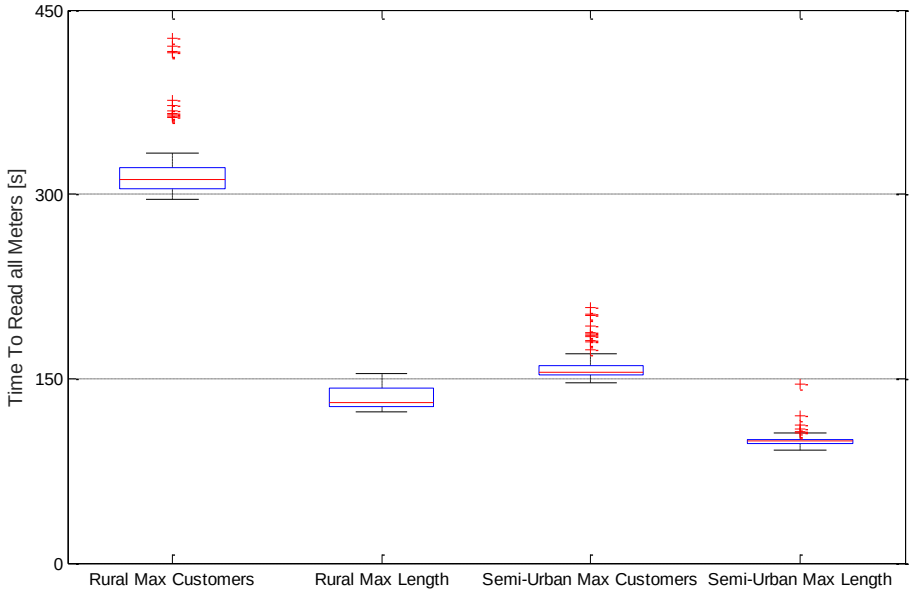


**Figure 3-21 Time to read all meters in the selected cases from the reference networks increasing the packet size to 2,000 Bytes**

In Figure 3-21 it can be also seen that this time the rural network with maximum number of customers performs practically all readings in more than 5 minutes, conversely to the results obtained with the 200 Bytes packet size. However, analysing in detail the results of this network with the 2,000 Bytes packet size it was found in the simulations that certain meters were not read several times because the maximum waiting time was reached. To better illustrate this effect, in Figure 3-22 the network is graphically presented with the node availability of these problematic nodes, where the green circles represent the service nodes, the blue lines the LV feeders, and the blue triangle in the centre of the figure is the base node. In this figure, it can be seen that the problematic nodes (marked in red) are located at the end of the LV feeders, because theses nodes present the highest attenuation from the base node. So, there are two nodes with 98% of availability, and one node with 87% of availability, which means that from 100 attempts to gather the readings, there are two nodes that failed two times and one node that failed 13 times. However, the overall network availability is 99.83%, which is in the range between the 99% and 99.99% recommended in (DOE, 2010).

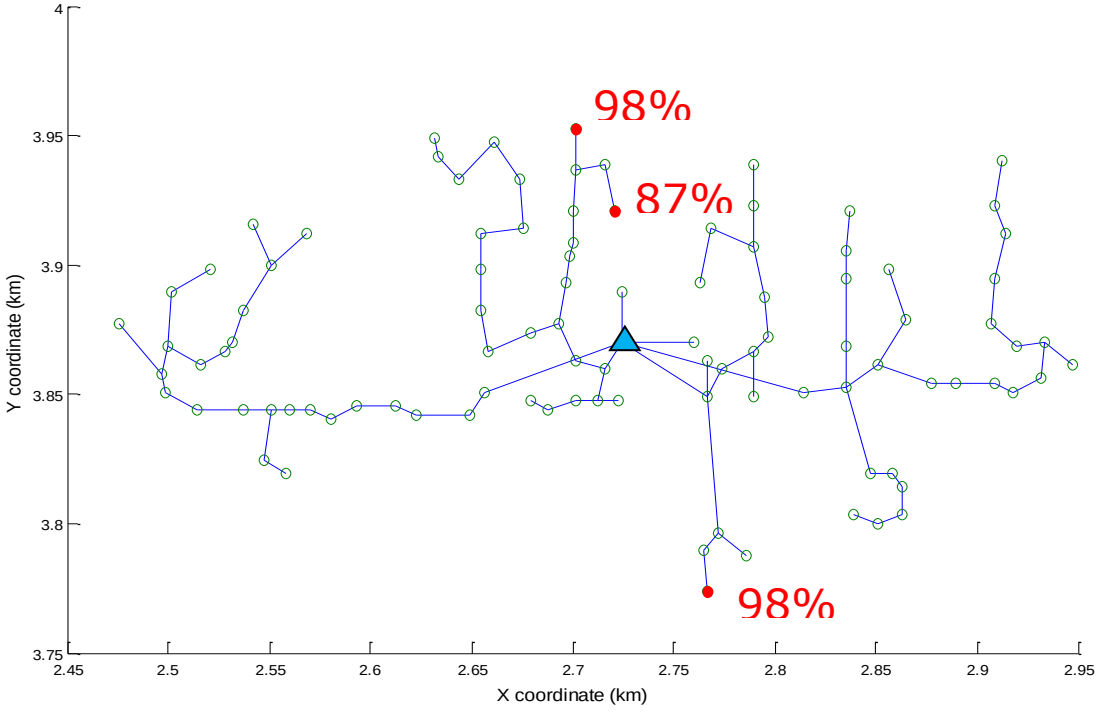


**Figure 3-22 Node availability in the Rural MC case with 2,000 Bytes packet size**

## 3.5. **Conclusions**

This chapter has presented a methodology to obtain the signal attenuation between any pair of nodes in a Power Line Communications (PLC) network with a tree topology based on transmission-line theory. As a result, the attenuation matrix can be obtained, which shows the impact of the topology and the loads and line impedances in the physical channel.

This methodology has been applied to compute the attenuation matrix of two case studies that represent real LV and MV networks, where different communication paths between the base node and different service nodes have been analysed. The obtained paths in both networks shown attenuations between 3 and 10 dB for neighbour nodes, which were aligned with values reported in the literature. Comparing both networks, the attenuation between the base node and the nodes at the end of the feeders was larger in the MV network, since the MV network was larger and presented four times more nodes than the LV network. These results are coherent with the conclusions from Chapter 2, where the branch length and the number of nodes were identified as critical factors for the network performance. The impact of the variation of the load impedance has been analysed for the MV network, where it has been concluded that doubling the value of the load impedance, which corresponds to reducing the consumption by half, causes the same reduction in the attenuation. For this reason, it is highly recommended to take advantage of off-peak scenarios to communicate with nodes that can present registration problems, and as far as the communications are not related to critical processes.

Additionally, the attenuation matrices of the LV and MV networks chosen as case studies have been used as input for the PLC simulation framework described in Chapter 2 to analyse their communication performance. With regards to the analysis carried out in the MV case, it has been concluded that the variation of the load impedance produces a different effect in the communication performance than the impact produced in the attenuation, because in this case the relationship is not linear and scenarios with low impedances due to high consumption present a very poor performance compared to the opposite scenarios. Indeed, in the scenario with the lowest value of load impedance, a significant proportion of nodes were not able to register. In cases where this situation can be permanent, alternative communication technologies could be used after exploiting all the capabilities and coverage of PLC. In the LV case, the effect of the impulsive noise on the communication performance has been analysed, where it has been concluded that this factor highly affects to the performance, especially for communications between nodes that are connected over longer distances. Noise cancellation techniques are very

useful to mitigate their negative effects, so their application should be considered as much as possible.

Finally, considering the differences that distribution networks present from different regions, this methodology has been also applied to large-scale networks obtained with a Reference Network Model (RNM). Considering the conclusions from the previous chapter, the most critical LV networks in terms of number of users and network length have been chosen. This selection allows analysing the most adverse scenarios for PLC communications, so the rest of the networks in the area are expected to provide a better performance. These simulations have also considered the effect of the packet size. Then, for small packet sizes, the results obtained have been very similar between the different networks, but when the packet size was larger, higher differences have been observed. Moreover, several problematic nodes have been found at the end of the feeders, which can jeopardize the system operation in case they are controllable nodes or manage critical information.

The conclusions derived from this study motivate the application of this kind of tool to the decision making process of communication network planning. The presented methodology allows knowing in which distribution networks PLC technologies can be effectively deployed to meet the communication requirements under different operating conditions. Hence, economic analyses can be supported by this technical approach to analyse the viability of a cost-effective solution like PLC. Indeed, smart grid functionalities can present different information and communication requirements, which should be analysed to adopt the most efficient decision for each case. However, the added value provided by better information and communication systems is very difficult to quantify, but is the only manner to know until which extend the investment in smart grid technologies and applications can be justified. For this reason, this question is handled in the next chapter to provide useful information about this important topic, focusing on one of the most extended smart grid functionalities: voltage control.

# Chapter 4: Information and Communication Requirements of Voltage Control

## 4.1. Introduction

One of the most important challenges that Distribution System Operators (DSOs) are facing due to the increase of Distributed Generation (DG) is the implementation of cost-effective voltage control mechanisms to keep voltage levels within the admissible limits. In this sense, smart grids are expected to maximize the integration of Renewable Energy Sources (RES) like PV in distribution networks thanks to advanced applications based on Information and Communication Technologies (ICT). Indeed, in Section 1.3 it was concluded that centralised voltage control with On-Load Tap Changers (OLTC) and PV inverters is a promising application to economically mitigate voltage violations due to the high PV penetration levels that are envisaged in the future.

The review carried out in Chapter 1 raised the need for more practical studies of the requirements of smart grid applications, considering both power and communication issues. This was mainly because of the high uncertainty related to the definition of the optimal level of information and control required by these new applications. In Chapters 2 and 3, the performance of Power Line Communications (PLC) networks was analysed from a technical point of view for different topologies and local implementation conditions, but the impact that this performance has in the operation of distribution networks was not addressed. In addition, technical benefits in system operation have to be quantified in monetary terms to adopt the most cost-effective solutions.

For all these reasons, this chapter is focused on the technical and economic assessment of a centralised voltage control application with OLTC and PV based on inverters to analyse the added value of better information and communication conditions, which will help to define their most appropriate requirements. This analysis is especially important for this application because it relies on the quality of the data used to calculate the set-points (forecast accuracy), and on the time interval used to send the set-points from the central unit to the P inverters (set-point timing). These aspects are directly related to the performance of the forecasting tools and communication systems, and their assessment provides a significant contribution to understand and improve the

performance of voltage control applications. In fact, none of the references analysed in Chapter 1 takes into account the added value of better information and communication in such application.

This chapter is structured as follows. First, the characteristics of voltage control applications in distribution networks are presented. Then, the methodology to assess the impact of forecasting and communication on a centralised voltage control scheme is explained. This methodology is carried out from a technical and economic point of view, and it is applied trough simulation in two real networks, one in LV and another in MV. Finally, the results from the forecasting and communication analysis in the selected scenarios are presented for both networks and the main conclusions are then discussed.

## 4.2. Voltage control in distribution networks

A simplified representation of the voltage variation along distribution feeders is presented in Figure 4-1 (Madureira, 2010), where (a) shows the effect of different load levels and (b) the effect of different DG levels. In Figure 4-1 (a) the following segments can be identified:

- A-B: Voltage drop in the MV feeder due to the loads
- B-C: Voltage increase due to the taps in the MV/LV secondary substation
- C-D: Voltage drop in the MV/LV secondary substation
- D-E: Voltage drop in the LV feeder due to the loads

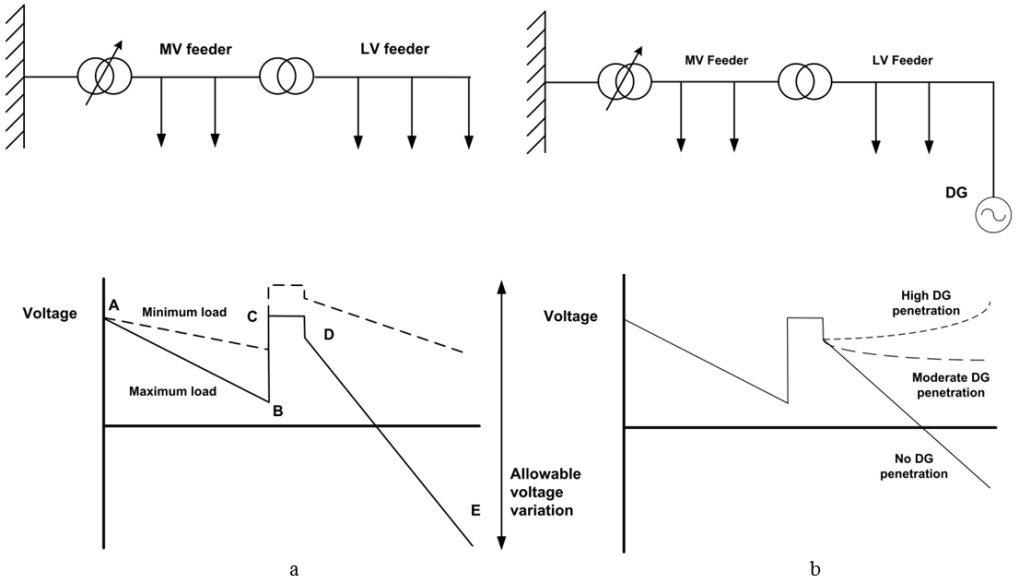


**Figure 4-1 Voltage variation in distribution feeders. (a) With different load levels (b) With different DG levels** (Madureira, 2010)

In Figure 4-1 (a) it can be seen that the taps of the MV/LV secondary substation can be adjusted to keep voltage levels within the admissible limits under maximum and minimum load conditions. These taps can be changed automatically with an OLTC, instead of the manual offline operations that are required without this device. Hence, taps can be stepped up in peak demand hours and stepped down in off-peak hours to maintain a good power quality while improving energy efficiency, for instance to reduce energy losses.

The presence of DG makes voltage control more complicated because the possible range of voltage variation is higher as depicted in Figure 4-1 (b), being the most unfavourable scenarios the ones with minimum load and maximum generation (maximum voltage), and maximum load and minimum generation (minimum voltage). Moreover, in case of having DG from RES, the fluctuations and uncertainty caused by the supply from these technologies turn this operation even more complex. To mitigate these problems, the inverters of the DG units can also be used for voltage control at the Point of Common Coupling (PCC), by changing the injected or absorbed amount of reactive power. This action can be generally performed through a power factor set-point or a voltage set-point. Despite voltage set-points are typically used in transmission networks, reactive power compensation is more effective when the reactance of the conductors is dominant over the resistance. Then, in LV and MV networks where the X/R ratio is typically low, power factor set-points with active power curtailment are more effective, especially for non-controllable DG units like wind or solar PV (Trebolle et al., 2012).

Active and reactive power control can be performed locally as a stand-alone application at the PCC, or in a more coordinated way where a central unit determines the control actions for all devices. Their main difference is that the coordinated approach requires information about the state of the network as well as communication between the central unit and the control devices. For instance, the devices used in the centralised voltage control application presented in (SUSTAINABLE project, 2016a) are shown in Figure 4-2.

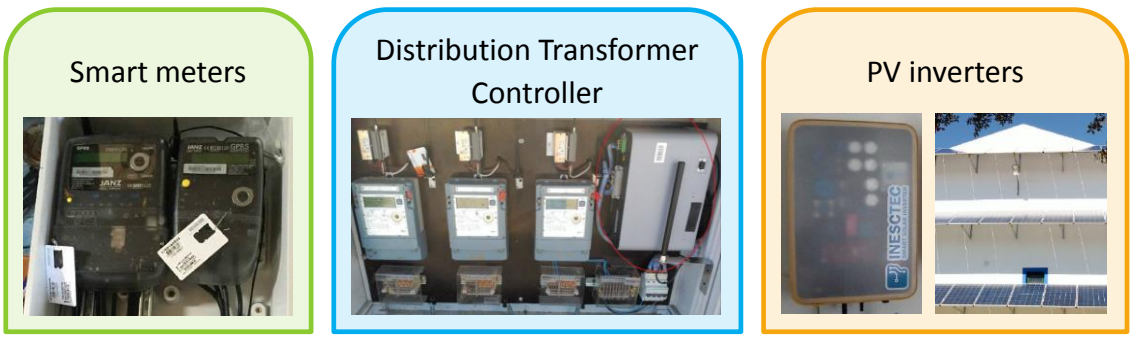


**Figure 4-2 Pictures of the devices used in a centralised voltage control functionality** (SUSTAINABLE project, 2016a)

In that case, the Distribution Transformer Controller (DTC) acts as the central unit and is located at the MV/LV secondary substation. This unit collects the information from the smart meters every 15 minutes to check if there is a voltage violation. If so, the DTC calculates the optimal control actions to solve the voltage problems and sends the resulting set-points to the PV inverters. Then, it can be expected that if the process to collect the information and to send the set-points were performed in a shorter time interval, voltage deviations would be solved faster. Conversely, in case these updates were less frequent, control signals would be worse adjusted to the actual needs. Additionally, the calculation of the set-points can be supported by forecasting tools, especially for longer updating periods where the accuracy of these tools is more relevant. For these reasons, the impact of forecasting and communication in this type of application is assessed in the next section from a technical and economic point of view.

## 4.3. Centralised voltage control assessment

### 4.3.1. Technical assessment

In this section, the methodology to technically assess the impact of forecast accuracy and set-point timing in a centralised voltage control application with OLTC and PV inverters is presented. The centralised voltage control strategy is based on an OPF formulation modelled with MATLAB® and MATPOWER (Zimmerman et al., 2011). The objective of the OPF is to minimize the total generation costs ($c_{j,h}^{G}$) of all generation units ($M$) at each time $h$, according to the standard formulation presented in equations from (4.1) to (4.7). The slack bus produces energy at an hourly cost and PV is dispatched at zero cost, so the ultimate objective is to maximize PV generation.

$$min \sum_{j \in M} c_{j,h}^{G} \qquad \forall h \in H \tag{4.1}$$

Subject to:

$$p_{i,h}^{G} - P_{i,h}^{D} = \sum_{k \in N} v_{i,h} \cdot v_{k,h} \cdot (G_{i,k} \cdot cos\ \theta_{i,k,h} + B_{i,k} \cdot sin\ \theta_{i,k,h}) \qquad \forall i \in N, h \in H \tag{4.2}$$

$$q_{i,h}^{G} - Q_{i,h}^{D} = \sum_{k \in N} v_{i,h} \cdot v_{k,h} \cdot (G_{i,k} \cdot sin\ \theta_{i,k,h} - B_{i,k} \cdot cos\ \theta_{i,k,h}) \qquad \forall i \in N, h \in H \tag{4.3}$$

$$s_{i,k,h} \leq S_{i,k}^{max} \qquad \forall i, k \in N, h \in H \tag{4.4}$$

$$V_r^{min} \leq v_{i,h} \leq V_r^{max} \qquad \forall i \in N, h \in H, r \in R \tag{4.5}$$

$$0 \leq p_{j,h}^{G} \leq P_{j,h}^{Gmax} \qquad \forall j \in M, h \in H \tag{4.6}$$

$$Q_{j,h}^{Gmin} \leq q_{j,h}^{G} \leq Q_{j,h}^{Gmax} \qquad \forall j \in M, h \in H \tag{4.7}$$

The power balance equations for each bus *i* and time *h* are represented in equations (4.2) and (4.3), where $p_{i,h}^{G}$ and $P_{i,h}^{D}$ are the active power generation and demand, respectively, $q_{i,h}^{G}$ and $Q_{i,h}^{D}$the analogue for the reactive power, $G_{ik}$ and $B_{ik}$ the real and imaginary parts of the element located in the row *i* and column *k* of the admittance matrix, $v_{i,h}$ the voltage magnitude at bus *i* and time *h*, and $\theta_{i,k,h}$ the angle difference between buses *i* and *k* at time *h*. The technical constraints are defined in equations (4.4) to (4.7), where $s_{i,k,h}$ is the apparent power flow between buses *i* and *k* at time *h*, $S_{ik}^{max}$ the maximum apparent power flow for buses *i* and *k*, $V_r^{min}$ and $V_r^{max}$ the minimum and maximum admissible voltage limits at iteration *r* until the feasibility of the OPF is reached, and $Q_{j,h}^{Gmin}$ and $Q_{j,h}^{Gmax}$ the minimum and maximum reactive power generation of unit *j* at time *h*.

The modelling of the centralised voltage control takes into account the computation of the set-points for the active and reactive power of the PV units (based on a power factor control more appropriate for distribution networks, as discussed in Section 4.2) as well as for the OLTC for all the times in the analysed period (*H*). Then, two control levels can be differentiated. The OLTC, which is managed by the DSO, and the PV units, which can be also managed by the DSO or by a third party like a VPP, and they can have different communication requirements.

The OLTC is modelled by changing the voltage of the node connected to the slack bus ($v_{1,h}$). The active power production of the PV units ($p_{j,h}^{G}$) is determined according to the profile of PV generation, and the reactive power provided by the PV inverter ($q_{i,h}^{G}$) is adjusted considering the limits of the reactive power consumed ($Q_{j,h}^{Gmin}$) or generated ($Q_{j,h}^{Gmax}$) with the limitation of the apparent power ($S^2 = P^2 + Q^2$). According to equation 4.1, PV curtailment is only used when no other control variable is available to mitigate voltage constraints. This represents how the DSO may decide the control actions. In case the voltage limits cannot be fulfilled with all the available control actions, the voltage limits are relaxed by ε to assess the amount of energy that would be served under undervoltage or overvoltage conditions. Then, the OPF is run again with the relaxed voltage limits repeating this process iteratively until the OPF converges (*R*). These voltage limits are obtained according to equations (4.8) and (4.9).

$$V_{r+1}^{min} = V_r^{min} - \varepsilon \qquad \forall r \in R \tag{4.8}$$

$$V_{r+1}^{max} = V_r^{max} + \varepsilon \qquad \forall r \in R \tag{4.9}$$

With the aim of taking into account the effect of the forecasting tools and communication systems in the simulations, the following methodology is presented. First, a forecast stage is defined to take into account the fact that the central unit has to determine the set-points for a future

scenario without perfect information. This means that the demand and generation profiles used for the calculation of the set-points are not very likely to coincide with the actual ones, so a forecast error is included. After this, a control stage is implemented to take into account the effect of the set-point timing that can be provided by the communication system. Hence, in this stage the time interval used to send the set-points from the central unit to the PV inverters is considered. For the purpose of this assessment, the set-points of the OLTC can be updated at any time because an independence of this device from the communication system is assumed. In practice, this means that the control station is implemented in the same location that this device, like in the centralised voltage control application developed in (SUSTAINABLE project, 2016a).

The objective of the forecast stage is to obtain the set-points that have to be applied to the actual profiles in the control stage, which are then naturally subject to forecast errors. Since forecast errors affect both load and PV estimation, two extreme scenarios can be considered in order to assess their impact: a) load overestimation and generation underestimation; and b) load underestimation and generation overestimation. The sensitivity to the forecast error is modelled by applying different errors to the actual profiles, adding or subtracting these errors depending on which case of overestimation or underestimation is analysed.

The set-points obtained in the previous stage can be sent periodically considering different time intervals taking into account the performance of the communication network. For instance, the central unit may perform the OPF with a time resolution of 1 minute, but the communication system may be limited to transmit this information to the control devices every 15 minutes. So, when the periodic control actions are taken in time intervals longer than in the forecasting stage, a method to decide the set-points for each interval of the control stage has to be defined. In this case, the median of all the set-points from the forecasting stage within the same time interval is used. In the previous example, it would be equivalent to use the 8$^{th}$ largest set-point in all the simulations of the 15-minutes interval. This process represents how the DSO may choose a representative set-point for every period considering the constraints of the communication network. With this process, every set-point is kept constant until the next set-point arrives. Then, another OPF is performed with the same time resolution used in the forecasting stage, but fixing the values of the set-points based on the previous criteria and being the OLTC located in the substation (slack bus) the only control variable. Finally, the results of the OPF at each time *h* for the following KPIs are obtained according to (4.10) to (4.12), respectively:

- $v_{i,h}^{VD}$: voltage deviation over the admissible limit at each node *i.*
- $p_{j,h}^{EC}$: energy curtailment at each generation unit *j*.
- $p_h^{EL}$: network energy losses.

$$v_{i,h}^{VD} = \begin{cases} v_{i,h} - V_0^{max}, & v_{i,h} > V_0^{max} \quad \forall i \in N, h \in H \\ 0, & V_0^{min} \leq v_{i,h} \leq V_0^{max} \quad \forall i \in N, h \in H \\ V_0^{min} - v_{i,h}, & v_{i,h} < V_0^{min} \quad \forall i \in N, h \in H \end{cases} \tag{4.10}$$

$$p_{j,h}^{EC} = P_{j,h}^{Gmax} - p_{j,h}^{G} \qquad \forall j \in M, h \in H \tag{4.11}$$

$$p_h^{EL} = p_{1,h}^{G} - \sum_{i \in N} P_{i,h}^{D} + \sum_{j \in M} p_{j,h}^{G} \qquad h \in H \tag{4.12}$$

### 4.3.2. **Economic assessment**

The economic impact of forecast accuracy and set-point timing is analysed considering the results of the control stage in the technical assessment through different monetization formulas to convert the technical KPIs into economic KPIs, according to common cost-benefit analysis methodologies for smart grid projects (EPRI, 2010; JRC, 2012a). Equations (4.13) to (4.15) show the computation of the cost of voltage deviation ($c^{VD}$), energy curtailment ($c^{EC}$) and energy losses ($c^{EL}$), where *UC* stands for the unitary cost of these parameters.

$$c^{VD} = \sum_{h \in H} \sum_{i \in N} P_{i,h}^{D} \cdot UC_{i,h}^{VD} \tag{4.13}$$

$$c^{EC} = \sum_{h \in H} \sum_{j \in M} p_{j,h}^{EC} \cdot UC_{h}^{EC} \tag{4.14}$$

$$c^{EL} = \sum_{h \in H} p_h^{EL} \cdot UC_h^{EL} \tag{4.15}$$

Note that these KPIs are computed ex-post, so they just quantify the costs from the technical assessment in monetary terms. The unitary costs used for this economic assessment are chosen considering a social perspective, which means that they are not actual costs but they somehow represent the benefits obtained from a better performance of this application.

For instance, the presence of voltage deviations over the technical limits jeopardizes electricity supply. For this reason, in Europe the Voltage Disturbances Standard EN 50160 sets a maximum voltage magnitude variation in MV and LV networks of ±10% for 95% of the week (Markiewicz & Klajn, 2004). However, some countries have implemented more restrictive limits, such as ±5% in Portugal or ±7% Spain (CEER, 2011). Therefore, in an extreme situation of voltage deviation, the social cost that may be borne is the cost of non-served energy (NSE), also referred as Value of Loss Load (VoLL), which represents the value that electricity users attribute to continuity of supply. This value can be used as an upper bound for the voltage deviation cost, so when the voltage exceeds a predetermined threshold, the associated cost can be approximated with the VoLL. For lower values, a linear or quadratic function can be used (Frías, 2008).

In Figure 4-3 an illustrative scheme of the cost function with a linear approach is shown, where the thresholds for the maximum and minimum voltage magnitudes associated to the VoLL are indicated as $V^{VoLL\_max}$ and $V^{VoLL\_max}$, respectively. So, the social cost of a voltage deviation at a certain node can be obtained by multiplying the consumption of that node by the corresponding penalty. The value of VoLL can be very different depending on the region and the customer sector (e.g. residential, industrial or commercial). Estimations of VoLL for different countries and sectors can be found in (Losa & Bertoldi, 2009), where authors concluded that in the long term VoLL values could lie in intervals of 5-25€/kWh for developed countries, and 2-5€/kWh for developing countries. In (Linares & Rey, 2013) an estimation of VoLL for the different sectors and regions of Spain can be found, where authors concluded that the cost of one kWh of NSE was above 4€/kWh but the economic signals sent to DSOs to avoid these interruptions were lower, which might result in underinvestment in short-term energy security. However, there are other European countries like Slovenia or Malta that present higher levels of interruptions, so this kind of incentive is especially important in these countries (CEER, 2016).

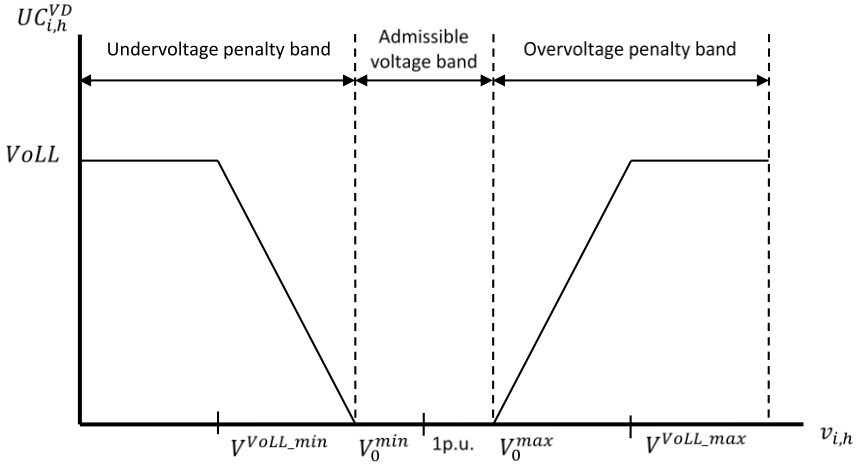


**Figure 4-3 Scheme of the voltage deviation cost function**

With regard to energy curtailment, the economic effect from the system point of view of reducing the production of renewable energy is that the same amount of energy has to be produced with conventional generation. This effect can be represented in a simplified way as an energy purchase at the wholesale market hourly price. This approach can be also applied to assess the economic impact of energy losses. As in the case of VoLL, wholesale energy prices present different values in each country, but in Europe these prices are currently in the range of 25-50€/MWh (European Commission, 2016). Finally, the flowchart of the complete centralised voltage control assessment described in this section can be found in Figure 4-4.

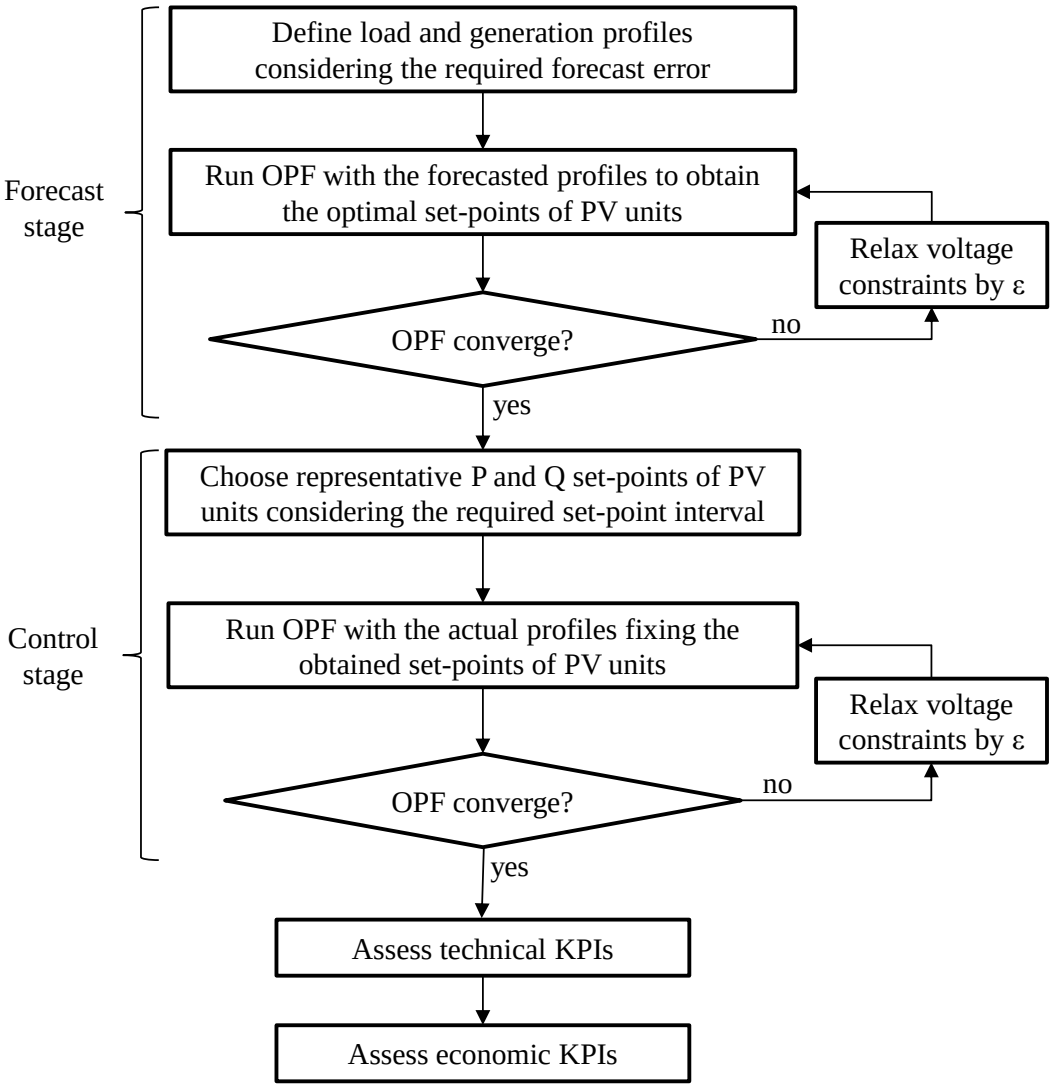


**Figure 4-4 Flowchart of the centralised voltage control assessment**

## 4.4. Case studies description

In this section, the case studies used to apply the presented assessment methodology are described. These case studies represent a rural LV network and a semi-urban MV network located in the region of Évora in Portugal (SUSTAINABLE project, 2016a). In Table 4-1 the main characteristics of these networks are summarized, whereas their geographical representation is shown in Figure 4-5 and Figure 4-6, respectively. The contracted power and installed capacity used in these case studies are significantly higher than the actual values to analyse the effect of the centralised voltage control in future scenarios. Although all DG units are based on PV generation, the presented methodology could be also applied with any other type of DG, like wind power or micro-cogeneration.

**Table 4-1 Characteristics of the case studies**

| | LV network | MV network |
|---|---|---|
| Voltage (kV) | 0.4 | 15 |
| Network length (m) | 650 | 7,550 |
| Number of LV customers (LV network) or MV/LV secondary substations (MV network) | 12 | 35 |
| Contracted power (MVA) | 0.65 | 28.41 |
| Number of PV units | 5 | 12 |
| PV installed capacity (MVA) | 0.25 | 46 |

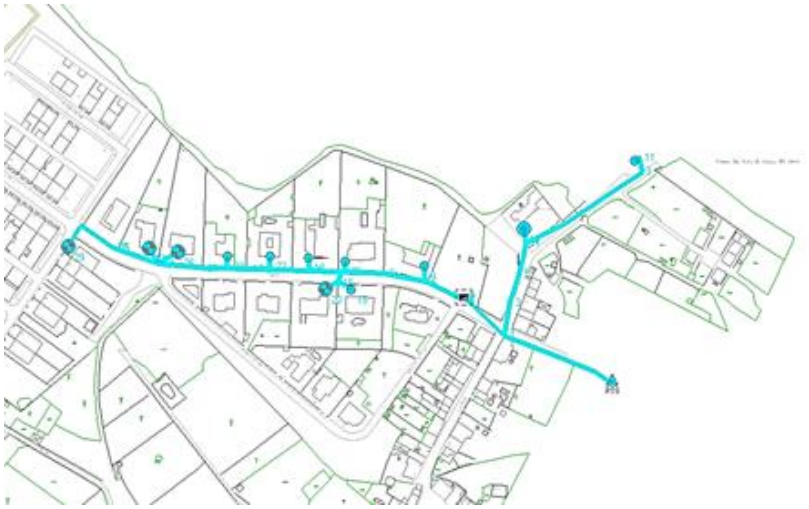

**Figure 4-5 Portuguese rural LV network case study (blue line)**
(SUSTAINABLE project, 2016a)

**Figure 4-6 Portuguese semi-urban MV network case study (red line)**
(SUSTAINABLE project, 2016a)

Although these scenarios are severe for the analysed networks, the conclusions obtained from the proposed methodology provide a useful insight about the impact of the forecast accuracy and set-point timing in a centralised voltage control application, which can be extrapolated to other networks facing voltage problems.

In the simulations, demand and generation profiles for a 24-hour interval with 1 minute resolution are used. The load profiles of the LV customers are obtained with the Load Profile Generator tool ("LoadProfileGenerator," 2016), a modelling tool for residential energy consumption. The characteristics of the load profiles used are the ones corresponding to the type of customer CHS01 (family, 2 children) in HT06 (normal detached house). Figure 4-7 shows a set of 6 samples of residential consumer profiles modelled with the previous software used in the LV case study. For the MV network, an aggregated consumer profile obtained with 65 residential profiles is used to represent a MV/LV secondary substation, which is shown in Figure 4-8. Figure 4-9 shows the PV generation profiles that are used in the study, which are from a real PV unit in the area, one for a sunny day and other for a cloudy day. Note that all the profiles are defined in p.u., so the actual consumption and supply are obtained multiplying these load and generation profiles by the contracted power or installed capacity of each customer or PV unit, respectively.

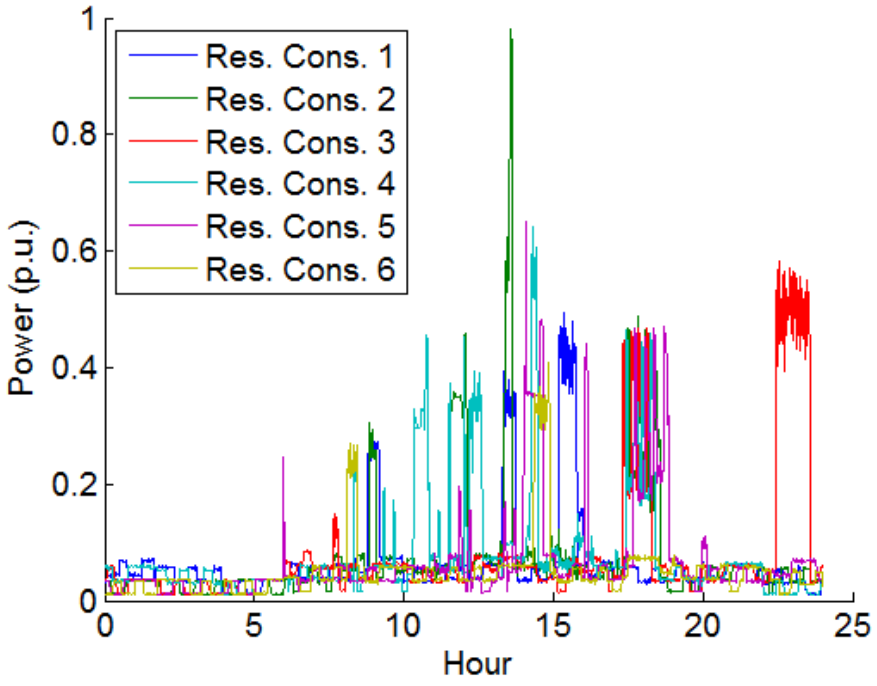


**Figure 4-7 Residential consumer profiles with 1 minute time resolution**
("LoadProfileGenerator," 2016)

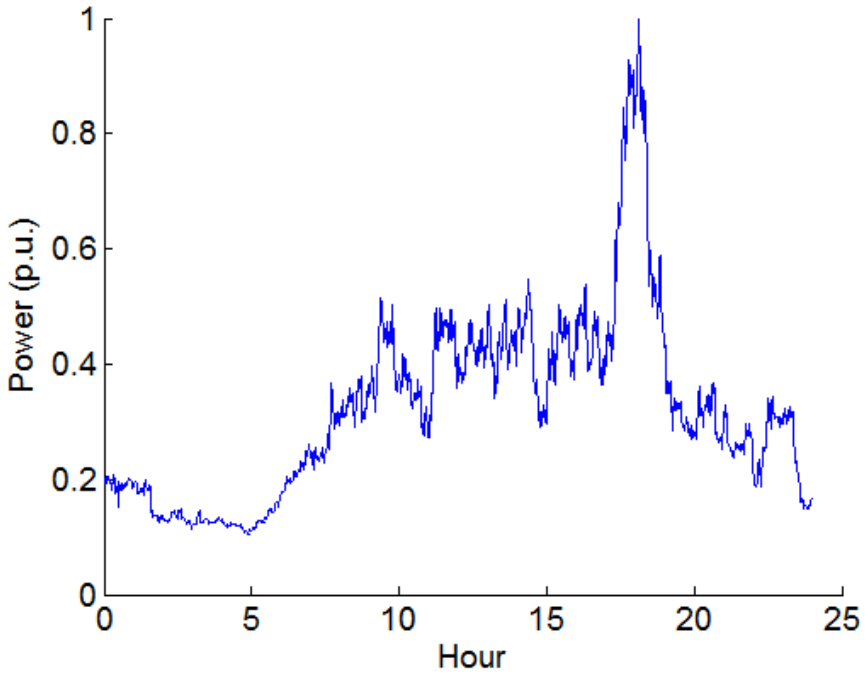


**Figure 4-8 MV/LV secondary substation profile with 1 minute resolution**
("LoadProfileGenerator," 2016)

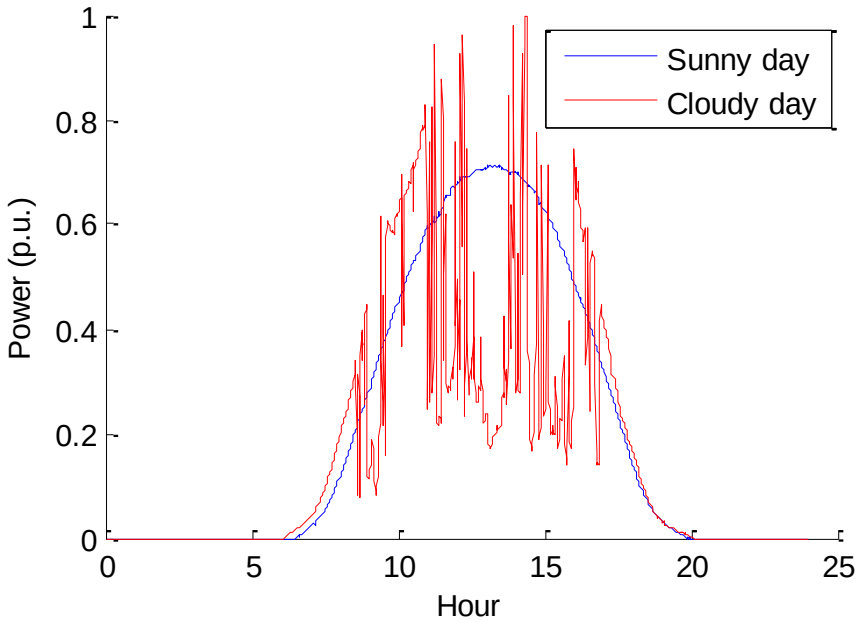


**Figure 4-9 PV generation profiles with 1 minute resolution**

In Table 4-2, the parameters used to obtain the voltage deviation cost function described in Section 4.3.2 are presented, and the resulting function is depicted in Figure 4-10. The admissible voltage limits are set to ±5% according to Portuguese legislation, whereas the threshold for the maximum penalty is set to ±20% to represent the situation where electricity supply can be damaged. The value for the VoLL is set to 3€/kWh according to (Rodriguez-Calvo, Frías, Reneses, Cossent, & Mateo, 2014), and the intermediate values are obtained with a linear interpolation. Besides, the value of the parameter ε described in Section 4.3.1 to relax the admissible voltage limits when the OPF does not converge is set to 0.01 p.u.

**Table 4-2 Parameters of the voltage deviation cost function and used values**

| Parameter | Value |
|---|---|
| $V_0^{min}$ | 0.95p.u. |
| $V_0^{max}$ | 1.05p.u. |
| $V^{VoLL\_min}$ | 0.8p.u. |
| $V^{VoLL\_max}$ | 1.2p.u. |
| $VoLL$ | 3€/kWh |

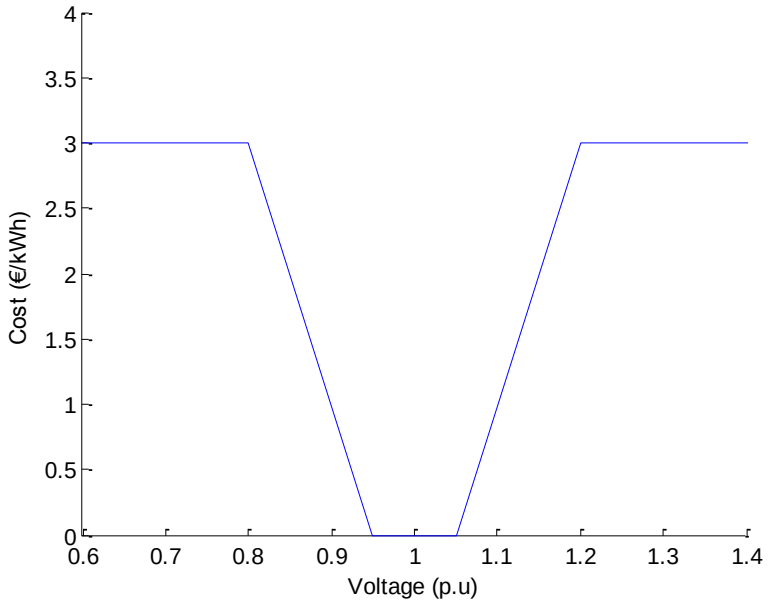


**Figure 4-10 Voltage deviation cost function**

Finally, the energy production cost function used to estimate the costs of energy curtailment and electricity losses related to these KPIs is represented in Figure 4-11. This function is also used in the OPF to define the hourly energy production cost of the slack bus. The values are obtained with the average hourly prices of the Iberian day-ahead electricity market in 2013 ("OMIE," 2016).

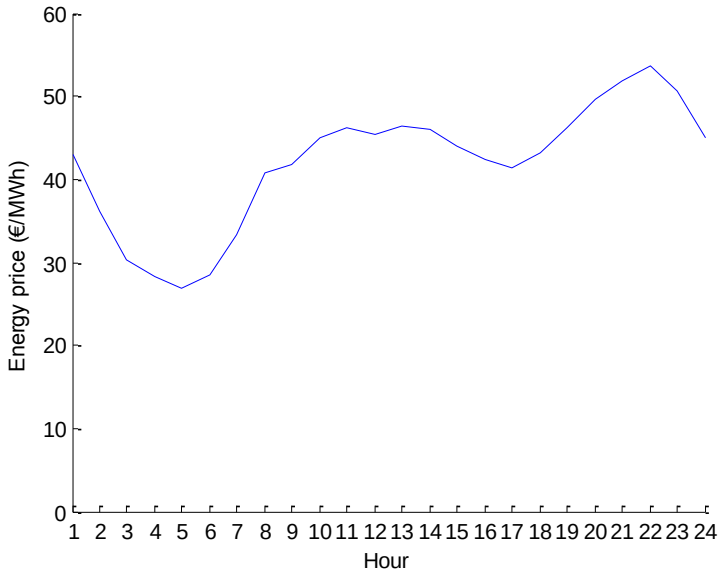


**Figure 4-11 Hourly energy price cost function**

## 4.5. Performance analysis

The analysis of the impact of forecasting and communication on a centralised voltage control application is presented in this section, where the methodology explained in Section 4.3 is applied to the case studies described in Section 4.4. Then, two type of analysis are carried out for each network:

- Forecasting analysis: impact of forecast accuracy to calculate the set-points.
- Communication analysis: impact of set-point timing to send the control signals.

The forecasting analysis is focused on the forecasting stage defined in Section 4.3, and is aimed to quantify the impact of the forecasting errors included in the load and generation profiles used by the centralised voltage control application to compute the set-points for the OLTC and the PV inverters. In this analysis, the following forecast errors are used: 0% (perfect forecast), 10%, 20%, 30% and 40%. These errors are applied for the scenarios of PV underestimation and demand overestimation, and PV overestimation and demand underestimation. Then, in this analysis the OPF is performed in the case studies with the forecasted 24-hour profiles and 1 minute resolution (1,440 simulations), and then the obtained set-points are applied in another OPF with the actual profiles considering also 1 minute set-point time interval to analyse the effect of the forecasting error alone. Thus, since there are five sensitivities for the forecasting errors, two scenarios, and two stages, a total of 28,800 simulations are carried out in this analysis.

The communication analysis aims to evaluate the impact of using different time intervals to send the set-points from the central unit to the PV inverters, so this time the focus is on the control stage defined in Section 4.3. In this case, the initial OPF is computed considering only a perfect forecast of the load and generation profiles, so the forecasting analysis does not interfere with this one. The following time intervals are used to analyse the impact of set-point timing: 1min, 5min, 15min, 30min, 1h, 2h, 4h, 8h and 24h. Notice that longer intervals are multiple of shorter intervals for a better comparison. Then, this time the OPF is carried out only in the forecasting stage with 1-minute resolution and 0% forecasting error, but in the control stage is performed for the 9 sensitivities of set-point interval. As explained in Section 4.3, when a time interval longer than 1-minute is analysed, the set-points applied in the each interval are chosen using the median of all the set-points from the previous simulation. Finally, this analysis is applied in two scenarios, one with the PV profile of the sunny day and the other with the cloudy day. In the forecasting analysis, only the cloudy day profile is used. Then, in both analysis the same number of simulations are performed. A summary of the described implementation details for each scenario is included in Table 4-3. The tables with all the results are included in Appendix E.

**Table 4-3 Implementation details of the analysed scenarios in the case studies**

| | **Forecasting analysis** | | **Communication analysis** | |
|---|---|---|---|---|
| | **Scenario 1** | **Scenario 2** | **Scenario 3** | **Scenario 4** |
| **PV forecasting error** | 0%, 10%, 20%, 30%, 40% underestimation | 0%, 10%, 20%, 30%, 40% overestimation | 0% | 0% |
| **Load forecasting error** | 0%, 10%, 20%, 30%, 40% overestimation | 0%, 10%, 20%, 30%, 40% underestimation | 0% | 0% |
| **Set-point time interval** | 1 min | 1 min | 1min, 5min, 15min, 30min, 1h, 2h, 4h, 8h, 24h | 1min, 5min, 15min, 30min, 1h, 2h, 4h, 8h, 24h |
| **PV profile** | Cloudy day | Cloudy day | Sunny day | Cloudy day |

### 4.5.1. Forecasting analysis

Figure 4-12 (a) shows the economic results of the defined KPIs (cost of voltage deviation, energy curtailment and energy losses) for the sensitivity of the forecast error using the PV profile of a cloudy day, for the case of PV generation underestimation and load overestimation in the LV network. As explained in Section 4.2, in this forecasting scenario the voltage profiles obtained with the OPF are expected to be lower than the actual ones. This means that overvoltages would be worse mitigated, but on the contrary undervoltages would be less likely to arise.

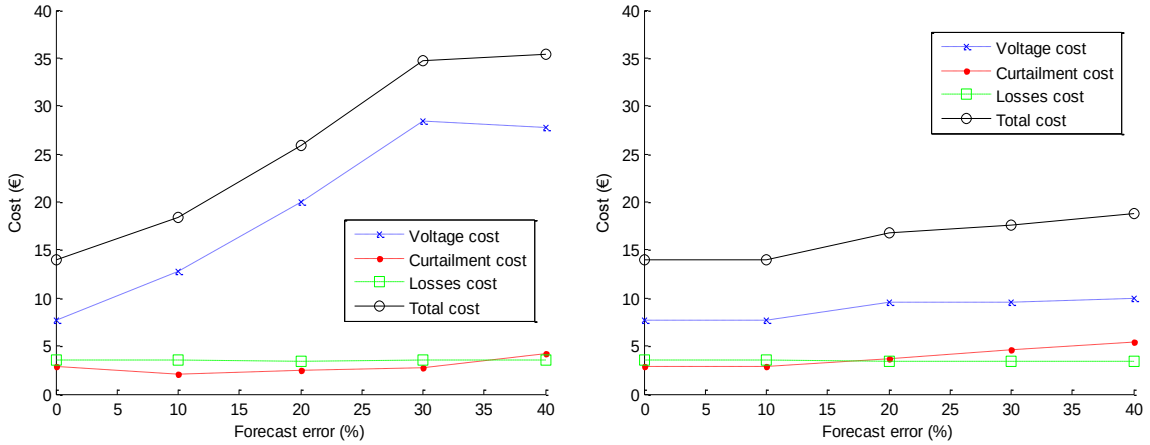


**Figure 4-12 Impact of the forecast error in a cloudy day in the LV case study. (a) PV underestimation and demand overestimation. (b) PV overestimation and demand underestimation**

Then, it can be seen that when underestimating PV generation, higher forecast errors cause a significant increase of voltage costs. This is mainly because the control signals dedicated to compensate the overvoltages are less intense than actually required. By contrast, it can be noted that the curtailment cost decreases with a forecast error of 10% compared to the situation of perfect forecast, but with higher forecast errors the curtailment costs also increase. Moreover, in the case of 40% forecast error, the higher increase in the curtailment cost causes a decrement in the voltage cost. This effect is due to the differences in the demand profiles between the different customers, which makes that for higher levels of demand, the OLTC is not able to keep all voltages within limits and curtailment is required since reactive power compensation has a very limited effect in LV networks. Indeed, in this network the demand is the dominant part. Then, it can be concluded that even when the amount of PV forecasted is small, the effect in voltage control can be substantial. Finally, it can be observed that the effect of the losses cost is similar to the curtailment cost, and is not very affected by the control actions.

Figure 4-12 (b) shows the results in the case of overestimating generation and underestimating demand, where it can be seen that curtailment costs increase with the increase of the forecast error. However, in this case this effect is more natural than in the previous scenario because when generation is overestimated, control signals for energy curtailment are higher than actually needed. Furthermore, since the demand forecast reduces the amount of expected consumption, the estimated voltages are significantly higher than in the previous case, so the control actions sent to the PV inverters are even more restrictive and make voltage costs keep practically constant.

Comparing both figures, it can be seen that the impact of the forecast error in total costs is higher in the PV underestimation than in the overestimation scenario, and the main driver in both cases is the voltage cost. Additionally, PV curtailment has been proved as an effective way to mitigate voltage deviations in this network, since small control actions can provide significant improvements in voltage profiles.

Figure 4-13 (a) and (b) show the sensitivity to the forecast error in the MV case study for the scenarios of underestimating PV generation and overestimating demand, and overestimating PV generation and underestimating demand, respectively.

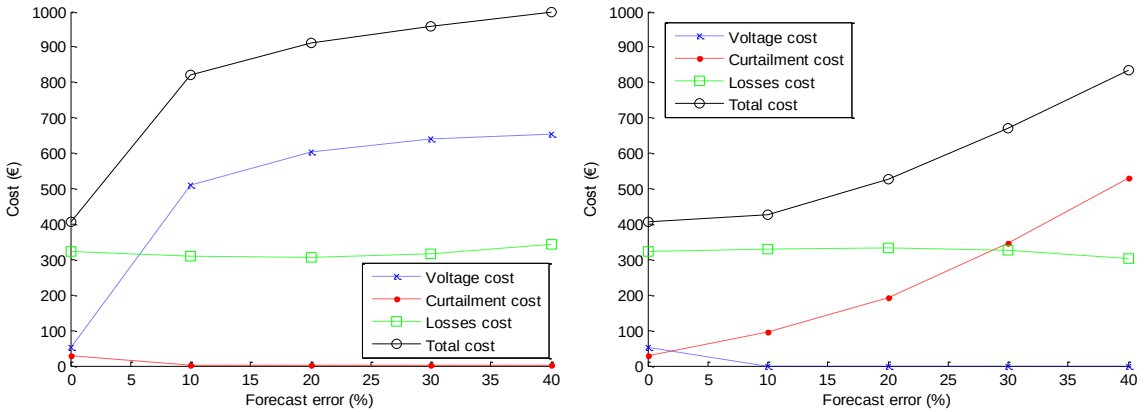


**Figure 4-13 Impact of the forecast error in a cloudy day in the MV case study. (a) PV underestimation and demand overestimation. (b) PV overestimation and demand underestimation**

The results obtained in this network are more aligned with what it may be expected for this forecasting analysis. In the case of PV underestimation, it can be seen that voltage costs increase with the increase of the forecast error whereas curtailment costs decrease. Then, when the forecast error for PV underestimation is higher, the obtained control actions do not include PV curtailment since overvoltages are not identified. For this reason, larger forecast errors cause additional voltage costs, but with a lower impact than in the case of perfect forecast, which is the only case with PV curtailment. In the case of PV overestimation, it can be noted that higher forecast errors result in higher curtailment costs, because the higher expected PV generation involves higher overvoltages that have to be mitigated. However, most of these actions are not necessary since the scenario with 10% of forecast error already presents no voltage deviation. Nevertheless, although this scenario removes the voltage cost due to the higher curtailment, the curtailment decisions are not made efficiently so additional system costs are incurred. Finally, the effect of network losses can be better identified in this case study, although small variations are observed. Despite in Figure 4-13 (a) the main cost driver is voltage deviation and in Figure 4-13

(b) the curtailment cost, for very high values of forecast error the total costs in both cases are quite similar. However, for lower values of this parameter, generation underestimation scenarios show higher total costs than in the case of generation overestimation.

From this analysis, it can be concluded that the worst scenario for the forecasting applications is the PV underestimation and demand overestimation, mainly in terms of voltage deviation costs. Indeed, it can be seen that in both networks a 10% forecast error for this scenario produces a total cost similar to the one obtained with a 40% forecast error in the PV overestimation and load underestimation scenario. However, scenarios with PV overestimation usually involve higher curtailment requirements, which penalise the DG. Then, the reduction of the forecast error leads to better results of the voltage control application, because more accurate forecasts enable more effective control actions. For instance, the forecasting tool developed in (A. Madureira et al., 2015) can achieve a normalized root mean square error of approximately 10%, being the highest performance reached when the forecast is carried out for short term periods. Then, if the information is frequently updated the control actions can be more effective, as it was also highlighted in (Ziadi et al., 2014). The impact of this effect is precisely analysed in the next section.

### 4.5.2. Communication analysis

Figure 4-14 (a) and (b) show the results for the sensitivity of the set-point interval in the LV network considering perfect forecasts for the PV profiles of the sunny and cloudy days, respectively. In both cases it can be seen that the reduction of the set-point interval involves lower voltage costs thanks to a better adjustment to the actual voltage profiles, especially when the time interval is lower than one hour.

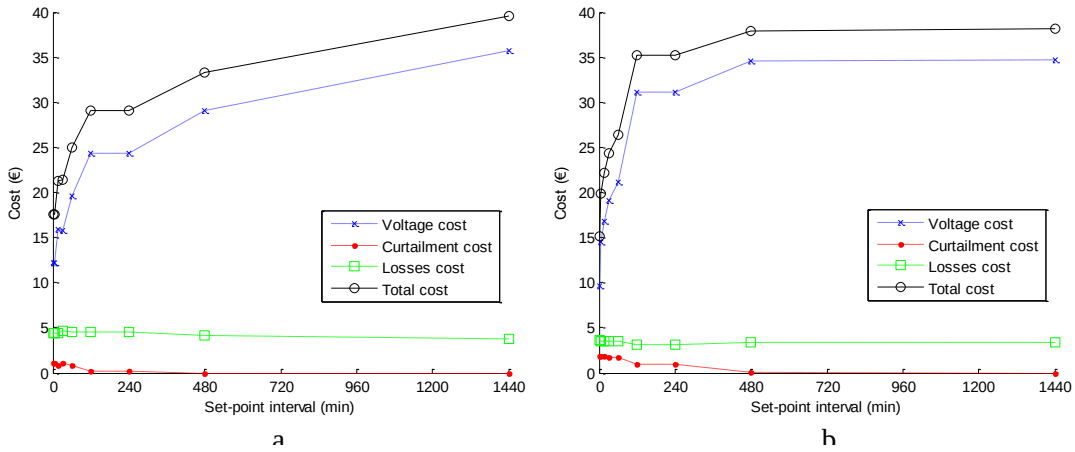


**Figure 4-14 Impact of the set-point interval with perfect forecast in the LV case study. (a) Sunny day. (b) Cloudy day**

Note that within this time interval the reduction of the voltage cost is related to a slight increase of the curtailment cost, which allows maintaining the voltages closer to the admissible limits. This effect is more intensified in the cloudy day, since the PV profile shows higher peak values. Therefore, even though in the cloudy day the curtailment actions are higher than in the sunny day for longer set-point intervals, the voltage costs are still higher. Then, in the sunny day PV voltage control is more effective. Finally, it can be seen that the effect of the set-point interval in energy losses in this network is not very high.

Figure 4-15 (a) and (b) show the same sensitivity in the MV network. In both cases total costs present a dramatic reduction with a set-point interval of 1 minute and saturate with intervals between 2h and 4h, and very similar values are obtained. However, in the cloudy day voltage costs are considerable lower than in the sunny day. This effect is caused by the lower voltage used at the slack bus in this scenario, which reduces the overvoltages but increases the energy losses. All these results show the complexity of the analysis, which is affected by many different factors but yields important conclusions.

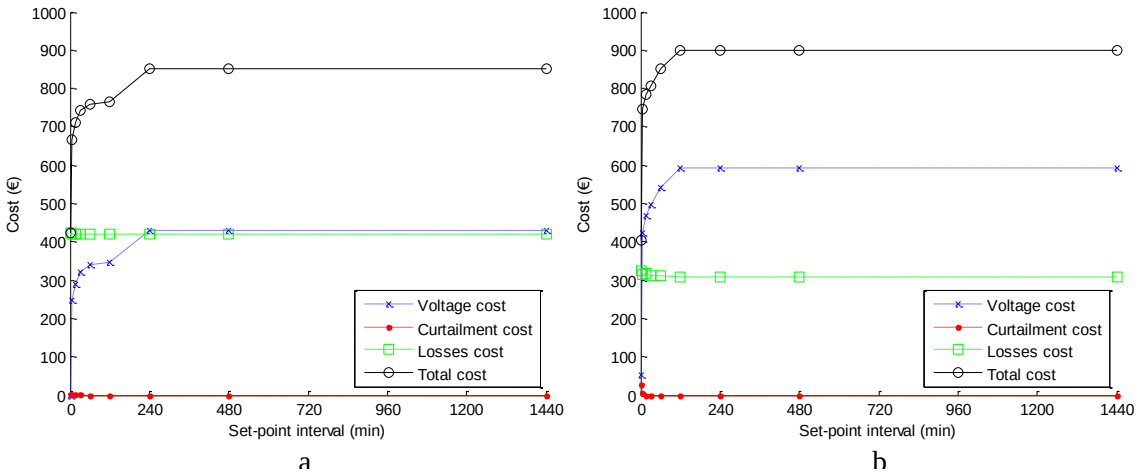


**Figure 4-15 Impact of the set-point interval with perfect forecast in the MV case study. (a) Sunny day. (b) Cloudy day**

The results from this communication assessment confirm that centralised voltage control applications with shorter set-point intervals are beneficial for the grid, regardless of the PV generation profile. Nevertheless, these improvements may be achieved only below a certain value of set-point interval. From the scenarios analysed in this study, it can be concluded that this threshold is approximately 1 hour.

In this sense, the communication technology and strategy used to transmit the set-points is very important. For instance, PLC is widely used in European low voltage networks, mainly

for smart metering applications. However, since it uses the electric cables as communication channel, the performance of this technology is highly affected by noise and signal attenuation as it was demonstrated in Chapters 2 and 3. Additionally, PV inverters produce high levels of impulsive noise, which can jeopardize the communication (Galli et al., 2011). Wireless communication technologies like GPRS are also used in monitoring and control applications, but they are affected by the quality of the local coverage. In terms of data transmission rates, both technologies can achieve a similar performance, since PLC based on PRIME standard provides data rates up to 130kbps, whereas GPRS provides 110kbps in the downlink and up to 26.8kbps in the uplink (G. López et al., 2015). Indeed, these are the technologies used in the SUSTAINABLE project (Bessa et al., 2014), and both can theoretically achieve time intervals up to 5 or 15 minutes, although their real performance depends on the local network conditions. However, since the voltage control application obtains the best performance with a set-point timing of 1 minute, especially in the MV, other communication technologies with higher data rates like optical fibre can be considered.

Finally, it is important to highlight that the voltage control technique used in this study is relatively simple, because the main objective is to illustrate the forecasting and communication sensitivities instead of the performance of a new voltage control approach. However, this methodology can be replicated with more sophisticated voltage control algorithms, but a simplified approach like this one has the advantage of drastically reducing the computation time required.

## 4.6. Conclusions

In this chapter, a methodology to analyse the impact of forecast accuracy and set-point timing for a centralised voltage control application has been presented. Although the presented analysis is particularized for the case of PV generation, the complete methodology can be perfectly applicable to any kind of DG, like wind power or micro-cogeneration. The main novelty of the presented approach is that it is focused on the assessment of the value of information considering forecasting and communication issues from a technical and economic point of view, which is a gap that has been found in the literature review. Additionally, sensitivities related to the type of forecast error (underestimation or overestimation) and the type of day for the PV generation profile (sunny or cloudy) have been taken into account to provide more practical conclusions. This methodology has been applied through simulations in two real networks. From the technical and economic assessment of the case studies it can be concluded that both the

forecast error and the set-point interval significantly affect the performance of the voltage control. Indeed, the results show that the enhancement of both factors provides similar benefits in the considered scenarios.

The forecast error leads to an increase of voltage cost when PV generation is underestimated. Conversely, when PV generation is overestimated, curtailment cost increases. Although drivers are different, in both cases the forecast error involves an increase of total cost, meaning that the lowest cost corresponds to perfect forecast. Hence, as expected it is preferable to make all related calculations with the actual load and generation profiles, but the savings obtained with an improved forecast should be compared to the cost to further reduce the forecast error.

With regard to the set-point interval, the results are very similar concerning sunny and cloudy days. It has been concluded that intervals shorter than 1 hour to send the set-points provide important voltage cost reductions, which has been found as the main cost driver for this assessment. In the case of the MV network, a the highest reduction is obtained with a time interval of 1 minute, so technologies like PLC or GPRS would not probably be appropriate for this application at this voltage level and other options with higher data rates like optical fibre can be considered. However, a much lower impact has been found when comparing set-point intervals between 4 hours and 24 hours, so a reduction in the time interval within this range would not be so interesting although under certain conditions important savings can be obtained, like in the LV case study for the sunny day scenario. As in the forecasting analysis, the cost reductions obtained with lower set-point intervals should be compared to the increase of the operation and maintenance costs of the control devices and the communication infrastructures, especially when more expensive technologies are needed to achieve the communication requirements.

All these conclusions highlight the importance of dedicating resources to improve both communication systems and forecasting tools. Nevertheless, the validity of this assessment is subject to the availability of the DSO to control DG that is established by the regulation at each country, as well as to the voltage quality requirements and remuneration schemes. In this sense, the presented methodology is particularly interesting in those cases where curtailment is allowed and voltage quality requirements are more stringent. Notwithstanding, the economic trade-off between voltage quality and RES curtailment highlighted in this chapter is a topic that has to be further investigated. Finally, it is important to bear in mind that the voltage cost is a fictitious cost that takes into account the social impact of having poor power quality conditions. For this reason, this effect was included as a constraint instead of in the objective function, so the effect of the voltage deviations can be assessed without affecting the actual system operation costs.

# Chapter 5: Conclusions, Contributions and Future Research

## 5.1. **Introduction**

In this thesis, the performance and the impact of Information and Communication Technologies (ICT) in current smart grids applications have been analysed from a novel technical and economic perspective, where many relevant findings have been obtained.

Communication infrastructures are essential for the deployment of smart grids. However, the review carried out in the introduction of this thesis confirmed the idea highlighted by previous authors about the current need for proper tools and methodologies dedicated to analyse the performance of smart grids from a technical and economic point of view.

Power Line Communications (PLC) was identified as the most cost-effective solution, since it allows the reutilization of the power infrastructure as communication channel. This technology has been widely used for AMI, especially in Europe due to the smart meters roll-out currently deployed in most countries. However, the performance of this technology is highly affected by the local network conditions. Among the different PLC protocols used for AMI, PRIME was found as the one that provides the best performance under favourable conditions.

The methodology developed in this thesis to analyse the performance of PLC PRIME networks has been shown as a very useful tool to provide practical results under different network conditions. The two KPIs defined for the analysis related to the number of registered nodes and the time to read all meters have reported really useful insights about the performance of the analysed networks, and the methodology has been satisfactory applied to distribution networks with a tree topology of any size. Additionally, the use of Reference Network Models (RNMs) has been identified as an interesting option to obtain representative networks that can be later analysed with the proposed methodology avoiding the use of confidential data from DSOs. The combination of both tools has resulted in a very powerful way to analyse the communication performance of PLC networks in regions of large size, focusing only on the most critical areas.

The conclusions obtained with the previous methodology provide valuable information for communication network planning and motivate the use of this methodology for this purpose. Thanks to this approach, it can be determined in which distribution networks PLC can be effectively deployed to meet the communication requirements under different operating

conditions. Furthermore, economic analyses can be supported by this methodology to analyse the viability of a cost-effective solution like PLC for different smart grids applications.

The added value provided by better information and communication systems in smart grids was also found as another gap in the literature review. Then, a methodology to analyse the impact of these systems in a centralised voltage control application with OLTC and PV based on inverters has been presented. The selection of this application was motivated by the high dependence of this functionality on ICT, as well as by the expected increase of solar PV in distribution networks and the beneficial effect of voltage control mechanisms to mitigate the voltage problems that might arise in scenarios with large PV penetration.

Since this kind of centralised voltage control application aims to send control set-points from the central unit to the OLTC and PV inverters to optimize the system operation, the presented methodology focused on the impact of the accuracy of the forecast used to calculate the set-points and the time interval used to update these set-points in the PV inverters. The voltage deviation cost, the energy curtailment cost, and the energy losses cost were chosen as KPIs, and have helped to reveal the impact of the previous concepts proving interesting conclusions in economic terms.

This conclusions chapter is divided as follows. First, the main conclusions derived along the research work are summarized. Then, the principal thesis contributions are explained and the future lines of research are presented. Finally, the related journal publications and international conference presentations are listed.

## 5.2. Main conclusions

In this section, the conclusions that have been drawn from the methodologies developed in this PhD related to the performance analysis of PLC PRIME networks for smart metering applications and ICT for centralised voltage control are presented below:

1. **The registration process highly affects the performance of PLC PRIME.**

In a PLC PRIME network, the registration of the service node by the base node is an essential requirement to proceed with the transmission of data between both devices. However, under certain conditions the base node is not able to maintain all the service nodes correctly registered, which causes important delays in the reading process. This is because the nodes try to retransmit the information until it is correctly received. The promotion of service nodes to the switch state can help to finish the registration process properly. Nevertheless, as the number of

switches increases, the complexity of the network also increases and the communication performance is substantially reduced.

In all the registration processes analysed, three differentiated stages have been observed. First, a high number of service nodes are registered directly by the base node. Then, the promotion of service nodes to the switch state enables the registration of new nodes in different steps. Finally, all the service nodes remain registered unless instability problems appear. These instability problems are usually due to collisions in the medium or channel congestion, and cause continuous registration and deregistration of certain of nodes that can seriously affect the performance. In cases where the instability problems are permanent or when a significant amount of nodes cannot be registered, alternative communication technologies can be used after exploiting all the capabilities and coverage of PLC. The areas where it is more likely to find nodes with instability problems are at the end of the feeders due to higher attenuations. On the one hand, this has the advantage that they do not cause cascade effects, but on the other hand, they can jeopardize the system operation in case they are controllable nodes or manage critical information.

With regard to the time to read all meters, when the registration process was performed correctly the reading time was usually lower than 15 minutes, which is a typical reference value used for smart metering scenarios. Another interesting conclusion is that faster registration processes do not necessary involve faster reading times, which means that the time required to finish the registration process is not a reliable indicator about the network communication performance.

**2. User density is a good indicator of the performance of PLC PRIME.**

User density can be used as a first indicator of the communication performance that can be expected in the network, where higher density networks generally present more demanding traffic management conditions, and networks with higher dispersion of users are more likely to show registration problems focused on specific nodes. The number of users is the parameter that affects the most to the performance. Indeed, in the analysed case studies with the highest number of users the 15 minutes threshold was normally exceeded. Conversely, in the networks with the lowest number of nodes, the time to read all meters was lower than 5 minutes. Moreover, it was proved that the relationship between these two parameters is not linear, but shows an exponential trend. The feeder length has also a noticeable impact, where a linear increase was found in the time to read all meters when increasing this parameter in the simulated scenarios.

The number of buildings per feeder and the number of feeders per secondary substation affect less to the communication performance, but two interesting conclusions have been found.

A maximum value for the reading time was found between scenarios with 3 and 9 buildings. This means that scenarios with lower user dispersion along the feeder favour the communication performance, which can be obtained in networks with high user concentration in the buildings, or high building concentration in the feeders. A minimum value was found between the scenarios with 3 and 9 feeders. This means that when all nodes are located in the same feeder their logical connection is easier since the amount of service nodes that can be connected through a switch is higher, but then the network is more congested because of more adverse traffic conditions.

With respect to the signal attenuation, both LV and MV networks showed attenuations between 3 and 10 dB for neighbour nodes in the base scenarios, which are aligned with the results obtained by other authors. However, the MV network showed higher attenuations between the base node and the nodes at the end of the feeders, since it was larger than the LV network and presented four times more nodes, which is also aligned with the aforementioned conclusions related to the impact of the number of nodes and feeder length.

**3. Noise, load and traffic conditions dynamically modify the performance of PLC.**

An important characteristic of the physical channel that presents a very high impact in the network performance is the impulsive noise, especially for communications between nodes that are connected over longer distances. For this reason, the application of noise cancellation techniques is highly recommended for any kind of PLC deployment. Another dynamic parameter that affects the performance is the value of the loads. Scenarios with low impedances due to high consumption present a very poor performance compared to the opposite scenarios. As a matter of fact, doubling the value of the load impedance causes a reduction in the attenuation by half. This situation happens when consumption is reduced in 50%. Off-peak scenarios should be chosen to communicate with nodes that can present registration problems, as far as the communications are not related to critical processes.

The size of the messages can also have an impact in the performance. Then, with small packet sizes (e.g. 200 Bytes) the probability of having registration problems is lower, and the communication performance is better than with large packet sizes (e.g. 2,000 Bytes). An increase of ten times the packet size resulted in an increase of three times the time to read all meters in the simulated scenarios, which means that this parameter is not critical for the network performance.

**4. The reduction of forecast errors and set-point intervals improves voltage control.**

From the forecasting analysis, in the case of PV underestimation and load overestimation, higher forecast errors have resulted in higher voltage costs and lower curtailment costs, because overvoltages are not identified and then the obtained control actions do not include PV curtailment. In the case of PV overestimation and load underestimation, higher forecast errors have resulted in higher curtailment costs, because the higher expected PV generation involves higher overvoltages that have to be mitigated. The impact of the forecast error has been found higher in the PV underestimation than in the overestimation scenario, being the voltage deviation the main cost driver. As a general conclusion, the reduction of the forecast error leads to better results of the voltage control application, because more accurate forecasts enable more effective control actions.

From the communication analysis, the reduction of the set-point interval has involved lower voltage costs thanks to a better adjustment to the actual voltage profiles, especially when the time interval was lower than one hour. This cost reduction obtained with shorter time intervals was usually related to a slight increase of the curtailment cost, which allows maintaining the voltages closer to the admissible limits. Moreover, the total cost reduction obtained with lower set-point intervals was higher in the LV network, despite that the ratio between PV generation and demand is higher in the MV case study. Then, this type of voltage control application should be encouraged in LV networks. However, a reduction in the time interval from 24 to 4 hours would not be very interesting, since the total costs within this range are in general very similar, so the communication requirements for this application should be at least 1 or 2 hours. Nevertheless, in the case of MV networks, there is a huge difference when using this application with 1 minute set-point interval, so in this voltage level the communication requirements would be much higher than in the LV.

The previous conclusions highlight the importance of dedicating resources to improve both communication systems and forecasting tools. As regards to the three defined KPIs, voltage deviation has been proved as the most important cost driver in all the simulated scenarios except for the case of PV overestimation in the MV network, where energy curtailment is clearly most important. PV curtailment has been proved as an effective way to mitigate voltage deviations from a technical point of view, since small control actions can provide significant improvements in voltage profiles. Energy losses have not been identified as an important cost driver, since only small differences have been obtained between all the scenarios. However, they can significantly contribute to the total costs, so they should be taken into account for any economic analysis.

## 5.3. Original contributions

The contributions achieved in this research work are aligned with the thesis objectives, and are summarized below:

1. **A methodology to assess the communication performance of PLC-PRIME networks to identify the most critical parameters has been defined.**

PLC performance is highly affected by the local conditions of distribution networks, but a lack of methodological processes to analyse their impact on the communication network behaviour was found in the literature review. The presented methodology proposed the use of two KPIs related to the registration and reading processes that were not exploited in previous publications to carry out a sensitivity analysis that provided valuable information about the impact of specific network design parameters in the communication performance. Additionally, the defined sensitivities are especially useful for the replicability analysis of PLC-PRIME networks, a hot topic in smart grid deployments that allows extrapolating the conclusions obtained under certain local conditions to scenarios with different characteristics. This contribution has led to a journal article published in IEEE Transactions on Smart Grids (González-Sotres, Mateo, Frías, Rodríguez-morcillo, & Matanza, 2016).

2. **The communication performance of PLC-PRIME in real distribution network topologies has been analysed and practical conclusions have been provided.**

The best way to analyse the performance of a PLC network is to test the technology in the field, but simulation tools can provide a fair approximation in a more economical way. However, the application of these tools by previous authors was limited to small cases and simple network configurations. Indeed, the simulation framework used in the methodology developed in this PhD for PLC-PRIME performance analysis was only applicable to configurations where all service nodes are connected to a main feeder, which is not generally true in real networks. For this reason, an algorithm to systematically compute the channel transfer function between any pair of nodes in real network configurations of any scale was developed. This algorithm is based on well-known transmission-line theory principles and is used to apply the previous methodology in real LV and MV networks, as well as in large-scale networks obtained with a Reference Network Model (RNM). Thus, this approach is very helpful to provide scaling-up rules of PLC deployments before installing any equipment and avoiding additional costs. These contributions have led to a journal article published in IET Communications (González-Sotres, Frías, & Mateo, 2017) and another one in IEEE Transactions on Power Delivery (González-Sotres et al., 2013).

3. **A methodology to assess the impact of information and communication on voltage control from a technical and economic point of view has been developed.**

The two previous contributions extend the PhD presented in (Matanza, 2013) and provide a significant improvement for the analysis of the performance of smart grid communication technologies. However, the impact that this performance has in the operation of distribution networks was identified as another important gap to be filled. With regards to centralised voltage control applications, none of the previous references analysed the added value of better information and communication systems. Furthermore, the number of authors that have published smart grid analyses combining technical and economic approaches is very low. Then, the novel methodology developed to analyse the impact of forecast accuracy and set-point timing provides an important contribution to the state of the art and presents practical results based on the economic KPIs of voltage deviation, energy curtailment and energy losses. This has led to an article submitted to Electric Power System Research that is currently under the second review.

## 5.4. Future lines of research

The development of this thesis has led to a number of different lines for future research, where some of them are detailed in the following:

- The methodology for communication performance analysis presented in this thesis does not include a detailed model of the customer loads and Distributed Generation (DG). For instance, the variation of the consumption and generation profiles as well as the impulsive noise that the PV inverters introduce in the PLC channel highly affect the communication performance, so a better characterization would provide more realistic results.
- This methodology has been only applied to PLC based on the PRIME standard. However, it would be really interesting to analyse other protocols like G3 or Meters and More and compare their performance. Other communication technologies like GPRS or optical fibre could be also analysed. With this regard, the methodology could be extended to hybrid architectures with different technologies.
- The analysis with the simulation framework could be complemented with real measurements from the field so results could be better contrasted and a better adjustment of the tool could be performed. Specifically, real measurements of signal attenuation or transmission delays under different network conditions would be of special interest.

- The development of a co-simulation framework that relates the effects of the communication network to the actions taken in the power system would provide a holistic representation of the performance of smart grids applications. Thanks to this approach, the impact of transmission delays or communication failures could be directly measured under certain distribution system operation conditions.
- The methodology to analyse the value of information and communication on a centralised voltage control application could be extended to other smart grid functionalities like demand response or substation automation. Each functionality would probably require a specific approach to measure the economic impact.
- The value of better information and communication should be compared with the additional costs required to achieve these improvements. These costs could be related for instance to investment on research and development activities, more expensive technologies or larger amount of monitoring or control devices. With this aim in view, a cost-benefit analysis could be performed to provide more practical results.

## 5.5. List of thesis related publications

In this section a list of relevant publications coming out from the research work presented in this document are presented.

### 5.5.1. Journal publications

- González-Sotres, L., Mateo, C., Frías, P., Rodríguez-Morcillo, C., & Matanza, J. (2016). Replicability Analysis of PLC PRIME Networks for Smart Metering Applications. IEEE Transactions on Smart Grid, 3053(c), 1–9. http://doi.org/10.1109/TSG.2016.2569487
- González-Sotres, L., Frías, P., & Mateo, C. (2017). Power Line Communication Transfer Function Computation in Real Network Configurations for Performance Analysis Applications. IET Communications, 1–8. http://doi.org/10.1049/iet-com.2016.0135
- González-Sotres, L., Frías, P., & Mateo, C. Techno-economic Assessment of Forecasting and Communication on Centralized Voltage Control with High PV Penetration. Submitted to Electric Power Systems Research on the 18th of November, 2016. Under second review.

- González-Sotres, L., Mateo, C., Sánchez-Miralles, Á., & Alvar Miró, M. (2013). Large-Scale MV/LV Transformer Substation Planning Considering Network Costs and Flexible Area Decomposition. IEEE Transactions on Power Delivery, 28(4), 2245–2253. https://doi.org/10.1109/TPWRD.2013.2258944

### 5.5.2. International conference publications

- González-Sotres, L., Mateo, C., Frías, P., Rodríguez-Morcillo, C., & Matanza, J Replicability analysis of PLC PRIME networks for smart metering applications. 12th IEEE PES PowerTech Conference. Towards and Beyond Sustainable Energy Systems. Manchester, UK, June 18-22, 2017
- González-Sotres, L., Matanza, J., Cordón Peralta, C. Análisis de rendimiento de comunicaciones para lectura de contadores inteligentes. II Congreso Smart Grids. Madrid, Spain, October 27-28, 2014.
- González-Sotres, L., Mateo, C., Gómez, T., Reneses, J., Rivier, M., & Sánchez-Miralles, Á. Assessing the Impact of Distributed Generation on Energy Losses using Reference Network Models. In Cigrè International Symposium on The Electric Power System of the Future: Integrating Supergrids and Microgrids. Bolonia, Italy, September 13-15, 2011.

### 5.5.3. Other

- González-Sotres, L. Performance of Smart Grid Technologies and Applications. Seminar presented at Universidad Pontificia Comillas in a Master's subject called Current development in power systems. Madrid, Spain, March 10, 2017.
- González-Sotres, L. Eye-lectricity: looking for the cost-effective observability and control of the smart grid. Eurelectric Annual Convention & Conference, e-lectricity: the power sector goes digital. Vilnius, Lithuania, June 6-7, 2016. Video presented at the student competition. Finalist in the student award.
  http://bit.ly/eyelectricity

# References

Aalamifar, F., Hassanein, H. S., & Takahara, G. (2012). Viability of powerline communication for the smart grid. *2012 26th Biennial Symposium on Communications, QBSC 2012*, 19–23. http://doi.org/10.1109/QBSC.2012.6221343

Aalamifar, F., Schl, A., Harris, D., & Lampe, L. (2013). Modelling Power Line Communication Using Network Simulator-3. *IEEE International Symposium on Power Line Communications and Its Applications (ISPLC)*, 1–6.

Aggarwal, A., Member, G. S., Kunta, S., & Pramode, K. (2010). A Proposed Communications Infrastructure for the Smart Grid, 1–5.

Alonso, E., Matanza, J., Rodriguez-Morcillo, C., & Alexandres, S. (2014). A Switch Promotion Algorithm for Improving PRIME PLC Network Latency, 278–283.

Amarsingh, A. A., Latchman, H. a., & Yang, D. (2014). Narrowband Power Line Communications: Enabling the Smart Grid. *IEEE Potentials*, *33*(1), 16–21. http://doi.org/10.1109/MPOT.2013.2249691

Ancillotti, E., Bruno, R., & Conti, M. (2013). The role of the RPL routing protocol for smart grid communications. *Communications Magazine, …*, (January), 75–83. Retrieved from http://ieeexplore.ieee.org/xpls/abs_all.jsp?arnumber=6400442

Andreadou, N., Guardiola, M., & Fulli, G. (2016). Telecommunication Technologies for Smart Grid Projects with Focus on Smart Metering Applications. *Energies*, *9*(5), 375. http://doi.org/10.3390/en9050375

Aziz, T., Mhaskar, U. P., Saha, T. K., & Member, S. (2013). An Index for STATCOM Placement to Facilitate Grid Integration of DER, *4*(2), 451–460.

Bahramirad, S., Svachula, J., & Juna, J. (2014). Trusting the Data. *IEEE Power & Energy Magazine*, (April), 107–111.

Banwell, T. C., & Galli, S. (2001). A new approach to the modeling of the transfer function of the Power Line Channel. In *IEEE International Symposium on Power Line Communications and Its Applications (ISPLC)*.

Bari, A., Jiang, J., Saad, W., & Jaekel, A. (2014). Challenges in the Smart Grid Applications: An Overview. *International Journal of Distributed Sensor Networks*, *2014*, 1–11. http://doi.org/10.1155/2014/974682

Bessa, R. J., Trindade, A., Monteiro, A., & Miranda, V. (2014). Solar Power Forecasting in Smart Grids Using Distributed Information. *Proceedings of the 18th Power Systems Computation Conference*. http://doi.org/10.1016/j.ijepes.2015.02.006

Bouhafs, F., Mackay, M., & Merabti, M. (2012). Links to the Future. *IEEE Power and Energy Magazine*, (february), 24–32. Retrieved from http://citeseerx.ist.psu.edu/viewdoc/download?doi=10.1.1.200.2841&rep=rep1&type=pdf

Bracale, A., Caramia, P., Carpinelli, G., Di Fazio, A. R., & Varilone, P. (2013). A Bayesian-Based Approach for a Short-Term Steady-State Forecast of a Smart Grid. *IEEE Transactions on Smart Grid*, *4*(4), 1760–1771. http://doi.org/10.1109/TSG.2012.2231441

Canale, S., Di Giorgio, A., Lanna, A., Mercurio, A., Panfili, M., & Pietrabissa, A. (2013). Optimal Planning and Routing in Medium Voltage PowerLine Communications Networks. *IEEE Transactions on Smart Grid*, *4*(2), 711–719. http://doi.org/10.1109/TSG.2012.2212469

Carmona-Delgado, C., Romero-Ramos, E., & Riquelme-Santos, J. (2013). Fast and reliable distribution load and state estimator. *Electric Power Systems Research*, *101*, 110–124. http://doi.org/10.1016/j.epsr.2013.03.004

Carneiro, M., Morelato, P., & Bishop, P. (1996). Long-range planning of power distribution systems: secondary networks. *Computers & Electrical Engineering*, *22*(3), 179–191.

Chang, B. R., Yuan, Y., Lv, H., Yin, W., & Yang, S. X. (2013). Selling the Smart Grid Part 1 - Why consumers must buy in for the smart grid to seceed, (April 2012).

Claessen, F. N., & La Poutré, J. a. (2014). Towards A European Smart Energy System -

ICT Innovation Goals And Considerations. Retrieved from http://oai.cwi.nl/oai/asset/22587/22587D.pdf

Collins, L., & Ward, J. K. (2015). Real and reactive power control of distributed PV inverters for overvoltage prevention and increased renewable generation hosting capacity. *Renewable Energy*, *81*, 464–471. http://doi.org/10.1016/j.renene.2015.03.012

Cossent, R., Gómez, T., & Frías, P. (2009). Towards a future with large penetration of distributed generation: Is the current regulation of electricity distribution ready? Regulatory recommendations under a European perspective. *Energy Policy*, *37*(3), 1145–1155. http://doi.org/10.1016/j.enpol.2008.11.011

Council of European Energy Regulators (CEER). (2011). *5th CEER Benchmarking Report on the Quality of Electricity Supply 2011*.

Council of European Energy Regulators (CEER). (2016). *6th CEER Benchmarking Report on the Quality of Electricity Supply*. Retrieved from http://www.ceer.eu/portal/page/portal/EER_HOME/EER_PUBLICATIONS/CEER_PAPERS/Electricity/Tab3/C13-EQS-57-03_BR5.1_19-Dec-2013_updated-Feb-2014.pdf

DECC. (2009). *Smarter Grids: The Opportunity*.

Degefa, M. Z., Lehtonen, M., Millar, R. J., Alahäivälä, A., & Saarijärvi, E. (2015). Optimal voltage control strategies for day-ahead active distribution network operation. *Electric Power Systems Research*, *127*, 41–52. http://doi.org/10.1016/j.epsr.2015.05.018

Delfanti, M., Merlo, M., & Monfredini, G. (2014). Voltage Control on LV Distribution Network: Local Regulation Strategies for DG Exploitation. *Research Journal of Applied Sciences, Engineering and Technology*, *7*(23), 4891–4905.

Depuru, S., Wang, L., & Devabhaktuni, V. (2011). Smart meters for power grid: Challenges, issues, advantages and status. *Renewable and Sustainable Energy Reviews*, *15*(6), 2736–2742. http://doi.org/10.1016/j.rser.2011.02.039

Di Bert, L., D'Alessandro, S., & Tonello, A. M. (2014). A G3-PLC simulator for access networks. *IEEE ISPLC 2014 - 18th IEEE International Symposium on Power Line Communications and Its Applications*, 99–104. http://doi.org/10.1109/ISPLC.2014.6812329

Díaz-Dorado, E., Cidrás, J., & Míguez, E. (2003). Planning of large rural low-voltage networks using evolution strategies. *IEEE Transactions on Power Systems*, *18*(4), 1594–1600. http://doi.org/10.1109/TPWRS.2003.818741

DISCERN project. (2016). Retrieved from http://www.discern.eu/

DLMS/COSEM. (2016). Retrieved from http://www.dlms.com/information/whatisdlmscosem/index.html

DOE. (2010). *Communication Requirements of Smart Grid Technologies*.

Duche, D., & Gogate, P. V. (2014). Signal Attenuation in Powerline Communication Channel. *International Journal of Emerging Trends & Technology in Computer Science (IJETICS)*, *3*(2).

Dupont, B., Meeus, L., & Belmans, R. (2010). Measuring the "Smartness" of the electricity grid. In *2010 7th International Conference on the European Energy Market, EEM 2010* (pp. 1–6). IEEE. http://doi.org/10.1109/EEM.2010.5558673

Durbak, D. W., & Stewart, J. R. (1990). PLC signal attenuation in branched networks. *IEEE Transactions on Power Delivery*, *5*(2), 878–883. http://doi.org/10.1109/61.53097

Ebad, M., & Grady, W. M. (2016). An approach for assessing high-penetration PV impact on distribution feeders. *Electric Power Systems Research*, *133*, 347–354. http://doi.org/10.1016/j.epsr.2015.12.026

EEGI. (2010). *The European Electricity Grid Initiative - Roadmap 2010-18 and Detailed Implementation Plan 2010-12*. *Transit*.

EEGI. (2013). European Electricity Grid Initiative Research and Innovation Roadmap 2013-2022, (January).

EPRI. (2010). *Methodological Approach for Estimating the Benefits and Costs of Smart Grid Demonstration Projects*.

ERGEG. (2010). *Position Paper on Smart Grids An ERGEG Conclusions Paper*.

Etherden, N., & Bollen, M. H. J. (2014). Overload and overvoltage in low-voltage and medium-voltage networks due to renewable energy Some illustrative case studies. *Electric Power Systems Research*, *114*, 39–48. http://doi.org/10.1109/ISGTEurope.2011.6162645

Eurelectric. (2011). *10 steps to smart grids*.

Eurelectric. (2013). *Power Distribution in Europe - Facts & Figures*. Retrieved from http://www.eurelectric.org/media/113155/dso_report-web_final-2013-030-0764-01-e.pdf

European Commission. (2009). *ICT for a Low Carbon Economy Smart Electricity*.

European Commission. (2010a). DIRECTIVE 2010/31/EU, 13–35.

European Commission. (2010b). *SET-Plan*.

European Commission. (2013a). Energy Technologies and Innovation - JRC Scientific and Policy Reports R & D Investment in the Technologies of the European Strategic Energy Technology Plan.

European Commission. (2013b). Energy Technologies and Innovation - Technology Assessment.

European Commission. (2014). Benchmarking smart metering deployment in the EU-27 with a focus on electricity.

European Commission. (2016). *Energy prices and costs in Europe*.

Falvo, M. C., Martirano, L., Sbordone, D., & Bocci, E. (2013). Technologies for Smart Grids: a brief review.

Ferreira, H., Lampe, L., Newbury, J., & Swart, T. (2010). *Power Line Communications: Theory and Applications for Narrowband and Broadband Communications over*

*Power Lines*. John Wiley and Sons.

Frías, P. (2008). *A regulatory model proposal for voltage control in electric power systems*.

Frias, P., Platero, C. A., Soler, D., & Blázquez, F. (2010). High-efficiency voltage regulator for rural networks. *IEEE Transactions on Power Delivery*, *25*(3), 1666–1672. http://doi.org/10.1109/TPWRD.2010.2046683

Galli, S., Scaglione, A., & Wang, Z. (2011). For the Grid and Through the Grid: The Role of Power Line Communications in the Smart Grid. *Proceedings of the IEEE*, *99*(6), 998–1027. http://doi.org/10.1109/JPROC.2011.2109670

Gellings, C. (2011). Power to the people. *IEEE Power and Energy Magazine*, 30–41.

Glassmire, J., Komor, P., & Lilienthal, P. (2012). Electricity demand savings from distributed solar photovoltaics. *Energy Policy*, *51*, 323–331. http://doi.org/10.1016/j.enpol.2012.08.022

González-Sotres, L., Frías, P., & Mateo, C. (2017). Power Line Communication Transfer Function Computation in Real Network Configurations for Performance Analysis Applications. *IET Communications*, 1–8. http://doi.org/10.1049/iet-com.2016.0135

González-Sotres, L., Mateo, C., Frías, P., Rodríguez-morcillo, C., & Matanza, J. (2016). Replicability Analysis of PLC PRIME Networks for Smart Metering Applications. *IEEE Transactions on Smart Grid*, *3053*(c), 1–9. http://doi.org/10.1109/TSG.2016.2569487

Gonzalez-Sotres, L., Mateo, C., Gomez, T., Reneses, J., Rivier, M., & Sanchez-Miralles, Á. (2011). Assessing the Impact of Distributed Generation on Energy Losses using Reference Network Models. In *Cigrè International Symposium on The Electric Power System of the Future: Integrating Supergrids and Microgrids*.

González-Sotres, L., Mateo Domingo, C., Sánchez-Miralles, Á., & Alvar Miró, M. (2013). Large-Scale MV/LV Transformer Substation Planning Considering Network Costs and Flexible Area Decomposition. *IEEE Transactions on Power*

*Delivery*, *28*(4), 2245–2253. http://doi.org/10.1109/TPWRD.2013.2258944

Gouveia, C., Rua, D., Soares, F. J., Moreira, C., Matos, P. G., & Lopes, J. A. P. (2015). Development and implementation of Portuguese smart distribution system. *Electric Power Systems Research*, *120*, 150–162. http://doi.org/10.1016/j.epsr.2014.06.004

Gungor, V. C., Sahin, D., Kocak, T., Ergut, S., Buccella, C., Cecati, C., & Hancke, G. P. (2011). Smart Grid Technologies: Communication Technologies and Standards. *Industrial Informatics, IEEE Transactions on*, *7*(4), 529–539. http://doi.org/10.1109/TII.2011.2166794

Gungor, V. C., Sahin, D., Kocak, T., Ergut, S., Buccella, C., Cecati, C., & Hancke, G. P. (2013). A Survey on smart grid potential applications and communication requirements. *IEEE Transactions on Industrial Informatics*, *9*(1), 28–42. http://doi.org/10.1109/TII.2012.2218253

Haghifam, M., & Shahabi, M. (2002). Optimal location and sizing of HV/MV substations in uncertainty load environment using genetic algorithm. *Electric Power Systems Research*, *63*(1), 37–50. http://doi.org/10.1016/S0378-7796(02)00087-1

Haidine, A., Tabone, A., & Muller, J. (2013). Deployment of power line communication by European utilities in advanced metering infrastructure. *2013 IEEE 17th International Symposium on Power Line Communications and Its Applications*, 126–130. http://doi.org/10.1109/ISPLC.2013.6525837

Han, X., Kosek, A. M., Morales Bondy, D. E., Bindner, H. W., You, S., Tackie, D. V., … Thordarson, F. (2014). Assessment of distribution grid voltage control strategies in view of deployment. *2014 IEEE International Workshop on Intelligent Energy Systems (IWIES)*, 46–51. http://doi.org/10.1109/IWIES.2014.6957045

Hashmi, M., Hänninen, S., & Mäki, K. (2011). Survey of Smart Grid Concepts , Architectures , and Technological Demonstrations Worldwide, 1–7.

Hidalgo, R., Abbey, C., & Joós, G. (2010). A Review of Active Distribution Networks Enabling Technologies. *Engineering*, 1–9.

Ho, Q., Gao, Y., & Le-Ngoc, T. (2013). Challenges and research opportunities in wireless communication networks for smart grid. *Wireless Communications, IEEE*, (June), 89–95. Retrieved from http://ieeexplore.ieee.org/xpls/abs_all.jsp?arnumber=6549287

Hooijen, O. G. (1998). A channel model for the residential power circuit used as a digital communications medium. *IEEE Transactions on Electromagnetic Compatibility*, *40*(4), 331–336. http://doi.org/10.1109/15.736218

Hooijen, O. G. (1998). On the Relation Between Network-Topology and Power Line Signal Attenuation. *International Symposium on Power Line Communications and Its Applications (ISPLC)*, 24–26.

Hu, X., Chen, Z., & Yin, F. (2014). Impulsive noise cancellation for MIMO power line communications. *Journal of Communications*, *9*(3), 241–247. http://doi.org/10.12720/jcm.9.3.241-247

Idlbi, B., Diwold, K., Stetz, T., Wang, H., & Braun, M. (2013). Cost-benefit analysis of central and local voltage control provided by distributed generators in MV networks. In *IEEE PowerTech*. http://doi.org/10.1109/PTC.2013.6652333

IEEE Power and Energy Magazine. (2011). Smart Grid: Reinventing the Electric Power System, 1–68.

International Energy Agency. (2011). *Technology Roadmap Smart Grids*.

International Energy Agency. (2013). *Photovoltaic and Solar Forecasting: State of the Art*.

Izadkhast, S., Garcia-Gonzalez, P., Frias, P., & Bauer, P. (2017). Design of Plug-in Electric Vehicle's Frequency-Droop Controller for Primary Frequency Control and Performance Assessment. *IEEE Transactions on Power Systems*, *8950*(c), 1–1. http://doi.org/10.1109/TPWRS.2017.2661241

Jimenez-Estevez, G., Vargas, L., & Marianov, V. (2010). Determination of Feeder Areas for the Design of Large Distribution Networks. *IEEE Transactions on Power Delivery*, *25*(3), 1912–1922. http://doi.org/10.1109/TPWRD.2010.2042468

Jimenez-Estevez, G., Vargas, L., & Palma-Behnke, R. (2007). An evolutionary approach for the greenfield planning problem in distribution networks. *Neural Networks, 2007*. Retrieved from http://ieeexplore.ieee.org/xpls/abs_all.jsp?arnumber=4371221

JRC. (2012a). *Guidelines for conducting a cost-benefit analysis of Smart Grid projects*.

JRC. (2012b). *Guidelines for Cost Benefit Analysis of Smart Metering Deployment*.

JRC. (2016). *From European Electricity Distribution Systems to Representative Distribution Networks*.

Karimi, B., & Namboodiri, V. (2012). Capacity analysis of a wireless backhaul for metering in the Smart Grid. *2012 Proceedings IEEE INFOCOM Workshops*, 61–66. http://doi.org/10.1109/INFCOMW.2012.6193520

KEMA. (2011). *The Virtual Power Plant*.

Kezunovic, M. (2011). Smart Fault Location for Smart Grids. *IEEE Transactions on Smart Grid*, *2*(1), 11–22. http://doi.org/10.1109/TSG.2011.2118774

Khan, R. H., & Khan, J. Y. (2013). A comprehensive review of the application characteristics and traffic requirements of a smart grid communications network. *Computer Networks*, *57*(3), 825–845. http://doi.org/10.1016/j.comnet.2012.11.002

Kim, I., Varadarajan, B., & Dabak, A. (2010). Performance Analysis and Enhancements of Narrowband OFDM Powerline Communication Systems. *Smart Grid Communications (SmartGridComm), 2010 First IEEE International Conference on*, 362–367. http://doi.org/10.1109/SMARTGRID.2010.5622070

Kolhe, M. (2012). Smart Grid: Charting a New Energy Future: Research, Development and Demonstration. *The Electricity Journal*, *25*(2). Retrieved from http://www.sciencedirect.com/science/article/pii/S104061901200019X

Korki, M., Vu, H. L., Foh, C. H., Lu, X., & Hosseinzadeh, N. (2011). MAC Performance Evaluation in Low Voltage PLC Networks. *ENERGY 2011 : The First International Conference on Smart Grids, Green Communications and IT*

*Energy-Aware Technologies*, (c), 135–140.

Korki, M., Zhang, C., & Vu, H. L. (2013). Performance evaluation of PRIME in smart grid. *2013 IEEE International Conference on Smart Grid Communications (SmartGridComm)*, 294–299. http://doi.org/10.1109/SmartGridComm.2013.6687973

Kural, F., & Şafak, M. (2002). An Experimental Investigation of Impulse Noise on Low Voltage Powerlines. *International Symposium on PowerLine Communication and Its Applications.*, 12–14.

Lampe, L., & Vinck, a. J. H. (2011). On cooperative coding for narrow band PLC networks. *AEU - International Journal of Electronics and Communications*, *65*(8), 681–687. http://doi.org/10.1016/j.aeue.2011.01.011

Lin, J., Nassar, M., & Evans, B. L. (2013). Impulsive Noise Mitigation in Powerline Communications Using Sparse Bayesian Learning, *31*(7), 1172–1183. http://doi.org/10.1109/JSAC.2013.130702

Linares, P., & Rey, L. (2013). The costs of electricity interruptions in Spain: Are we sending the right signals? *Energy Policy*, *61*, 751–760. http://doi.org/10.1016/j.enpol.2013.05.083

Lloret, J., & Valencia, U. P. De. (2013). A multi-agent system architecture for smart grid management and forecasting of energy demand in virtual power plants. *Communications …*, (January), 106–113. Retrieved from http://ieeexplore.ieee.org/xpls/abs_all.jsp?arnumber=6400446

LoadProfileGenerator. (2016). Retrieved from http://www.loadprofilegenerator.de/

López, G., Moreno, J. I., Amarís, H., & Salazar, F. (2015). Paving the road toward Smart Grids through large-scale advanced metering infrastructures. *Electric Power Systems Research*, *120*, 194–205. http://doi.org/10.1016/j.epsr.2014.05.006

López, G., Moura, P. S., Custodio, V., Moreno, J. I., & Iii, C. (2013). Modeling the Neighborhood Area Networks of the Smart Grid. *IEEE ICC 2012 - Selected Areas in Communications Symposium*. http://doi.org/10.1109/ICC.2012.6364501

Losa, I., & Bertoldi, O. (2009). Regulation of continuity of supply in the electricity sector and cost of energy not supplied. *International Energy Workshop 2009, Venice, Italy, June 17-19, 2009*, 1–10.

Luan, W., Sharp, D., & Lancashire, S. (2010). Smart grid communication network capacity planning for power utilities. *Transmission and Distribution …*, 1–4. Retrieved from http://ieeexplore.ieee.org/xpls/abs_all.jsp?arnumber=5484223

Madureira, A., Bessa, R., Meirinhos, J., Fayzur, D., Filipe, J., Messias, A. A., … Matos, P. G. (2015). The Impact of Solar Power Forecast Errors on Voltage Control in Smart Distribution Grids. In *Proceedings of the 23rd International Conference on Electricity Distribution (CIRED 2015), Lyon, France*.

Madureira, A. G. (2010). Coordinated and optimized voltage management of distribution networks with multi-microgrids, (July), 234.

Madureira, A. G., & Peças Lopes, J. A. (2012). Ancillary services market framework for voltage control in distribution networks with microgrids. *Electric Power Systems Research*, *86*, 1–7. http://doi.org/10.1016/j.epsr.2011.12.016

Markiewicz, H. (Cooper D. A., & Klajn, A. (Wroclaw U. of T. (2004). *Voltage Disturbances Standard EN 50160. Power quality Application Guide* (Vol. 5.4.2). Retrieved from www.cda.org.uk; www.brass.org; www.eurocopper.org;

Matanza, J. (2013). *Improvements in the PLC Systems for Smart Grids Environments*. Retrieved from https://www.iit.upcomillas.es/publicaciones/mostrar_tesis_doctorado.php.en?id=10076

Matanza, J., Alexandres, S., & Rodríguez-Morcillo, C. (2014). Advanced metering infrastructure performance using European low-voltage power line communication networks. *IET Communications*, *8*(7), 1041–1047. http://doi.org/10.1049/iet-com.2013.0793

Mateo, C., Gomez, T., Sanchez-Miralles, Á., Peco, J., & Candela, A. (2011). A Reference Network Model for Large-Scale Distribution Planning With Automatic

Street Map Generation. *IEEE Transactions on Power Systems*, *26*(1), 190–197. Retrieved from http://ieeexplore.ieee.org/xpls/abs_all.jsp?arnumber=5504171

Matos, P., & Messias, A. (2013). Inovgrid, a smart vision for a next generation distribution system. *... Distribution (CIRED ...*, (536), 10–13. Retrieved from http://ieeexplore.ieee.org/xpls/abs_all.jsp?arnumber=6683390

McHann, S. E. (2013). Grid analytics: How much data do you really need? *2013 IEEE Rural Electric Power Conference (REPC)*, C3-1-C3-4. http://doi.org/10.1109/REPCon.2013.6681858

Mets, K., Ojea, J. A., & Develder, C. (2014). Combining power and communication network simulation for cost-effective smart grid analysis. *IEEE Communications Surveys and Tutorials*, *16*(3), 1771–1796. http://doi.org/10.1109/SURV.2014.021414.00116

Middleton, D. (1972). Statistical-Physical Models of Urban Radio-Noise Environments - Part I: Foundations. *IEEE Transactions on Electromagnetic Compatibility, EMC-14*(2), 38–56. http://doi.org/10.1109/TEMC.1972.303188

Míguez, E., Díaz-Dorado, E., & Cidrás, J. (1998). An Application of an Evolution Strategy in Power Distribution System Planning. *IEEE International Conference on Evolutionary Computation Proceedings*, 241–243.

Miranda, V., Ranito, J., & Proença, L. (1994). Genetic algorithms in optimal multistage distribution network planning. *IEEE Transactions on Power Systems*, *9*(4), 1927–1933.

Morgan, M. G., Apt, J., Lave, L. B., Ilic, M. D., Sirbu, M., & Peha, J. M. (2009). The many meanings of " Smart Grid ." *Computer Engineering*, (July).

Najafi, S., Hosseinian, S. H., Abedi, M., Vahidnia, A., & Abachezadeh, S. (2009). A Framework for Optimal Planning in Large Distribution Networks. *IEEE Transactions on Power Systems*, *24*(2), 1019–1028. http://doi.org/10.1109/TPWRS.2009.2016052

Nassar, M., Gulati, K., Mortazavi, Y., & Evans, B. L. (2011). Statistical Modeling of

Asynchronous Impulsive Noise in Powerline Communication Networks. *Proc. IEEE Int. Global Communications Conf., Dec. 2011, Houston, TX USA.*, 1–6. http://doi.org/10.1109/GLOCOM.2011.6134477

Navarro, A., & Rudnick, H. (2009a). Large-scale distribution planning-Part I: Simultaneous network and transformer optimization. *IEEE Transactions on Power Systems*, *24*(2), 744–751.

Navarro, A., & Rudnick, H. (2009b). Large-scale distribution planning—Part II: Macro-optimization with Voronoi´s diagram and Tabu search. *IEEE Transactions on Power Systems*, *24*(2), 752–758. http://doi.org/10.1109/TPWRS.2009.2016594

NIST. (2012). *SmartGrid: A Beginner's Guide*.

NIST. (2013). *Strategic R&D Opportunities for the Smart Grid*.

NRECA-DOE. (2013). *Communications: The Smart Grid's Enabling Technology*.

Olivera, A. F., Escalona, A. S., Galdos, I. U., Arenas, J. M., & Buceta, P. A. (2013). Analysis of PRIME PLC Smart Metering Networks Performance. In *International Conference on Renewable Energies and Power Quality (ICREPQ'13)*.

OMIE. (2016). Retrieved from http://www.omie.es/en/inicio

Papadopoulos, T. A., Kaloudas, C. G., Chrysochos, A. I., & Papagiannis, G. K. (2013). Application of narrowband Power-Line communication in medium-voltage smart distribution grids. *IEEE Transactions on Power Delivery*, *28*(2), 981–988. http://doi.org/10.1109/TPWRD.2012.2230344

Parikh, P. P., Member, S., & Kanabar, M. G. (2010). Opportunities and Challenges of Wireless Communication Technologies for Smart Grid Applications, (Cc).

Patel, A., Aparicio, J., Tas, N., Loiacono, M., & Rosca, J. (2011). Assessing communications technology options for smart grid applications. *2011 IEEE International Conference on Smart Grid Communications (SmartGridComm)*, 126–131. http://doi.org/10.1109/SmartGridComm.2011.6102303

Pérez-Arriaga, I. J., & Knittel, C. (2016). *Utility of the future, An MIT Energy Initiative*

*response to an industry in transition*.

Pérez-Arriaga, I. J., Ruester, S., Schwenen, S., Battle, C., & Glachant, J. (2013). *From Distribution Networks to Smart Distribution Systems: Rethinking the Regulation of European Electricity DSOs*. Retrieved from http://cadmus.eui.eu/handle/1814/27615

Pieltain Fernandez, L., Gomez San Roman, T., Cossent, R., Mateo Domingo, C., & Frias, P. (2011). Assessment of the Impact of Plug-in Electric Vehicles on Distribution Networks. *IEEE Transactions on Power Systems*, *26*(1), 206–213. http://doi.org/10.1109/TPWRS.2010.2049133

PRIME Alliance. (2016). Retrieved from http://www.prime-alliance.org/

Ramirez-Rosado, I. J., & Bernal-Agustin, J. L. (2001). Reliability and costs optimization for distribution networks expansion using an evolutionary algorithm. *IEEE Transactions on Power Systems*, *16*(1), 111–118. http://doi.org/10.1109/59.910788

Ribeiro, P. (2012). Planning and Designing Smart Grids: Philosophical Considerations. *Technology and Society …*. Retrieved from http://ieeexplore.ieee.org/xpls/abs_all.jsp?arnumber=6313612

Rodriguez-Calvo, A., Frías, P., Reneses, J., Cossent, R., & Mateo, C. (2014). Optimal investment in smart MV/LV substations to improve continuity of supply. *International Journal of Electrical Power & Energy Systems*, *62*, 410–418. http://doi.org/10.1016/j.ijepes.2014.04.062

Rohjans, S., Danekas, C., & Uslar, M. (2012). Requirements for Smart Grid ICT-architectures. *2012 3rd IEEE PES Innovative Smart Grid Technologies Europe (ISGT Europe)*, 1–8. http://doi.org/10.1109/ISGTEurope.2012.6465617

Rönnberg, S., Bollen, M., & Larsson, A. (2014). Emission from small scale PV-installations on the low voltage grid. In *International Conference on Renewable Energies and Power Quality (ICREPQ'14)* (Vol. 1).

Rönnberg, S. K., Bollen, M. H. J., & Wahlberg, M. (2011). Interaction between

narrowband power-line communication and end-user equipment. *IEEE Transactions on Power Delivery*, *26*(3), 2034–2039. http://doi.org/10.1109/TPWRD.2011.2130543

Saputro, N., Akkaya, K., & Uludag, S. (2012). A survey of routing protocols for smart grid communications. *Computer Networks*, *56*(11), 2742–2771. http://doi.org/10.1016/j.comnet.2012.03.027

Selga, J. M., Zaballos, A., & Navarro, J. (2013). Solutions to the Computer Networking Challenges of the Distribution Smart Grid. *IEEE Communications Letters*, *17*(3), 588–591. http://doi.org/10.1109/LCOMM.2013.020413.122896

Sendin, A., Guerrero, R., & Angueira, P. (2011). Signal injection strategies for smart metering network deployment in multitransformer secondary substations. *IEEE Transactions on Power Delivery*, *26*(4), 2855–2861. http://doi.org/10.1109/TPWRD.2011.2165737

Sendin, A., Peña, I., & Angueira, P. (2014). Strategies for power line communications smart metering network deployment. *Energies*, *7*(4), 2377–2420. http://doi.org/10.3390/en7042377

Sendin, A., Sanchez-Fornie, M. A., Berganza, I., Urrutia, I., & Simon, J. (2016). *Telecommunication for Networks for Smart Grids*. Artech House. Retrieved from https://books.google.es/books?id=NxHgjwEACAAJ

Sexauer, J., Javanbakht, P., & Mohagheghi, S. (2013). Phasor measurement units for the distribution grid: Necessity and benefits. In *2013 IEEE PES Innovative Smart Grid Technologies Conference, ISGT 2013*. http://doi.org/10.1109/ISGT.2013.6497828

Shahraeini, M. (2011). Comparison between communication infrastructures of centralized and decentralized wide area measurement systems. *Smart Grid, IEEE …*, *2*(1), 206–211. Retrieved from http://ieeexplore.ieee.org/xpls/abs_all.jsp?arnumber=5668520

Shrestha, G. M., & Jasperneite, J. (2012). Performance Evaluation of Cellular Communication Systems for M2M Communication in Smart Grid Applications,

352–359.

SmartGrids ERA-NET. (2012). Mapping & Gap Analysis of current European Smart Grids Projects, (April).

SolarPower Europe. (2014). Global Market Outlook for Solar Power 2015-2019, 32.

Stetz, T., Diwold, K., Kraiczy, M., Geibel, D., Schmidt, S., & Braun, M. (2014). Techno-economic assessment of voltage control strategies in low voltage grids. *IEEE Transactions on Smart Grid*, *5*(4), 2125–2132. http://doi.org/10.1109/TSG.2014.2320813

SUSTAINABLE project. (2016a). *Deliverable 6.2: Description of tools integration on existing infrastructure*. Retrieved from http://www.sustainableproject.eu/Portals/0/news/Deliverables/Sustainable_D6.2.pdf

SUSTAINABLE project. (2016b). Retrieved from http://www.sustainableproject.eu/

Tonello, A. M., & Versolatto, F. (2011). Bottom-up statistical PLC channel modeling-part I: Random topology model and efficient transfer function computation. *IEEE Transactions on Power Delivery*, *26*(2), 891–898. http://doi.org/10.1109/TPWRD.2010.2096518

Tonello, A., Song, J., Weiss, S., & Yang, F. (2012). PLC for the Smart Grid: State-of-the-Art and Challenges. In *Proceedings of Conference on Mobility and Computing*. Retrieved from http://www.diegm.uniud.it/tonello/PAPERS/CONFERENCES/CMC2012.pdf

Trebolle, D., Frías, P., Maza, J. M., & Tello, J. (2012). El control de tensión en redes de distribución con generación distribuida (II). *Anales de Ingeniería Mecánica*, *LXXXIX*(II), 11–19.

V.Klonari, J.F.Toubeau, Z.De Greve, O.Durieux, J.Lobry, F. V. (2015). Probabilistic Analysis Tool of the Voltage Profile in Low Voltage Grids. *23rd CIRED*, (June), 15–18.

Vandenbergh, M., Craciun, D., Helmbrecht, V., Hermes, R., Lama, R., Sonvilla, P. M., … Concas, G. (2013). *Prioritisation of Technical Solutions Available for the Integration of PV into the Distribution Grid*.

von Appen, J., Braun, M., Stetz, T., Diwold, K., & Geibel, D. (2013). Time in the sun: the challenge of high PV penetration in the German electric grid. *IEEE Power & Energy Magazine*, *3*(2), 55–64. http://doi.org/10.1109/MPE.2012.2234407

Zaballos, A., Vallejo, A., Majoral, M., & Selga, J. M. (2009). Survey and Performance Comparison of AMR Over PLC Standards. *IEEE Transactions on Power Delivery*, *24*(2), 604–613. http://doi.org/10.1109/TPWRD.2008.2002845

Zaballos, A., Vallejo, A., & Selga, J. M. (2011). Heterogeneous Communication Architecture for the Smart Grid, (October), 30–37.

Zaw, N. L., Kyaw, H. A., & Ye, K. Z. (2013). Power Line Cable Transfer Function for the Broadband Power Line Communication Channel. *Universal Journal of Control and Automation*, *1*(4), 103–110. http://doi.org/10.13189/ujca.2013.010403

Ziadi, Z., Oshiro, M., Senjyu, T., Yona, A., Urasaki, N., Funabashi, T., & Kim, C. H. (2014). Optimal voltage control using inverters interfaced with PV systems considering forecast error in a distribution system. *IEEE Transactions on Sustainable Energy*, *5*(2), 682–690. http://doi.org/10.1109/TSTE.2013.2292598

Ziari, I., Ledwich, G., & Wishart, M. (2009). Initial steps in optimal planning of a distribution system. In *AUPEC 2009*. Retrieved from http://ieeexplore.ieee.org/xpls/abs_all.jsp?arnumber=5356616

Zimmerman, R. D., Murillo-Sanchez, C. E., & Thomas, R. J. (2011). MATPOWER: Steady-State Operations, Planning, and Analysis Tools for Power Systems Research and Education. *IEEE Transactions on Power Systems*, *26*(1), 12–19. http://doi.org/10.1109/TPWRS.2010.2051168

# Appendix A. Methodology for large-scale distribution network planning

## A.1 Introduction

In Chapter 4 a Reference Network Model (RNM) was used to design large scale distribution networks. The characteristics of real distribution networks are not publicly available because this information is considered confidential by the DSOs. For this reason an RNM can be considered a good alternative to obtain a fair approximation of these data. In that chapter, the networks obtained with the RNM were used to analyse the communication performance of PLC PRIME. In a PLC network the data concentrator is usually located in the secondary substation and the network topology highly affects the communication performance. For these reasons, a methodology for large-scale distribution network planning has been developed to obtain representative networks where the communication performance can be analysed.

The combinatorial optimization problem of distribution network planning can be considered NP-hard and classical optimization methods may not provide a solution in a reasonable computational time (Jimenez-Estevez, Vargas, & Marianov, 2010). Heuristic algorithms have been developed to deal with problems of large size, where evolutionary algorithms have been shown as the most used technique in the past due to their flexibility for dealing with multi-stage planning and multi-objective optimization (Miranda, Ranito, & Proença, 1994; Ramirez-Rosado & Bernal-Agustin, 2001).

The first step in distribution network planning is to obtain the location and size of distribution transformers. In (Míguez, Díaz-Dorado, & Cidrás, 1998) authors codified the coordinates of the candidate substations and applied an evolutionary algorithm by using mutation and crossover operators to find the optimal location. In order to consider the real constraints of the environment, some authors have taken the location of the substations as input data (Jimenez-Estevez, Vargas, & Palma-Behnke, 2007), or considered a number of predetermined locations (Haghifam & Shahabi, 2002; Najafi, Hosseinian, Abedi, Vahidnia, & Abachezadeh, 2009).

Since the location of the transformers will determine somehow the layout of feeders, some authors have tried to do both optimizations simultaneously. Several authors have used the concept of Minimum Spanning Tree (MST) to obtain an approximation of the initial network, as indication of the optimal network layout when geographical or electrical constraints are not considered

(Jimenez-Estevez et al., 2007; Najafi et al., 2009). A MST is a weighted connected graph whose total edge cost is minimal. In (Díaz-Dorado, Cidrás, & Míguez, 2003) a methodology for planning large rural LV networks based on this concept was described. The authors obtained an initial MST with all the load points and then they obtained different sets of subtrees by removing and exchanging their branches iteratively using evolution strategies, where each subtree was fed by one substation. An approximation of the MV network costs was also included in the cost function by connecting all the substations with another MST.

A different methodology for simultaneous LV network and transformer planning was presented in (Navarro & Rudnick, 2009a, 2009b). In this case, the authors divided the planning area into regular mini-zones of 500x500 meters, and then they applied a repetitive process based on the use of a k-means algorithm. The objective is to obtain the optimal number of subsets that minimize the cost function, so that one transformer feeds each subset. The authors assumed that as more transformers are installed, transformation costs increase but network costs decrease. This condition was also demonstrated by other authors in (Ziari, Ledwich, & Wishart, 2009), and allows the algorithm to obtain a minimum number. In (Navarro & Rudnick, 2009b) the authors presented a post-optimization process to improve the solution obtained in (Navarro & Rudnick, 2009a), in order to take into account the possibility of planning together different mini-zones, since the division into mini-zones was arbitrary.

This appendix presents the methodology to plan the location, size and service area of substations, specially focusing on the MV/LV transformer substations using an alternative methodology to divide the whole planning area into more appropriate regions to be planned separately. The advantage of this methodology respect to (Navarro & Rudnick, 2009a) is that a post-optimization process is not required to achieve a reasonable solution, but on the other hand new features are needed to be included in order to adapt the algorithm, which will be explained across the following sections. Section A.2 describes the methodology that has been developed to carry out the optimization of the transformer substations. In Section A.3 two case studies are presented in order to show the features of this algorithm and in Section A.4 the main conclusions are stated.

## A. 2 Methodology

The methodology presented is aimed to plan very large areas with a size of a Spanish province, which average size is approximately $10^4$ $km^2$. Logically, the direct optimization of the whole area would be very costly in terms of computational burden. For this reason, a correct

division of the planning area into smaller regions is required so that the complexity of the problem is greatly reduced. The proposed methodology can be divided into three main stages, which are:

1. Identification of isolated areas.
2. Flexible decomposition of isolated areas of medium size into regions of smaller size.
3. Optimization of small regions.

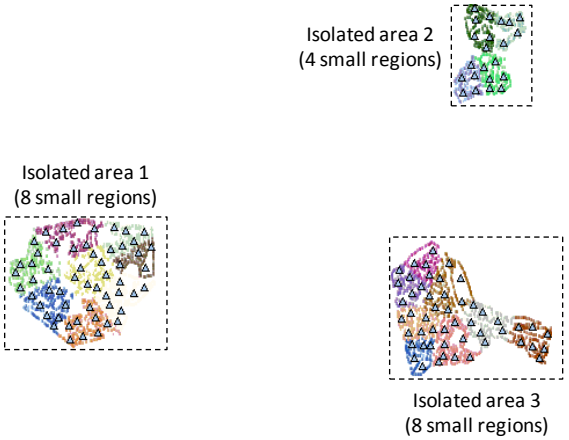


**Figure A-1 Example of application of the proposed methodology**

In order to provide a general overview of the methodology, an example of application is shown in Figure A-1, where the triangles represent the resulting MV/LV transformer substations. First, the isolated areas are identified based on a maximum distance criterion. Then, these areas are decomposed in smaller regions based on an estimation of the minimum number of transformers that will be required to supply the demand located at each region. Finally, the small regions are optimized independently in order to obtain the optimal number, location and service area of the MV/LV transformer substations. These three stages are explained in detail in the following subsections.

This methodology begins with the identification of isolated areas that can be planned independently, because they are located clearly too far from the others. In (Díaz-Dorado et al., 2003) authors applied an evolution strategy to remove the branches of the MST of all the nodes with the aim of obtaining subsets of nodes that can be fed by one transformer. A similar idea is used in the first stage of this methodology, but only for obtaining the isolated areas. To this end, the MST of all the load points in the LV level is built and then, the branches which length exceeds a maximum threshold are removed. The threshold was set to 3 km in the case of the LV network, because in practice LV lines should not be longer than this distance.

The previous stage may provide areas of a reasonable size to be planned with an optimization technique, especially in rural areas where the load is rather dispersed. However, in areas with higher load density, the size of the isolated areas may still be too large. For this reason, another division should be performed. In (Navarro & Rudnick, 2009a) the authors proposed to use a division into regular mini-zones of 500x500 meters. This arbitrary approach requires a post-optimization process to improve the initial solution so that the neighbouring areas can be planned together, as it was presented in (Navarro & Rudnick, 2009b).

With the aim of avoiding a post-optimization process to obtain a global reasonable solution, a flexible decomposition into smaller regions is proposed. This decomposition is based on the Theoretical Minimum Number of Transformers (TMNT) that is required to supply an area, considering only the capacity constraint of the transformers (Carneiro, Morelato, & Bishop, 1996). This number can be obtained by dividing the total demand of the area over the capacity of the maximum available transformer in that area. The total demand is calculated as the sum of the demanded power of all the load points in the analysed scenario. Simultaneity factors are taken into account to estimate the total demand (Mateo, Gomez, Sanchez-Miralles, Peco, & Candela, 2011), as well as a security margin for the transformers.

The objective of this stage is to obtain small regions in which their TMNT does not exceed a predetermined value, which is represented by their Characteristic TMNT (CTMNT). This classification is carried out with the k-means clustering technique. The k-means algorithm is used in this paper to classify a set of $m$ loads into $k$ clusters. Every cluster is represented by their centroid, which is located in the centre of gravity of the loads that constitute the cluster. After applying k-means to all the loads in an isolated area, $k$ centroids are obtained, so that every load is assigned to their nearest centroid. The number of centroids represents the number of small regions in which an isolated area will be divided, and it is taken as input by the k-means algorithm. This value is obtained by dividing the TMNT over the CTMNT.

Since the k-means algorithm only guarantees the number of clusters but not the size of them, this step is recursively applied to every new region until the TMNT of all the regions is lower than their CTMNT. Consequently, the computational burden required to optimize each region will not be too high. For all the simulations presented, the value of the CTMNT has been set to 8 transformers. However, this parameter can be adjusted with different values depending on the characteristics of the area, so that in urban areas with very high load density a higher value could be chosen.

Once the whole planning zone has been divided into smaller regions, the following optimization process described can be applied separately to each one. The presented algorithm is used to optimize the location, size and service area of the MV/LV transformer substations at each small area. This algorithm is based on the idea described in (Navarro & Rudnick, 2009a) and (Ziari et al., 2009), where was demonstrated that as more transformers are installed in a determined area, transformation costs increase but network costs decrease. Therefore, the objective of this stage is to find the set of clusters that minimize the cost function, where each cluster is fed by one transformer. The following costs are considered in the cost function:

- Estimation of the cost of the LV network that will connect the customers to the MV/LV transformers.
- The cost of the MV/LV transformers.
- Estimation of the cost of the MV network that will be required to connect all these transformers.

The developed optimization algorithm is shown in Figure A-2. The algorithm aims to obtain the optimal number of transformers to be installed at each small region. The number of transformers is initially set to one, and is increased incrementally until the cost function reaches a minimum value. Then, the algorithm stops and the clusters that constitute the minimum cost solution (Sol_Min) are returned. This process is described in more detail below:

1. **Initialization:** The algorithm begins considering infinite as the initial value of the cost function, which will be reduced during the optimization process.

2. **K-means, increasing K:** The first step is to apply k-means to all the loads of the small region beginning with K=1, which means that all the loads are fed by only one transformer. This number is increased by one at the end of each iteration, so that an iterative process is performed until the optimal solution is found. Then, the feasibility of each cluster obtained by the k-means is checked. If one cluster is considered unfeasible, that cluster is divided into feasible clusters by means of a specific algorithm that will be explained in the next subsection. In order to be identified as feasible, a cluster must fulfil three constraints, which are:

    - Maximum capacity of the transformer.
    - Maximum distance from each load to the transformer.
    - Maximum electric moment from each load to the transformer.

3. **Cluster cost assessment:** When all the clusters are considered feasible the costs related to each cluster are calculated, which consist of the cost of the LV network and the cost of the

MV/LV transformer that feeds the cluster. The MST is used to estimate the cost of the LV network. However the MST is only an approximation to obtain a quick estimation for planning MV/LV transformer substations. The algorithms to plan the LV network will be explained in subsequent publications. First, the MST of all the load points of the cluster is built. In this case, a source node has to be defined when building the MST in order to be able to aggregate power for estimating a power flow. The closest load point to the centre of gravity of the cluster is chosen as the source node of the tree. This selection has the advantage of being close to the center of gravity, so that only the branches of the MST are required. Thus, the MST can be explored in a sorted way by adding the power demanded at each node from one end of the tree to the source node. Consequently, the downstream power at each node can be obtained, which can be used to calculate the size of the conductor that is required to supply such demand, and then the related costs. Several conductors are considered in the cost evaluation if the downstream power is higher than the maximum conductor size, or if the estimation of the voltage drop exceeds the maximum that is allowed. Finally, the cost of the energy losses is also evaluated for each conductor, considering that the voltage is 1 p.u.

4. **MV network cost assessment:** In the presented algorithm the cost of the MV network is assessed after obtaining the cost of all the clusters, as it was also performed in (Díaz-Dorado et al., 2003). To this end, the MST of all the transformers that feed each cluster is obtained and then, the cost of the maximum available conductor that connects each transformer according to the branches of the MST is calculated. Obviously, the approximation of the MV network with the MST is less accurate than in the case of the LV network, because the topology of the MV network tends to be more complex. However, the impact in the choice of the most economic solution is quite high, as it will be shown in a case study in Section IV.

5. **Stop criterion:** The condition to stop the iterative process is finding a minimum in the cost function. This situation can be identified when the following two conditions are fulfilled:

    a. The current value of the objective function (Cost_K) is higher than the value of the minimum cost solution (Cost_Min).

    b. The current number of initial transformer substations (K) is higher than the number of transformers in the minimum cost solution (NT_Min).

When one cluster is not feasible and the number of transformers is increased in the k-means algorithm, it may happen that the new location of the transformers do not resolve the unfeasibility, with the result that another transformer will be added. This process will continue until the k-means algorithm locates all the transformers in the correct place, meanwhile increasing

the cost of the solution unnecessarily because of the addition of previous transformers. Nevertheless, this problem can be solved if instead of increasing the number of transformers when a cluster is not feasible, the algorithm focuses on the unfeasible cluster and divides it into feasible clusters.

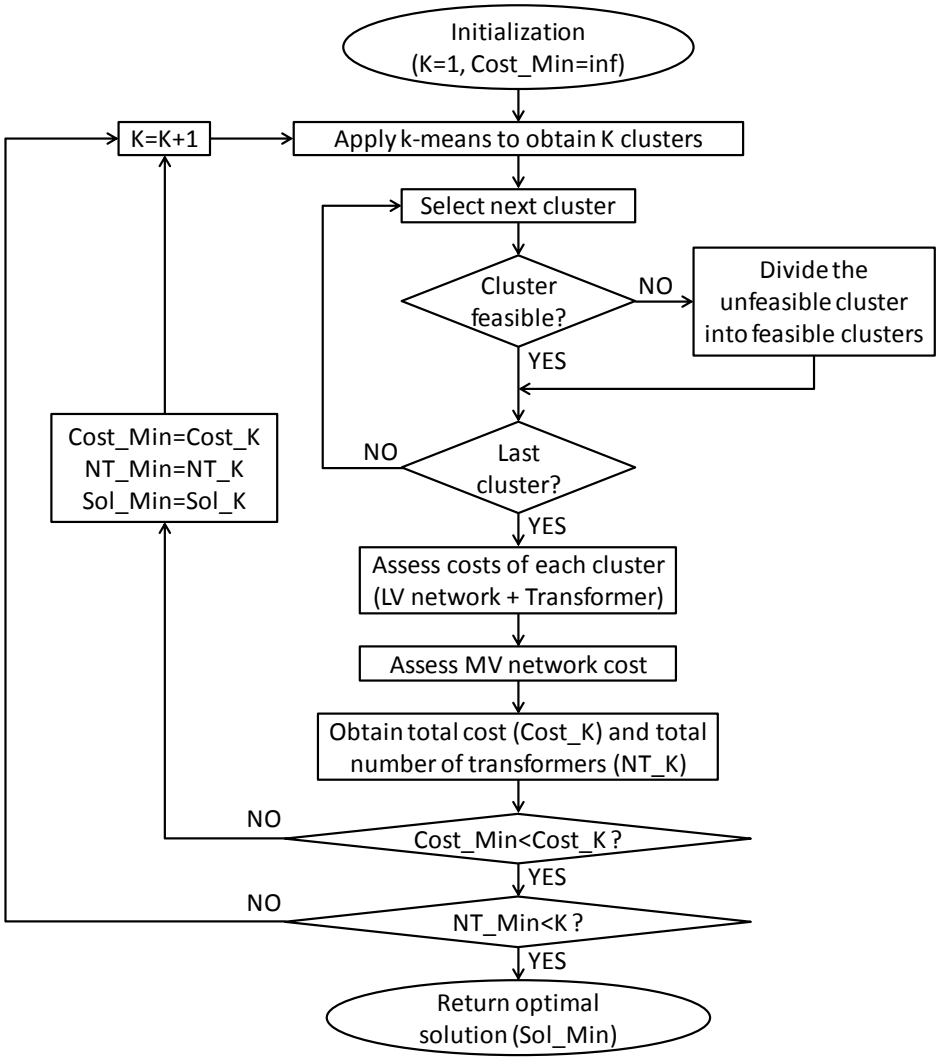


**Figure A-2 Optimization algorithm applied to each small region**

Figure A-3 shows the module implemented to convert an unfeasible cluster into feasible clusters, which is performed by the optimization algorithm when a cluster is considered unfeasible, and was introduced in the previous subsection. The main idea of this module is to find feasible subgroups within the unfeasible cluster. To this end, the algorithm performs a process in which the number of unfeasible nodes is reduced until all the nodes are assigned to a feasible subgroup.

The algorithm begins applying k-means to the initial unfeasible cluster, increasing the K until one of the new clusters is feasible. The nodes of the clusters that are still unfeasible are inserted in a list of unfeasible nodes (L_UN). The algorithm starts with K=2 because the solution with K=1 has already been considered unfeasible. In the event that all the clusters obtained with the k-means are feasible, the algorithm returns these clusters and the process is finished. If only some of them are feasible, the algorithm tries to reallocate the nodes of the list L_UN to their nearest feasible cluster, taking into account that the reallocation is only carried out if the receiver cluster remains feasible. Then, if all the nodes of the list have been reallocated, or if the remaining nodes of the list form a feasible cluster, the process is finished. Otherwise, the algorithm starts the process again but only considering the nodes that are still unfeasible (nodes in L_UN). Thus, although this module is also based on a repetitive process, in this case only the unfeasible nodes are taken into account in each iteration. Hence, the resulting feasible clusters are stored, removing their nodes from the next initial unfeasible cluster.

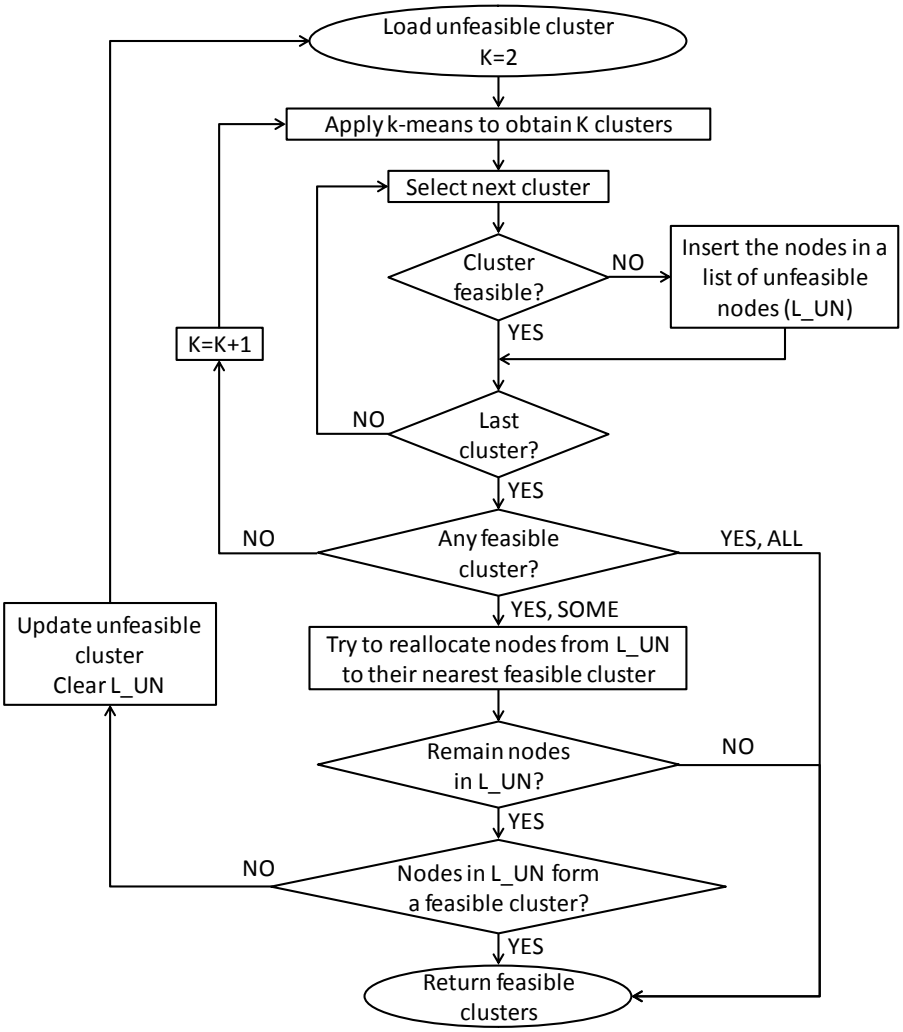


**Figure A-3 Division of an unfeasible cluster into feasible clusters**

When the optimal number of small regions has been found and the location and size of the transformer substation has been defined, an initial approximation of the network topology can be obtained with the MST. However, another algorithm can be used to obtain a better optimised network. In this case, a branch exchange technique is used to optimise the total cost of the network, where the weight of each branch takes into account the investment and operation costs, energy losses, and other orography factors.

The order in which the nodes are tested is very important, since it can determine the success of the final solution and the time required to achieve it. So, instead of using a random order, in this methodology the reverse order of the DFS is used. This criteria was also used in Chapter 3.2 to find a sub-tree in the computation of the PLC transfer function. Then, starting with a solution where all the nodes are directly connected to the transformer substation, new branches are tested following this order. With this process, the feeders are designed from back to front checking voltage and thermal limits at each step, which ensures getting to a feasible solution. Indeed, in case there are no feasibility problems, the final solution will be precisely the MST. An example of this process is presented in Figure A-4 for a simple network with eight nodes, in which the branches tested in steps 3 and 5 lead to an unfeasible solution so no branches are exchanged for these cases.

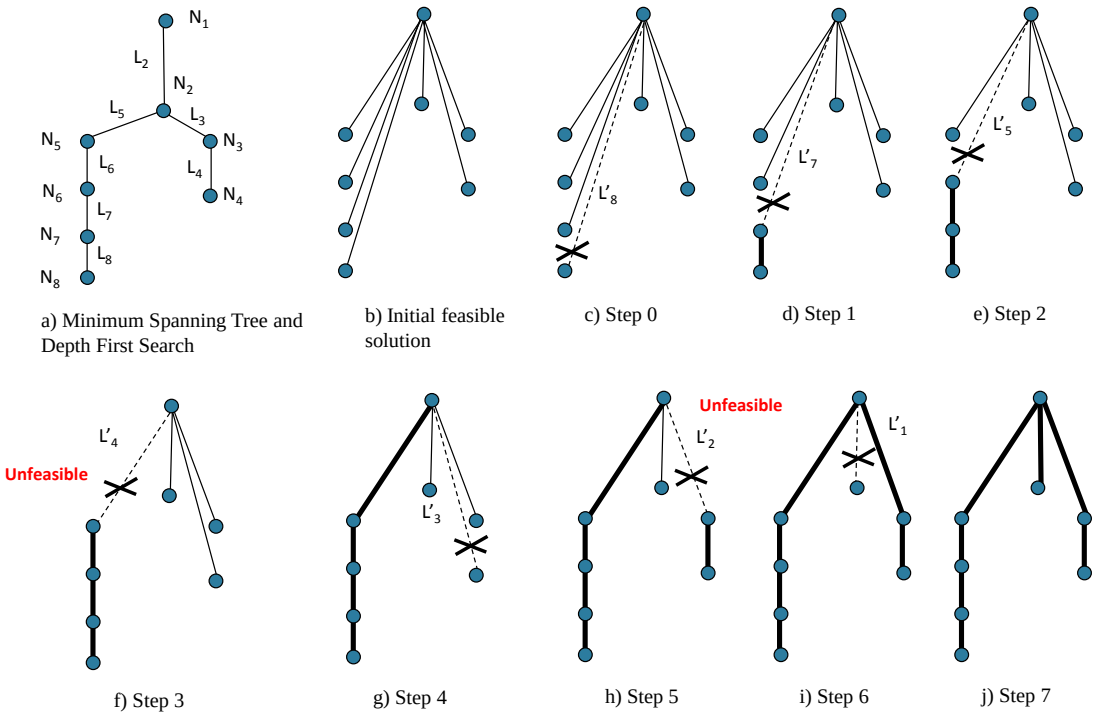


**Figure A-4 Branch-exchange process using the reverse order of the Depth First Search of a Minimum Spanning Tree**

# Appendix B. Sensitivity analysis statistics

A summary of the statistics of the results obtained for all the simulations performed in the sensitivity analysis of Chapter 2 is presented in Figure B-1. The values provided for each scenario of each case study include the number of samples, the mean value, the median value, the standard deviation, the maximum value and the minimum value.

**Table B-1 Statistics of scenarios simulated in the sensitivity analysis of Chapter 2**

| | | Scenario 1 | Scenario 2 | Scenario 3 | Scenario 4 |
|---|---|---|---|---|---|
| **Case U-L** | **Samples** | 11 | 12 | 4 | 2 |
| | **Mean** | 911.1 | 963.3 | 1352.4 | 1660.9 |
| | **Median** | 699.2 | 928.2 | 1348.8 | 1660.9 |
| | **Std deviation** | 352.0 | 324.8 | 67.4 | 431.2 |
| | **Maximum** | 1520.0 | 1504.2 | 1437.6 | 1965.8 |
| | **Minimum** | 599.3 | 558.7 | 1274.4 | 1356.0 |
| **Case U-M** | **Samples** | 543 | 299 | 90 | 7 |
| | **Mean** | 65.5 | 123.2 | 382.0 | 1277.1 |
| | **Median** | 64.4 | 119.8 | 331.5 | 1799.3 |
| | **Std deviation** | 8.9 | 15.2 | 214.1 | 708.7 |
| | **Maximum** | 171.3 | 222.5 | 1615.9 | 1886.4 |
| | **Minimum** | 56.1 | 109.9 | 274.4 | 491.7 |
| **Case U-S** | **Samples** | 290 | 108 | 8 | 6 |
| | **Mean** | 133.8 | 297.5 | 236.2 | 324.8 |
| | **Median** | 129.8 | 207.1 | 173.1 | 172.2 |
| | **Std deviation** | 15.9 | 286.7 | 162.2 | 375.2 |
| | **Maximum** | 231.3 | 1750.7 | 635.4 | 1090.7 |
| | **Minimum** | 118.3 | 191.3 | 170.1 | 169.5 |
| **Case U-XS** | **Samples** | 123 | 224 | 275 | 19 |
| | **Mean** | 289.6 | 172.7 | 127.0 | 412.5 |
| | **Median** | 278.9 | 170.6 | 124.3 | 134.2 |
| | **Std deviation** | 28.0 | 10.5 | 13.2 | 587.8 |
| | **Maximum** | 396.3 | 217.8 | 233.6 | 1947.1 |

# Appendix C. Network data

In this Appendix, the network data of the case studies analysed in Chapter 3 are provided. Table C-1 includes the technical characteristics of the conductors used in the LV network, where the values of the resistance R inductance L and capacitance C are provided per unit of length (km). Table C-2 provides the conductor used in each line of this network, defined by the start and end nodes, as well as the length of each line. Tables C-3 and C-4 provide the respective data for the MV case study analysed in the same chapter.

**Table C-1 List of conductors of the LV network analysed in Chapter 3**

| Code | R (Ω/km) | L (mH/km) | C (nF/km) |
|---|---|---|---|
| **BT_LXS16** | 2.083 | 0.3183 | 4.8 |
| **BT_LXS25** | 1.333 | 0.3183 | 4.8 |
| **BT_LXS50** | 0.667 | 0.3183 | 4.8 |
| **BT_LXS70** | 0.476 | 0.3183 | 4.8 |
| **LXS_2X10** | 3.060 | 0.4775 | 4.8 |
| **LXS_2x16** | 1.910 | 0.4775 | 4.8 |
| **LXS_4x10** | 3.060 | 0.4775 | 4.8 |
| **LXS_4x16** | 1.910 | 0.4775 | 4.8 |
| **LXS_4x50** | 0.641 | 0.4775 | 4.8 |
| **VV_2x4** | 4.450 | 0.3183 | 4.8 |
| **XS_2x4** | 4.610 | 0.4775 | 4.8 |
| **XS_4x2c5** | 7.130 | 0.4775 | 4.8 |
| **XS_4x4** | 4.610 | 0.4775 | 4.8 |
| **XS_4x6** | 2.970 | 0.4775 | 4.8 |

**Table C-2 Type of conductor and line length of the LV network analysed in Chapter 3**

| Line ID | Start Node | End Node | Code | Length (m) |
|---|---|---|---|---|
| 1 | 1 | 2 | BT_LXS50 | 85 |
| 2 | 1 | 3 | BT_LXS70 | 40 |
| 3 | 1 | 4 | BT_LXS50 | 55 |
| 4 | 2 | 5 | BT_LXS70 | 65 |
| 5 | 3 | 6 | LXS_4x50 | 120 |
| 6 | 3 | 7 | BT_LXS50 | 105 |
| 7 | 4 | 8 | BT_LXS50 | 100 |
| 8 | 5 | 9 | BT_LXS50 | 70 |
| 9 | 5 | 10 | XS_4x6 | 35 |
| 10 | 5 | 11 | BT_LXS16 | 105 |
| 11 | 6 | 12 | BT_LXS16 | 140 |
| 12 | 7 | 13 | BT_LXS50 | 35 |
| 13 | 8 | 14 | LXS_4x10 | 65 |
| 14 | 8 | 15 | LXS_2x16 | 65 |
| 15 | 9 | 16 | BT_LXS50 | 35 |
| 16 | 11 | 17 | XS_4x2c5 | 35 |
| 17 | 11 | 18 | LXS_4x16 | 50 |
| 18 | 12 | 19 | BT_LXS70 | 80 |

| | | | | |
|---|---|---|---|---|
| 19 | 13 | 20 | LXS_4x16 | 80 |
| 20 | 13 | 21 | XS_4x4 | 105 |
| 21 | 14 | 22 | XS_4x2c5 | 170 |
| 22 | 15 | 23 | LXS_2x16 | 140 |
| 23 | 16 | 24 | BT_LXS25 | 35 |
| 24 | 18 | 25 | XS_4x4 | 35 |
| 25 | 19 | 26 | BT_LXS70 | 50 |
| 26 | 20 | 27 | BT_LXS16 | 90 |
| 27 | 23 | 28 | VV_2x4 | 210 |
| 28 | 24 | 29 | XS_2x4 | 40 |
| 29 | 26 | 30 | BT_LXS25 | 40 |
| 30 | 27 | 31 | LXS_2X10 | 70 |
| 31 | 28 | 32 | XS_2x4 | 70 |
| 32 | 31 | 33 | XS_2x4 | 35 |

**Table C-3 List of conductors of the MV network analysed in Chapter 3**

| Code | R (Ω/km) | L (mH/km) | C (nF/km) |
|---|---|---|---|
| **AA_020_A_RT** | 1.6425 | 1.3029 | 8.8636 |
| **AA_030_A_RT** | 1.1810 | 1.2698 | 9.1040 |
| **AA_050_A_SG** | 0.7309 | 1.2541 | 9.2228 |
| **AA_090_A_SG** | 0.4112 | 1.1966 | 9.6854 |
| **AM_020_A_RT** | 1.6080 | 1.3029 | 8.8636 |
| **CU_025_A_SG** | 0.7334 | 1.3179 | 8.7586 |
| **LEHIV_070_S** | 0.5323 | 0.3508 | 215.1960 |
| **LXHIOV_070_S** | 0.5680 | 0.3508 | 215.1960 |
| **LXHIOV_120_S** | 0.3244 | 0.3229 | 261.7361 |
| **PHCA_016_S** | 1.3760 | 0.3893 | 220.0000 |
| **PHCA_025_S** | 0.8699 | 0.3597 | 240.0000 |
| **PHCA_035_S** | 0.6270 | 0.3498 | 270.0000 |
| **PHCA_050_S** | 0.4630 | 0.3298 | 300.0000 |

**Table C-4 Type of conductor and line length of the MV network analysed in Chapter 3**

| Line ID | Start Node | End Node | Code | Length (m) |
|---|---|---|---|---|
| 1 | 206 | 202 | LXHIOV_120_S | 68 |
| 2 | 206 | 201 | LXHIOV_120_S | 71 |
| 3 | 206 | 203 | LXHIOV_120_S | 50 |
| 4 | 203 | 183 | AA_050_A_SG | 1872 |
| 5 | 183 | 177 | AA_050_A_SG | 195 |
| 6 | 177 | 166 | AA_050_A_SG | 453 |
| 7 | 166 | 125 | AA_050_A_SG | 2295 |
| 8 | 125 | 115 | AA_050_A_SG | 1261 |
| 9 | 115 | 106 | AA_050_A_SG | 935 |
| 10 | 106 | 99 | AA_050_A_SG | 712 |
| 11 | 99 | 103 | AA_050_A_SG | 1494 |
| 12 | 103 | 108 | AA_050_A_SG | 954 |
| 13 | 108 | 116 | AA_050_A_SG | 2589 |
| 14 | 116 | 120 | AA_050_A_SG | 1698 |
| 15 | 120 | 126 | AA_050_A_SG | 913 |
| 16 | 126 | 129 | AM_020_A_RT | 457 |
| 17 | 129 | 136 | AM_020_A_RT | 268 |
| 18 | 136 | 113 | AA_050_A_SG | 3080 |
| 19 | 113 | 95 | AA_050_A_SG | 988 |
| 20 | 95 | 88 | AA_050_A_SG | 387 |
| 21 | 88 | 64 | AA_050_A_SG | 1552 |
| 22 | 120 | 121 | AM_020_A_RT | 9 |

| | | | | |
|---|---|---|---|---|
| 23 | 126 | 123 | AA_050_A_SG | 167 |
| 24 | 129 | 128 | AA_030_A_RT | 275 |
| 25 | 88 | 89 | AA_050_A_SG | 13 |
| 26 | 183 | 178 | AA_030_A_RT | 64 |
| 27 | 106 | 92 | AA_030_A_RT | 1058 |
| 28 | 166 | 169 | AA_030_A_RT | 38 |
| 29 | 125 | 124 | AA_030_A_RT | 30 |
| 30 | 136 | 156 | AM_020_A_RT | 1363 |
| 31 | 156 | 189 | AM_020_A_RT | 1611 |
| 32 | 189 | 196 | AA_030_A_RT | 548 |
| 33 | 196 | 199 | LXHIOV_070_S | 480 |
| 34 | 156 | 158 | AA_050_A_SG | 1310 |
| 35 | 189 | 192 | AM_020_A_RT | 100 |
| 36 | 116 | 140 | AA_030_A_RT | 1559 |
| 37 | 140 | 148 | AA_030_A_RT | 405 |
| 38 | 148 | 145 | AA_030_A_RT | 61 |
| 39 | 145 | 143 | AA_030_A_RT | 63 |
| 40 | 140 | 154 | AA_030_A_RT | 821 |
| 41 | 148 | 141 | AA_030_A_RT | 343 |
| 42 | 108 | 134 | AM_020_A_RT | 1714 |
| 43 | 134 | 142 | AM_020_A_RT | 494 |
| 44 | 142 | 146 | AM_020_A_RT | 180 |
| 45 | 146 | 147 | AM_020_A_RT | 68 |
| 46 | 147 | 149 | CU_025_A_SG | 20 |
| 47 | 134 | 135 | AA_030_A_RT | 119 |
| 48 | 103 | 91 | AM_020_A_RT | 649 |
| 49 | 146 | 138 | AA_050_A_SG | 634 |
| 50 | 138 | 139 | LXHIOV_070_S | 35 |
| 51 | 142 | 153 | AA_050_A_SG | 1009 |
| 52 | 153 | 164 | AA_050_A_SG | 699 |
| 53 | 153 | 155 | AA_030_A_RT | 245 |
| 54 | 99 | 78 | AA_050_A_SG | 1380 |
| 55 | 78 | 57 | AA_050_A_SG | 1476 |
| 56 | 57 | 52 | AA_050_A_SG | 879 |
| 57 | 52 | 50 | AA_050_A_SG | 204 |
| 58 | 50 | 43 | AA_050_A_SG | 1536 |
| 59 | 43 | 38 | AA_050_A_SG | 320 |
| 60 | 38 | 37 | AA_020_A_RT | 199 |
| 61 | 52 | 54 | AA_030_A_RT | 272 |
| 62 | 38 | 35 | AA_050_A_SG | 138 |
| 63 | 78 | 63 | AM_020_A_RT | 1404 |
| 64 | 57 | 56 | AA_030_A_RT | 481 |
| 65 | 43 | 44 | AA_030_A_RT | 735 |
| 66 | 44 | 45 | AA_030_A_RT | 661 |
| 67 | 44 | 34 | AA_050_A_SG | 634 |
| 68 | 50 | 48 | AA_050_A_SG | 1798 |
| 69 | 48 | 31 | AA_050_A_SG | 3460 |
| 70 | 31 | 36 | AA_050_A_SG | 1177 |
| 71 | 48 | 51 | AA_050_A_SG | 758 |
| 72 | 31 | 28 | AA_050_A_SG | 594 |
| 73 | 202 | 194 | AA_090_A_SG | 1144 |
| 74 | 194 | 179 | AA_090_A_SG | 625 |
| 75 | 179 | 173 | AA_090_A_SG | 364 |
| 76 | 173 | 137 | AA_090_A_SG | 3436 |
| 77 | 137 | 131 | AA_090_A_SG | 669 |
| 78 | 131 | 87 | AA_090_A_SG | 3561 |
| 79 | 87 | 83 | AA_090_A_SG | 536 |
| 80 | 83 | 59 | AA_090_A_SG | 1449 |
| 81 | 59 | 49 | AA_090_A_SG | 2060 |
| 82 | 49 | 42 | AA_090_A_SG | 2311 |
| 83 | 42 | 32 | AA_090_A_SG | 952 |

| | | | | |
|---|---|---|---|---|
| 84 | 32 | 29 | AA_090_A_SG | 518 |
| 85 | 29 | 15 | AA_090_A_SG | 2412 |
| 86 | 15 | 6 | AA_090_A_SG | 1188 |
| 87 | 6 | 3 | AA_050_A_SG | 436 |
| 88 | 42 | 40 | AA_050_A_SG | 12 |
| 89 | 32 | 33 | AA_050_A_SG | 257 |
| 90 | 29 | 30 | AA_050_A_SG | 323 |
| 91 | 15 | 16 | AA_050_A_SG | 21 |
| 92 | 6 | 5 | AA_030_A_RT | 394 |
| 93 | 194 | 208 | AA_020_A_RT | 1364 |
| 94 | 173 | 172 | AA_030_A_RT | 136 |
| 95 | 49 | 46 | AA_050_A_SG | 696 |
| 96 | 179 | 159 | AA_050_A_SG | 1117 |
| 97 | 159 | 162 | AA_050_A_SG | 161 |
| 98 | 162 | 144 | AM_020_A_RT | 1073 |
| 99 | 162 | 163 | AA_050_A_SG | 105 |
| 100 | 131 | 133 | AM_020_A_RT | 406 |
| 101 | 137 | 132 | AM_020_A_RT | 2286 |
| 102 | 132 | 122 | AA_050_A_SG | 27 |
| 103 | 132 | 112 | AA_050_A_SG | 756 |
| 104 | 112 | 105 | AM_020_A_RT | 1891 |
| 105 | 112 | 76 | AM_020_A_RT | 517 |
| 106 | 159 | 168 | AA_050_A_SG | 703 |
| 107 | 168 | 171 | AM_020_A_RT | 364 |
| 108 | 168 | 167 | AA_030_A_RT | 56 |
| 109 | 167 | 157 | AM_020_A_RT | 325 |
| 110 | 167 | 170 | AA_030_A_RT | 516 |
| 111 | 59 | 62 | AA_050_A_SG | 454 |
| 112 | 62 | 58 | AA_050_A_SG | 604 |
| 113 | 62 | 65 | AA_050_A_SG | 550 |
| 114 | 65 | 73 | AA_030_A_RT | 528 |
| 115 | 65 | 67 | AA_050_A_SG | 379 |
| 116 | 67 | 68 | AA_050_A_SG | 175 |
| 117 | 67 | 72 | AA_050_A_SG | 243 |
| 118 | 68 | 66 | AA_050_A_SG | 669 |
| 119 | 68 | 61 | AA_050_A_SG | 555 |
| 120 | 83 | 82 | AA_050_A_SG | 1833 |
| 121 | 87 | 90 | AA_050_A_SG | 395 |
| 122 | 90 | 86 | AA_050_A_SG | 163 |
| 123 | 90 | 96 | AA_050_A_SG | 682 |
| 124 | 201 | 190 | AA_050_A_SG | 1349 |
| 125 | 190 | 187 | PHCA_050_S | 183 |
| 126 | 187 | 186 | LEHIV_070_S | 13 |
| 127 | 186 | 185 | PHCA_050_S | 94 |
| 128 | 185 | 191 | LXHIOV_070_S | 250 |
| 129 | 191 | 193 | PHCA_050_S | 54 |
| 130 | 193 | 188 | PHCA_025_S | 482 |
| 131 | 188 | 181 | PHCA_016_S | 152 |
| 132 | 181 | 184 | LXHIOV_120_S | 154 |
| 133 | 184 | 182 | LXHIOV_120_S | 236 |
| 134 | 185 | 174 | LEHIV_070_S | 536 |
| 135 | 174 | 176 | LXHIOV_120_S | 490 |
| 136 | 176 | 175 | LXHIOV_120_S | 90 |

# Appendix D. Attenuation matrix

Table D-1 includes the attenuation matrix obtained for the LV case study analysed in Chapter 3, which provides the signal attenuation between each pair of nodes, expressed in dB.

**Table D-1 Attenuation matrix of the LV network analysed in Chapter 3**

| Node | 1 | 2 | 3 | 4 | 5 | 6 | 7 | 8 | 9 | 10 | 11 |
|---|---|---|---|---|---|---|---|---|---|---|---|
| **1** | -1000 | -9.70 | -16.63 | -23.75 | -27.93 | -31.84 | -36.44 | -20.68 | -25.27 | -28.77 | -32.43 |
| **2** | -13.58 | -1000 | -11.68 | -18.90 | -23.03 | -26.96 | -31.57 | -15.50 | -19.97 | -23.39 | -27.10 |
| **3** | -17.23 | -8.89 | -1000 | -10.49 | -14.65 | -18.40 | -23.01 | -7.10 | -11.87 | -15.15 | -18.75 |
| **4** | -26.83 | -18.02 | -12.50 | -1000 | -7.22 | -11.85 | -16.01 | -14.24 | -15.60 | -22.04 | -24.10 |
| **5** | -29.65 | -20.80 | -15.28 | -6.44 | -1000 | -6.51 | -11.70 | -17.07 | -18.43 | -24.90 | -27.01 |
| **6** | -34.57 | -25.28 | -19.56 | -11.79 | -7.22 | -1000 | -7.89 | -21.69 | -23.15 | -29.65 | -31.68 |
| **7** | -42.15 | -32.78 | -27.06 | -18.75 | -15.09 | -10.50 | -1000 | -29.17 | -30.75 | -37.10 | -39.23 |
| **8** | -25.49 | -16.25 | -10.73 | -13.71 | -17.77 | -22.15 | -28.49 | -1000 | -14.23 | -20.53 | -22.68 |
| **9** | -27.98 | -18.82 | -13.35 | -15.94 | -19.99 | -24.16 | -30.40 | -14.91 | -1000 | -7.17 | -11.39 |
| **10** | -33.45 | -24.21 | -18.57 | -21.52 | -25.66 | -30.17 | -36.47 | -20.62 | -9.45 | -1000 | -14.02 |
| **11** | -35.99 | -27.01 | -21.28 | -24.25 | -28.49 | -33.11 | -39.47 | -23.58 | -12.36 | -14.68 | -1000 |
| **12** | -40.76 | -31.98 | -26.05 | -29.18 | -33.43 | -38.06 | -44.37 | -28.49 | -17.06 | -19.21 | -8.38 |
| **13** | -9.02 | -14.26 | -19.11 | -27.53 | -31.80 | -36.17 | -42.47 | -26.60 | -27.75 | -34.20 | -36.29 |
| **14** | -14.85 | -20.71 | -25.54 | -33.94 | -38.21 | -42.58 | -48.89 | -33.01 | -34.70 | -41.08 | -43.43 |
| **15** | -20.87 | -26.48 | -31.32 | -39.73 | -44.00 | -48.19 | -54.02 | -38.80 | -40.49 | -46.86 | -49.22 |
| **16** | -25.98 | -31.63 | -36.41 | -44.81 | -48.99 | -53.23 | -59.61 | -43.87 | -45.67 | -52.04 | -54.40 |
| **17** | -30.47 | -35.70 | -40.53 | -48.99 | -53.24 | -57.40 | -63.63 | -48.03 | -50.14 | -56.51 | -58.54 |
| **18** | -34.68 | -39.91 | -44.76 | -53.25 | -57.39 | -61.77 | -68.21 | -52.39 | -54.24 | -60.79 | -62.65 |
| **19** | -16.66 | -22.24 | -27.10 | -35.50 | -39.77 | -44.14 | -50.45 | -34.57 | -36.36 | -42.90 | -45.05 |
| **20** | -18.21 | -23.98 | -28.80 | -37.21 | -41.48 | -45.85 | -52.15 | -36.28 | -37.99 | -44.52 | -46.70 |
| **21** | -30.07 | -35.73 | -40.57 | -48.98 | -53.25 | -57.62 | -63.92 | -48.05 | -49.73 | -56.12 | -58.46 |
| **22** | -34.01 | -39.69 | -44.52 | -52.93 | -57.20 | -61.57 | -67.87 | -52.00 | -53.68 | -60.07 | -62.42 |
| **23** | -41.77 | -47.44 | -52.28 | -60.69 | -64.96 | -69.32 | -75.63 | -59.75 | -61.44 | -67.81 | -70.17 |
| **24** | -45.85 | -51.53 | -56.37 | -64.77 | -69.04 | -73.41 | -79.72 | -63.84 | -65.53 | -71.90 | -74.26 |
| **25** | -28.25 | -33.92 | -38.75 | -47.16 | -51.24 | -55.55 | -61.95 | -46.22 | -47.92 | -54.29 | -56.65 |
| **26** | -11.59 | -16.34 | -21.29 | -29.94 | -34.17 | -38.96 | -45.50 | -29.62 | -30.25 | -36.85 | -38.80 |
| **27** | -16.69 | -21.80 | -26.67 | -35.07 | -39.38 | -43.70 | -50.02 | -34.25 | -36.14 | -42.74 | -44.58 |
| **28** | -24.84 | -30.30 | -35.16 | -43.61 | -47.93 | -52.49 | -58.92 | -43.04 | -44.27 | -50.84 | -52.97 |
| **29** | -28.59 | -33.85 | -38.68 | -47.09 | -51.18 | -55.25 | -60.74 | -45.92 | -47.56 | -54.12 | -56.03 |
| **30** | -24.93 | -30.21 | -35.15 | -43.66 | -47.89 | -52.58 | -58.97 | -43.08 | -44.46 | -51.01 | -53.04 |
| **31** | -27.11 | -32.07 | -36.91 | -45.76 | -50.12 | -54.73 | -61.20 | -45.32 | -46.06 | -52.44 | -54.80 |
| **32** | -33.21 | -38.37 | -43.23 | -51.63 | -55.79 | -60.35 | -66.05 | -50.90 | -51.84 | -58.41 | -60.13 |
| **33** | -41.29 | -46.55 | -51.41 | -59.91 | -64.09 | -68.44 | -74.75 | -58.86 | -60.55 | -66.92 | -69.28 |
| **Node** | **12** | **13** | **14** | **15** | **16** | **17** | **18** | **19** | **20** | **21** | **22** |
| **1** | -35.51 | -6.67 | -13.09 | -17.09 | -22.93 | -28.41 | -30.80 | -14.28 | -16.79 | -25.36 | -29.67 |
| **2** | -30.29 | -15.33 | -21.83 | -27.33 | -32.59 | -37.10 | -41.45 | -22.70 | -26.49 | -35.03 | -40.22 |
| **3** | -21.77 | -19.30 | -25.34 | -30.88 | -36.16 | -40.76 | -45.15 | -26.26 | -30.02 | -38.57 | -43.76 |
| **4** | -29.47 | -29.01 | -35.05 | -40.58 | -45.63 | -50.22 | -54.64 | -35.97 | -39.73 | -48.28 | -53.46 |
| **5** | -32.43 | -31.87 | -37.91 | -43.45 | -48.47 | -53.07 | -57.49 | -38.83 | -42.59 | -51.14 | -56.33 |
| **6** | -37.29 | -36.30 | -42.22 | -47.42 | -52.60 | -57.33 | -61.96 | -43.26 | -47.02 | -55.57 | -60.76 |
| **7** | -44.92 | -43.78 | -49.67 | -54.49 | -60.02 | -64.80 | -69.57 | -50.74 | -54.50 | -63.05 | -68.24 |
| **8** | -28.19 | -27.16 | -33.50 | -38.73 | -43.86 | -48.46 | -53.05 | -34.11 | -37.87 | -46.43 | -51.61 |
| **9** | -14.63 | -29.39 | -35.90 | -41.43 | -46.71 | -51.54 | -56.05 | -36.87 | -40.63 | -49.12 | -54.31 |
| **10** | -19.20 | -34.93 | -41.30 | -46.83 | -52.12 | -56.95 | -61.55 | -42.34 | -46.11 | -54.53 | -59.71 |

| | | | | | | | | | | | |
|---|---|---|---|---|---|---|---|---|---|---|---|
| **11** | -7.13 | -37.70 | -44.25 | -49.78 | -55.07 | -59.57 | -63.93 | -45.16 | -48.93 | -57.48 | -62.66 |
| **12** | -1000 | -42.62 | -49.14 | -54.67 | -59.63 | -64.26 | -68.73 | -50.05 | -53.81 | -62.37 | -67.55 |
| **13** | -41.77 | -1000 | -10.18 | -14.45 | -20.33 | -25.75 | -28.01 | -11.61 | -14.15 | -22.27 | -26.65 |
| **14** | -48.88 | -10.38 | -1000 | -8.10 | -13.32 | -19.07 | -21.14 | -13.22 | -17.35 | -25.69 | -30.90 |
| **15** | -54.66 | -15.66 | -8.81 | -1000 | -10.31 | -15.15 | -17.41 | -18.57 | -22.51 | -30.91 | -36.11 |
| **16** | -59.62 | -20.84 | -13.79 | -10.09 | -1000 | -9.11 | -11.58 | -23.92 | -27.74 | -36.11 | -41.29 |
| **17** | -63.79 | -25.28 | -18.45 | -13.73 | -8.07 | -1000 | -5.22 | -28.12 | -31.83 | -40.27 | -45.50 |
| **18** | -67.97 | -29.69 | -22.76 | -18.03 | -12.63 | -7.34 | -1000 | -32.27 | -36.06 | -44.62 | -49.76 |
| **19** | -50.44 | -11.97 | -13.68 | -18.88 | -24.19 | -28.79 | -33.12 | -1000 | -6.33 | -14.26 | -18.63 |
| **20** | -52.14 | -13.57 | -16.09 | -21.34 | -26.47 | -30.98 | -35.36 | -5.71 | -1000 | -11.86 | -15.87 |
| **21** | -63.91 | -24.88 | -27.31 | -32.68 | -37.71 | -42.35 | -46.78 | -16.84 | -14.56 | -1000 | -9.47 |
| **22** | -67.86 | -28.85 | -31.35 | -36.75 | -41.77 | -46.43 | -50.90 | -20.84 | -18.23 | -9.52 | -1000 |
| **23** | -75.61 | -36.60 | -38.71 | -43.94 | -49.05 | -53.77 | -58.33 | -28.61 | -26.01 | -15.94 | -11.95 |
| **24** | -79.70 | -40.68 | -42.67 | -47.89 | -53.07 | -57.84 | -62.39 | -32.68 | -30.16 | -20.34 | -15.71 |
| **25** | -62.00 | -23.08 | -25.63 | -30.90 | -36.27 | -41.10 | -45.69 | -14.91 | -12.99 | -15.65 | -21.07 |
| **26** | -44.26 | -13.15 | -19.34 | -24.81 | -29.86 | -34.48 | -39.03 | -20.18 | -23.98 | -32.52 | -37.71 |
| **27** | -49.87 | -18.43 | -24.59 | -30.14 | -35.42 | -40.25 | -44.62 | -25.52 | -29.27 | -37.83 | -43.01 |
| **28** | -58.26 | -26.84 | -32.72 | -38.25 | -43.54 | -48.37 | -52.75 | -33.84 | -37.60 | -45.95 | -51.13 |
| **29** | -61.60 | -30.22 | -36.59 | -40.89 | -47.01 | -51.95 | -56.47 | -37.29 | -41.07 | -49.17 | -54.37 |
| **30** | -58.29 | -26.73 | -32.78 | -38.31 | -43.59 | -48.42 | -52.92 | -33.69 | -37.45 | -46.00 | -51.19 |
| **31** | -60.24 | -29.63 | -34.94 | -39.60 | -45.03 | -49.72 | -54.77 | -37.24 | -40.99 | -49.63 | -54.79 |
| **32** | -65.94 | -34.88 | -40.94 | -45.08 | -51.22 | -56.14 | -60.96 | -42.24 | -46.01 | -54.06 | -59.22 |
| **33** | -74.57 | -42.88 | -49.12 | -54.08 | -59.37 | -64.20 | -68.97 | -49.93 | -53.71 | -61.78 | -66.96 |
| **Node** | **23** | **24** | **25** | **26** | **27** | **28** | **29** | **30** | **31** | **32** | **33** |
| **1** | -37.90 | -40.93 | -23.55 | -8.11 | -13.58 | -22.05 | -24.69 | -22.83 | -26.47 | -30.66 | -36.25 |
| **2** | -47.15 | -52.24 | -34.14 | -16.91 | -22.33 | -30.45 | -35.10 | -30.39 | -34.80 | -39.50 | -46.61 |
| **3** | -50.69 | -55.78 | -38.00 | -20.68 | -26.13 | -34.11 | -38.92 | -34.15 | -38.33 | -43.63 | -50.54 |
| **4** | -60.40 | -65.49 | -47.50 | -30.53 | -35.86 | -43.93 | -48.49 | -43.86 | -48.14 | -53.29 | -59.94 |
| **5** | -63.26 | -68.35 | -50.36 | -33.40 | -38.72 | -46.76 | -51.36 | -46.68 | -50.95 | -56.15 | -62.79 |
| **6** | -67.69 | -72.78 | -54.75 | -38.42 | -43.39 | -51.53 | -55.79 | -51.59 | -55.43 | -60.15 | -66.95 |
| **7** | -75.17 | -80.26 | -62.23 | -45.90 | -51.06 | -59.02 | -63.27 | -59.07 | -62.82 | -66.96 | -74.43 |
| **8** | -58.54 | -63.64 | -45.64 | -29.28 | -34.48 | -42.39 | -46.64 | -42.44 | -46.62 | -51.62 | -58.08 |
| **9** | -61.24 | -66.33 | -48.30 | -31.19 | -36.74 | -44.69 | -49.34 | -44.84 | -48.89 | -52.65 | -60.50 |
| **10** | -66.64 | -71.74 | -53.71 | -36.76 | -42.33 | -50.24 | -54.81 | -50.29 | -54.29 | -58.59 | -65.90 |
| **11** | -69.59 | -74.69 | -56.44 | -39.32 | -44.99 | -52.81 | -57.78 | -52.97 | -57.24 | -61.54 | -68.85 |
| **12** | -74.48 | -79.58 | -61.37 | -44.19 | -49.74 | -57.62 | -62.56 | -57.72 | -62.13 | -66.64 | -73.78 |
| **13** | -34.62 | -37.52 | -20.19 | -12.39 | -17.80 | -25.50 | -29.73 | -25.51 | -30.00 | -35.02 | -41.52 |
| **14** | -37.67 | -42.54 | -24.96 | -18.80 | -24.29 | -31.90 | -36.15 | -31.95 | -35.70 | -39.03 | -47.31 |
| **15** | -42.75 | -47.57 | -30.17 | -24.55 | -30.07 | -37.68 | -41.93 | -37.73 | -41.48 | -44.82 | -53.09 |
| **16** | -48.01 | -53.13 | -35.71 | -29.64 | -35.25 | -42.86 | -48.12 | -42.92 | -46.92 | -52.14 | -59.16 |
| **17** | -52.25 | -57.28 | -40.12 | -33.86 | -39.46 | -47.33 | -51.93 | -47.39 | -51.14 | -56.04 | -62.90 |
| **18** | -56.61 | -61.76 | -44.16 | -38.07 | -43.60 | -51.49 | -56.64 | -51.58 | -55.53 | -60.76 | -67.75 |
| **19** | -26.86 | -29.88 | -11.47 | -20.32 | -25.85 | -33.78 | -38.53 | -33.51 | -38.79 | -43.64 | -50.29 |
| **20** | -23.96 | -27.11 | -9.49 | -22.06 | -27.55 | -35.36 | -40.13 | -35.21 | -40.36 | -45.36 | -51.95 |
| **21** | -16.44 | -19.72 | -15.88 | -33.81 | -39.32 | -46.95 | -51.18 | -46.98 | -51.67 | -56.56 | -62.98 |
| **22** | -12.38 | -15.18 | -20.63 | -37.76 | -43.27 | -50.90 | -55.19 | -50.93 | -55.82 | -60.60 | -67.07 |
| **23** | -1000 | -7.13 | -27.89 | -45.52 | -51.02 | -58.63 | -62.89 | -58.69 | -62.86 | -67.73 | -74.09 |
| **24** | -8.19 | -1000 | -31.93 | -49.60 | -55.11 | -62.72 | -66.97 | -62.77 | -66.66 | -71.47 | -78.13 |
| **25** | -27.63 | -32.62 | -1000 | -31.89 | -37.50 | -45.11 | -50.42 | -45.16 | -49.09 | -54.56 | -61.54 |
| **26** | -44.64 | -49.73 | -31.70 | -1000 | -10.32 | -18.17 | -21.26 | -18.09 | -22.42 | -26.57 | -32.49 |
| **27** | -49.95 | -55.04 | -37.28 | -10.06 | -1000 | -12.40 | -14.62 | -12.82 | -16.39 | -20.10 | -25.51 |
| **28** | -58.06 | -63.16 | -45.88 | -17.48 | -12.32 | -1000 | -6.80 | -16.13 | -20.49 | -25.39 | -32.20 |
| **29** | -60.59 | -65.29 | -49.06 | -21.45 | -15.28 | -7.92 | -1000 | -19.31 | -24.20 | -28.97 | -36.05 |
| **30** | -58.12 | -63.21 | -45.69 | -17.54 | -12.37 | -16.14 | -20.34 | -1000 | -7.94 | -12.34 | -17.92 |
| **31** | -61.42 | -66.52 | -48.47 | -20.12 | -14.63 | -18.75 | -24.01 | -6.46 | -1000 | -6.81 | -12.04 |
| **32** | -66.10 | -70.85 | -53.86 | -25.65 | -20.10 | -24.00 | -29.19 | -12.32 | -7.83 | -1000 | -10.20 |
| **33** | -73.89 | -78.99 | -62.20 | -34.15 | -28.18 | -32.26 | -37.30 | -20.06 | -17.02 | -12.28 | -1000 |

# Appendix E. Voltage control KPIs

Tables E-1 and E-2 include the values of the Key Performance Indicators (KPIs) obtained in the forecasting and communication analyses carried out in Chapter 4 for the LV and MV case studies, respectively. Both tables present the same structure, where the Scenario 1 corresponds to the forecast error analysis with PV underestimation and load overestimation, Scenario 2 with the PV overestimation and load underestimation, Scenario 3 to the set-point interval analysis with the sunny day PV profile, and Scenario 4 with the cloudy the PV profile.

**Table E-1 Results of the KPIs in the LV network analysed in Chapter 4**

| | | Voltage deviation | | | | Curtailment | | Losses | | Total |
|---|---|---|---|---|---|---|---|---|---|---|
| | Value | Voltage (p.u.) | Number of buses | Energy (kWh) | Cost (€) | Energy (kWh) | Cost (€) | Energy (kWh) | Cost (€) | Cost (€) |
| Scenario 1 | 0% | 18.46 | 305 | 32.01 | 7.68 | 62.13 | 2.81 | 76.93 | 3.49 | 13.98 |
| | 10% | 66.71 | 1,160 | 66.06 | 12.72 | 46.70 | 2.10 | 77.08 | 3.51 | 18.33 |
| | 20% | 94.84 | 1,532 | 76.95 | 20.06 | 54.33 | 2.41 | 75.66 | 3.45 | 25.92 |
| | 30% | 109.31 | 1,611 | 77.12 | 28.44 | 63.01 | 2.75 | 77.13 | 3.51 | 34.70 |
| | 40% | 106.35 | 1,541 | 73.97 | 27.76 | 95.58 | 4.15 | 77.13 | 3.52 | 35.43 |
| Scenario 2 | 0% | 18.46 | 305 | 32.01 | 7.68 | 62.13 | 2.81 | 76.93 | 3.49 | 13.98 |
| | 10% | 18.46 | 305 | 32.01 | 7.68 | 62.13 | 2.81 | 76.93 | 3.49 | 13.98 |
| | 20% | 23.75 | 397 | 40.08 | 9.61 | 82.22 | 3.71 | 76.14 | 3.45 | 16.77 |
| | 30% | 23.81 | 396 | 39.07 | 9.57 | 102.07 | 4.60 | 75.55 | 3.41 | 17.58 |
| | 40% | 25.51 | 426 | 40.93 | 9.93 | 121.72 | 5.48 | 74.61 | 3.36 | 18.78 |
| Scenario 3 | 1min | 48.33 | 837 | 60.21 | 12.17 | 23.56 | 1.07 | 95.78 | 4.36 | 17.61 |
| | 5min | 48.33 | 837 | 60.21 | 12.17 | 23.56 | 1.07 | 95.78 | 4.36 | 17.61 |
| | 15min | 57.85 | 973 | 68.19 | 15.93 | 18.82 | 0.85 | 97.88 | 4.46 | 21.25 |
| | 30min | 57.14 | 968 | 66.20 | 15.76 | 23.22 | 1.04 | 101.34 | 4.62 | 21.42 |
| | 1h | 73.62 | 1,218 | 81.19 | 19.57 | 18.78 | 0.85 | 100.63 | 4.59 | 25.01 |
| | 2h | 101.97 | 1,667 | 92.49 | 24.37 | 3.56 | 0.15 | 100.43 | 4.56 | 29.08 |
| | 4h | 101.97 | 1,667 | 92.49 | 24.37 | 3.56 | 0.15 | 100.43 | 4.56 | 29.08 |
| | 8h | 112.95 | 1,803 | 101.19 | 29.13 | 0.00 | 0.00 | 91.60 | 4.16 | 33.29 |
| | 24h | 136.67 | 2,155 | 117.81 | 35.74 | 0.00 | 0.00 | 83.02 | 3.78 | 39.52 |
| Scenario 4 | 1min | 33.08 | 570 | 41.04 | 9.61 | 41.10 | 1.87 | 80.25 | 3.64 | 15.12 |
| | 5min | 54.76 | 908 | 57.77 | 14.54 | 41.04 | 1.85 | 77.98 | 3.54 | 19.93 |
| | 15min | 59.63 | 966 | 60.89 | 16.82 | 40.61 | 1.83 | 78.81 | 3.58 | 22.22 |
| | 30min | 65.91 | 1,057 | 66.23 | 19.15 | 38.01 | 1.71 | 77.94 | 3.54 | 24.39 |
| | 1h | 79.85 | 1,283 | 74.67 | 21.20 | 39.36 | 1.76 | 76.60 | 3.47 | 26.43 |
| | 2h | 117.78 | 1,743 | 90.46 | 31.08 | 21.99 | 0.93 | 69.69 | 3.18 | 35.19 |
| | 4h | 117.78 | 1,743 | 90.46 | 31.08 | 21.99 | 0.93 | 69.69 | 3.18 | 35.19 |
| | 8h | 135.36 | 2,000 | 99.89 | 34.54 | 0.85 | 0.04 | 73.67 | 3.35 | 37.93 |
| | 24h | 135.27 | 2,001 | 100.74 | 34.66 | 0.00 | 0.00 | 75.42 | 3.43 | 38.09 |

The results for the voltage deviation KPI include the total voltage in p.u. that is out of the admissible limits, the number of buses where this situation occurs, the amount of energy affected and the total cost that these voltage deviations represent with the considered methodology. The results for the energy curtailment KPI include the amount of energy that is curtailed and their cost. Similarly, the results for the energy losses include the amount of energy losses and their cost. Finally, the total cost as the sum of the costs of the three KPIs is included.

**Table E-2 Results of the KPIs in the MV network analysed in Chapter 4**

| | | Voltage deviation | | | | Curtailment | | Losses | | Total |
|---|---|---|---|---|---|---|---|---|---|---|
| | Value | Voltage (p.u.) | Number of buses | Energy (kWh) | Cost (€) | Energy (kWh) | Cost (€) | Energy (kWh) | Cost (€) | Cost (€) |
| Scenario 1 | 0% | 5.90 | 106 | 488.71 | 52.86 | 634.46 | 28.53 | 7,155.04 | 323.41 | 404.79 |
| | 10% | 40.44 | 684 | 2,378.41 | 511.50 | 31.79 | 1.45 | 6,829.91 | 308.39 | 821.35 |
| | 20% | 44.52 | 735 | 2,508.22 | 603.26 | 2.93 | 0.10 | 6,804.84 | 307.24 | 910.60 |
| | 30% | 46.42 | 764 | 2,596.80 | 640.97 | 6.65 | 0.23 | 7,001.74 | 316.23 | 957.43 |
| | 40% | 46.96 | 771 | 2,629.46 | 652.95 | 12.49 | 0.44 | 7,626.36 | 344.46 | 997.85 |
| Scenario 2 | 0% | 5.90 | 106 | 488.71 | 52.86 | 634.46 | 28.53 | 7,155.04 | 323.41 | 404.79 |
| | 10% | 0.00 | 0 | 0.00 | 0.00 | 2,116.03 | 95.94 | 7,274.93 | 328.96 | 424.89 |
| | 20% | 0.00 | 0 | 0.00 | 0.00 | 4,240.07 | 192.98 | 7,370.96 | 332.75 | 525.72 |
| | 30% | 0.00 | 0 | 0.00 | 0.00 | 7,591.71 | 345.72 | 7,218.93 | 324.63 | 670.36 |
| | 40% | 0.00 | 0 | 0.00 | 0.00 | 11,681.21 | 530.90 | 6,749.38 | 302.48 | 833.38 |
| Scenario 3 | 1min | 0.00 | 0 | 0.00 | 0.00 | 0.00 | 0.00 | 9,347.46 | 421.92 | 421.92 |
| | 5min | 21.17 | 372 | 1,327.27 | 246.68 | 0.45 | 0.02 | 9,315.15 | 420.44 | 667.13 |
| | 15min | 25.24 | 444 | 1,564.24 | 290.32 | 1.23 | 0.04 | 9,304.23 | 419.94 | 710.30 |
| | 30min | 28.29 | 498 | 1,739.09 | 322.38 | 0.20 | 0.01 | 9,298.80 | 419.69 | 742.08 |
| | 1h | 30.01 | 529 | 1,829.12 | 338.68 | 0.00 | 0.00 | 9,297.42 | 419.62 | 758.30 |
| | 2h | 30.68 | 541 | 1,870.97 | 346.29 | 0.00 | 0.00 | 9,308.83 | 420.14 | 766.43 |
| | 4h | 36.73 | 650 | 2,330.33 | 429.42 | 0.00 | 0.00 | 9,339.48 | 421.27 | 850.69 |
| | 8h | 36.73 | 650 | 2,330.33 | 429.42 | 0.00 | 0.00 | 9,339.48 | 421.27 | 850.69 |
| | 24h | 36.73 | 650 | 2,330.33 | 429.42 | 0.00 | 0.00 | 9,339.48 | 421.27 | 850.69 |
| Scenario 4 | 1min | 5.90 | 106 | 488.71 | 52.86 | 634.46 | 28.53 | 7,155.04 | 323.41 | 404.79 |
| | 5min | 30.28 | 504 | 1,810.98 | 423.26 | 131.18 | 5.82 | 6,988.62 | 315.83 | 744.90 |
| | 15min | 32.34 | 533 | 1,900.64 | 466.53 | 0.00 | 0.00 | 7,035.93 | 317.94 | 784.47 |
| | 30min | 35.58 | 589 | 2,001.38 | 496.40 | 0.00 | 0.00 | 6,889.53 | 311.17 | 807.57 |
| | 1h | 38.20 | 626 | 2,188.47 | 541.48 | 0.00 | 0.00 | 6,866.26 | 310.09 | 851.57 |
| | 2h | 44.02 | 727 | 2,442.84 | 591.47 | 0.00 | 0.00 | 6,835.16 | 308.35 | 899.82 |
| | 4h | 44.02 | 727 | 2,442.84 | 591.47 | 0.00 | 0.00 | 6,835.16 | 308.35 | 899.82 |
| | 8h | 44.02 | 727 | 2,442.84 | 591.47 | 0.00 | 0.00 | 6,835.16 | 308.35 | 899.82 |
| | 24h | 44.02 | 727 | 2,442.84 | 591.47 | 0.00 | 0.00 | 6,835.16 | 308.35 | 899.82 |